CHAPTER 4 RESULT AND DISCUSSION

This chapter demonstrates the results to improvement and testing of Thai sail windmill for water pumping. As mentioned earlier separated in configurations studied as follows:

- Field survey of the local wisdom of Thai sail windmill
- Laboratory scale testing
- Large scale testing
- Cost of windmill for water pumping

4.1 Field survey of the local wisdom of Thai sail windmill

A survey of the local Thai sail windmill in Thailand should be carried out to determine the characteristics of the windmill for water pumping at the salt farms which are widely used in the region near Samut Sakorn and Samut Songkram. A few years ago the Thai sail windmills were replaced by diesel and gasoline engine pumps because of the advantages of portability and greater control over water pumping. The salt workers along the two shores of the upper reaches of the Gulf of Thailand also use wind driven pumps to move the water from which they recover salt by evaporation. Some of the pumps are locally constructed using simple wood, bamboo, metals cloth materials and requires only carpentering skills. The result of experimental Thai sail windmill technology are as follows: type, sail, rotor and hub, Spar and main shaft, power transmission, tower structure, pump and operating data we carry out the characteristics of 14 the Thai sail windmills with a discussion of the results found.

4.1.1 Type

The Thai sail windmill is a type of low wind speed turbine, horizontal axis, bi direction to receive the wind and sail windmill. The windmill have been applied for the brine pumping at the salt farm, locally constructed windmill have been used for salt farming for at least 60 years. The oldest windmills were constructed from wood and bamboo mate which often carried 6 triangular sails are shown in Figure 4.1. In the modern Thai sail windmills, the salt farmer use cloth sails, sack sail or canvas sail which have a long lifetime more than bamboo mat sail are shown in Figure 4.2.

4.1.2 Sail

There are 6 sails made of triangular mate woven from split bamboo, cloth sail or sack canvas sail are shown in Figure 4.2 and are reinforced with nylon cord. Each sail is fastened by wooden slats and nails along its long edge to a bamboo spar radiating from the hub. The apex of each sail is held tight by a nylon cord loop connected to a 1-1.2 cm diameter nylon rope are shown in Figure 4.3 which is starched around the rotor circumference between the tips of each spar. There is a manually activated, the quick-release sail-feathering device is incorporated at each loop connection are shown in Figure 4.4. The rotor solidity of Thai sail windmill is the total swept area divided by total frontal area of blades is about 22-30 percent are shown in Table 4.1.

Figure 4.1 Thai bamboo mate windmill

Figure 4.2 Thai modern sail windmill

Figure 4.3 Circumference nylon cord

4.1.3 Quick-release sail-feathering device

A manually-activated, quick-release sail-feathering device is incorporated at each loop connection. The tips of each spar are braced by steel wires looped to points near the opposite end of the main shaft are shown in Figure 4.4. The quick-release sail-feathering device in salt farm was called “Ta-ling-Ping”; it was made form bamboo stick 15 cm long.

Figure 4.4 The quick-release sail-feathering device

Table 4.1 Solidity of Thai sail windmill in field survey

Number of windmill	Solidity		
	Small windmill	Medium windmill	Large windmill
1	23.35	26.06	22.24
2	30.32	24.70	22.96
3	26.27	25.43	28.91
4	-	27.77	22.82
5	-	24.84	-
6	-	23.28	-
7	-	24.35	-
Average	26.40	25.30	24.30

4.1.4 Rotor and hub

The sail rotor is 6.7-7.8 m of diameter for small windmill, 8.1-8.9 m for medium windmill and 9.1-9.3 m for large windmill. The rotor consists of a 30 cm diameter wooden hub mounted or steel hub mounted in the centre of a square main shaft 10 cm x 10 cm x 4.5-5.0 m, or 10 cm of diameter steel pipe . A laminated wooden hub of 30 cm diameter are shown in Figure 4.5 or steel hub of 30-60 cm diameter are shown in Figure 4.6 , was used because of its simplicity of construction on Thai sail rotors.

4.1.5 Spar and main shaft

Spars-Commonly, six bamboo spars, radiate out from the hub to form a total windmill diameter of 6.7-9.3 m. The tips of each spar are braced by steel wire of 0.3 cm diameter to points near the opposite ends of the main shaft which is between the two wooden pole. The bearing of the main shaft are rounded to fit in a mouth cut in to the top of the two wooden supporting pole are shown in Figure 4.5 to Figure 4.6. No lubrication in used.

Figure 4.5 Wooden hub and bamboo spar

Figure 4.6 Steel hub and bamboo spar

4.1.6 Power transmission

Chains are widely used for power transmission in the Thai sail windmill are shown in Figure 4.7 to Figure 4.8 Power is transferred by 10-12 m diagonally with a steel chain of 0.6 cm diameter and 2.5 cm long open links from a upper pulley of 0.7-1.0 m diameter mounted at one end of the main shaft are shown in Figure 4.9 to Figure 4.10, to lower pulley of 0.5-0.75 m diameter near the ground are shown in Figure 4.11 to Figure 4.12, which drives the power shaft of an open-trough wooden-pallet chain pump. The power transmission ratio of Thai sail windmills is 1.25-1.5 : 1 for small windmill, 1.33-1.67 : 1 for medium and large windmill are shown in Table 4.2.

4.1.7 Tower structure

The stationary support tower structure of two wood poles is set in the ground in a fixed direction to receive the winds. They are fixed in azimuth which is the angle between the north point, rotating one way in the southwest monsoon and reversing direction in the northeast monsoon. The two wood poles are square 15 cm x 15 cm x 4.0-5.3 m from the ground. The azimuth angle of the Thai sail windmill is 15° to 30° from the north point are shown in Table 4.3.

Figure 4.7 Power transmission chain for upper pulley

Figure 4.8 Power transmission chain for lower pulley

Figure 4.9 Wooden upper pulley

Figure 4.10 Steel upper pulley

Figure 4.11 Wooden lower pulley

Figure 4.12 Steel lower pulley

Table 4.2 Power transmission ratio of Thai sail windmill in field survey

Number of windmill	Power transmission ratio		
	Small windmill	Medium windmill	Large windmill
1	1.50	1.33	1.50
2	1.49	1.43	1.67
3	1.25	1.67	1.33
4	-	1.50	1.36
5	-	1.50	-
6	-	1.48	-
7	-	1.67	-
Average	1.41	1.51	1.45

Table 4.3 Azimuth angle of Thai sail windmill in field survey

Number of windmill	Azimuth angle		
	Small windmill	Medium windmill	Large windmill
1	30°	25°	20°
2	25°	30°	25°
3	15°	20°	20°
4	-	20°	25°
5	-	15°	-
6	-	25°	-
7	-	20°	-
Average	23.3°	22.1°	22.5°

4.1.8 Pump and operating data

The square-wooden-pallet chain pump or water ladder pump is commonly used in Thailand consists of rectangular wooden pallets or paddles mounted on a continuous wooden chain that runs up an inclined square-section open wooden trough which drives the power shaft of the square-wooden-pallet by chains transmission power from the windmill are shown in Figure 4.13. This type of pump is commonly used with Thai sail rotors windmill. The square-wooden-pallet chain pump slope is about 30° to 45°; width 15 cm and 3-5 m long. The performance of the square-wooden-pallet chain pump 3.0 m long and 15 cm width upon wind speed are shown in Figure 4.14, by using the data of Klungnak, P. Study on Horizontal Canvas Windmill System. Department of Irrigation Engineering, Kasetsart University, 2002 [36]. Testing in the field found that the discharge is 32 to 35 lps are shown in Figure 4.15.

Figure 4.13 Wooden-pallet chain pump

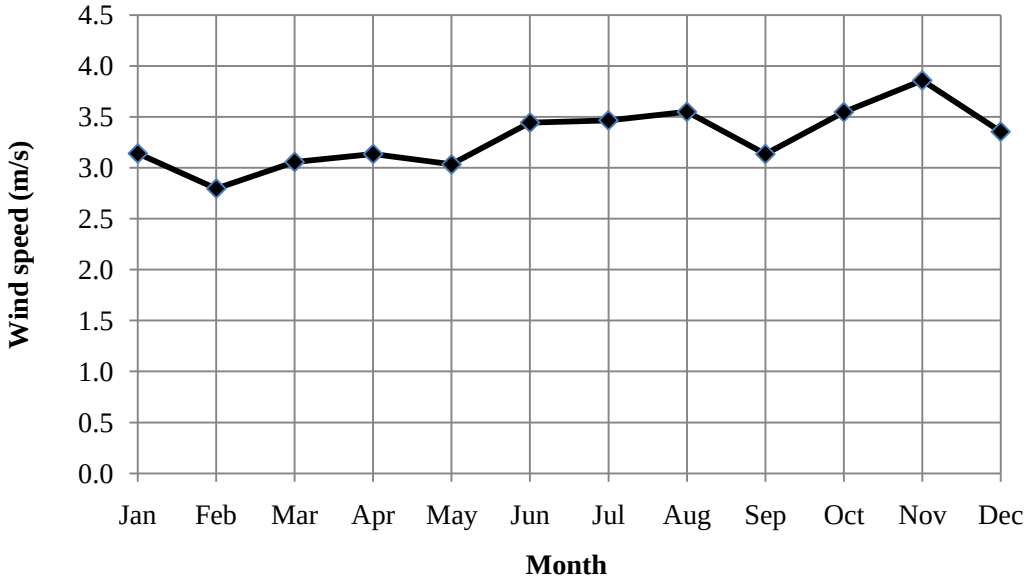

Figure 4.14 Wind speed for difference mouths

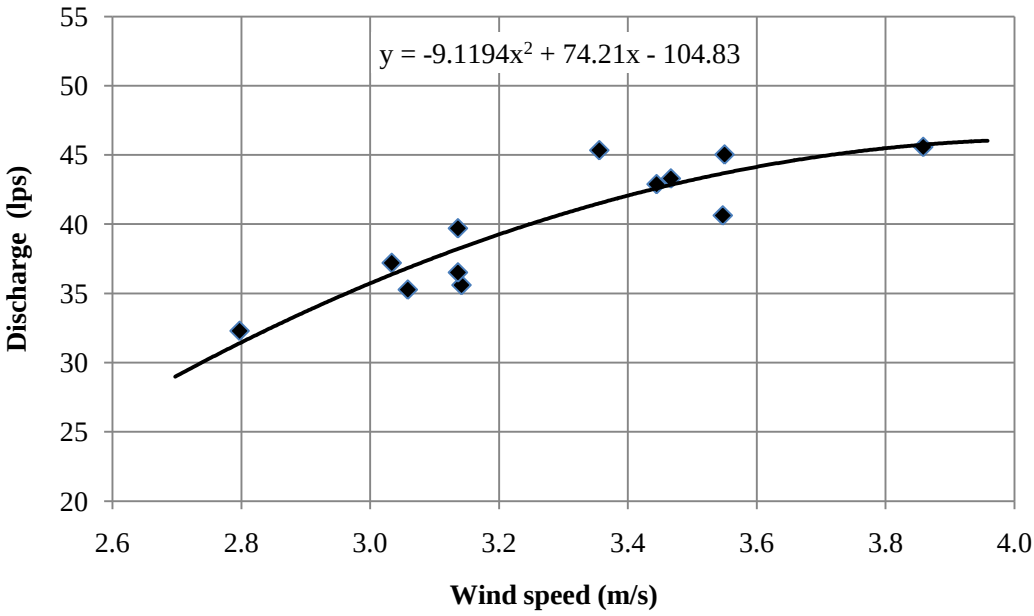

Figure 4.15 Wind speed versus discharge curve

4.2 Laboratory scale of Thai sail rotor model testing

The performance of the TSRM depends on the different parameters like number of blades, geometry of the blades. The best way of optimizing the various parameters is to carryout number of experiments on the different types of rotors in a low-speed open test section wind tunnel. The experiments have been conducted with a total of 17 different types of rotors by varying number of blades, four blades, six blades, eight blades and twelve blades, and varying size of the blades to optimize the Thai sail rotor model.

4.2.1 Thai sail rotor model four blades testing

The power coefficient (Cp) and Tip speed ratio (TSR) for varying between 1 to 5 m/s are shown in Figure 4.16 to Figure 4.20 for the TSRM four blades; 4B-T1, 4B-T2, 4B-T3, 4B-T4, and 4B-T5.

The torque coefficient (Cq) and Tip speed ratio (TSR) for varying between 1 to 5 m/s are shown in Figure 4.21 to Figure 4.25 for the TSRM four blades; 4B-T1, 4B-T2, 4B-T3, 4B-T4, and 4B-T5.

It can be observed that for the five models tested, the optimum power coefficient (Cp) occurs at tip speed ratio (TSR) of about 1.1 as shown in Figure 4.17. The TSRM 4B-T2 rotor solidity of 0.23 gives the highest power coefficient (Cp), as shown in Figure 4.26. The corresponding Cp for the five model is 0.085, 0.11, 0.10, 0.085 and 0.04 respectively.

The optimum torque coefficient (Cq) occurs at tip speed ratio (TSR) of about 0.5 as shown in Figure 4.22. Similarly TSRM 4B-T2 rotor solidity of 0.23 gives the higher optimum torque coefficient (Cq). The corresponding Cq for the five model is 0.07, 0.08, 0.09, 0.08 and 0.05 respectively.

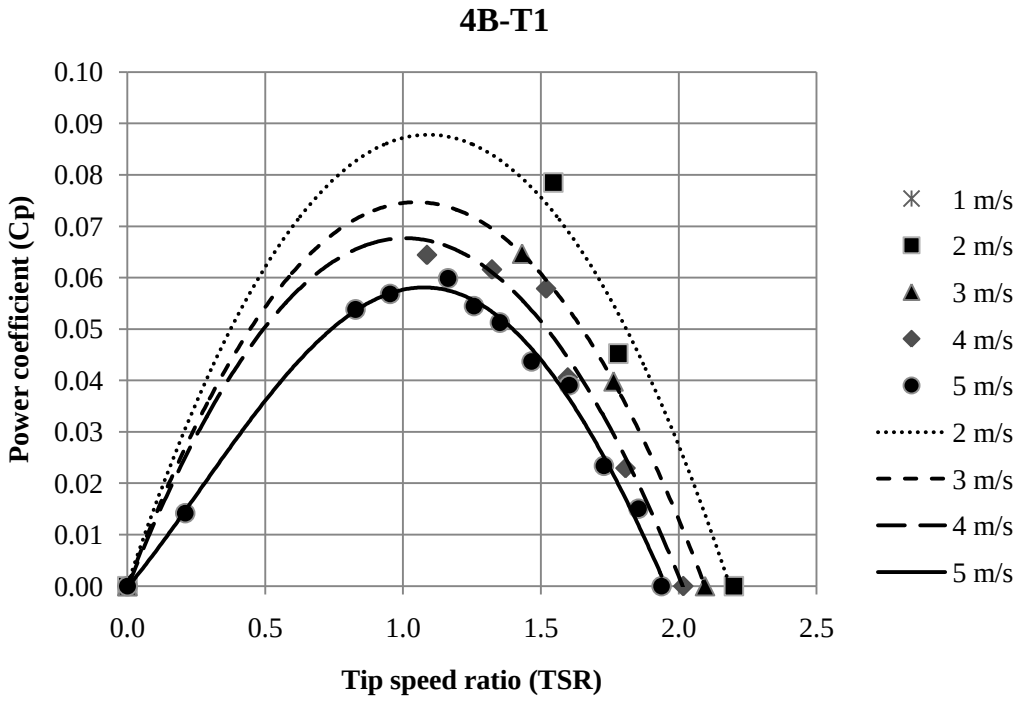

Figure 4.16 Relationship between power coefficient (Cp) and tip speed ratio (TSR) of TSRM 4B-T1 at wind speed 1-5 m/s

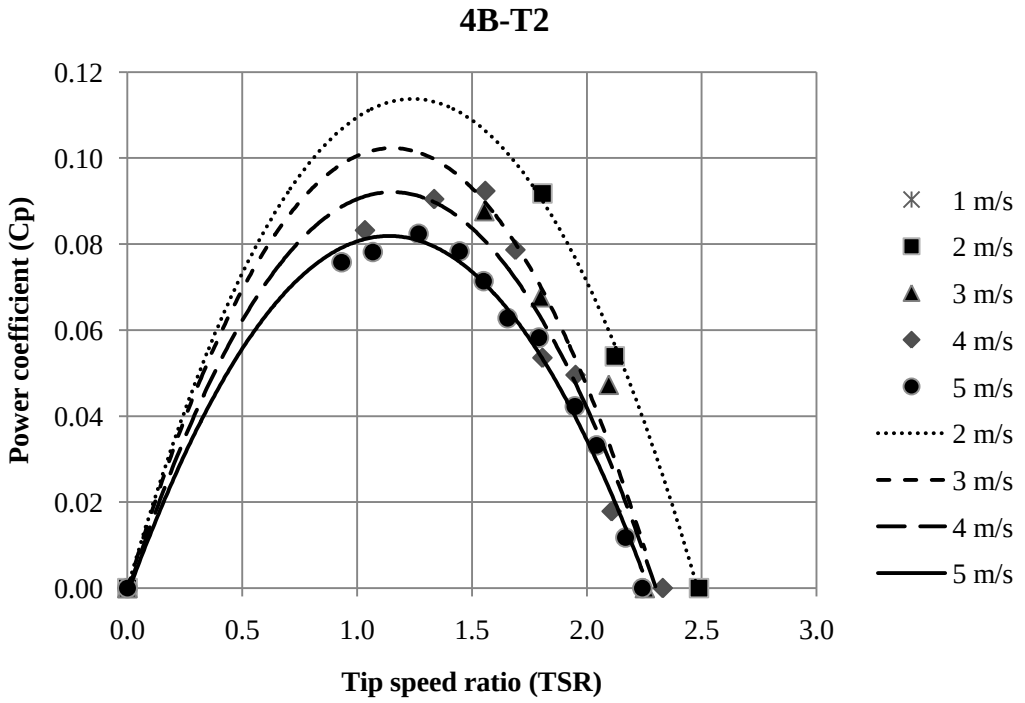

Figure 4.17 Relationship between power coefficient (Cp) and tip speed ratio (TSR) of TSRM 4B-T2 at wind speed 1-5 m/s

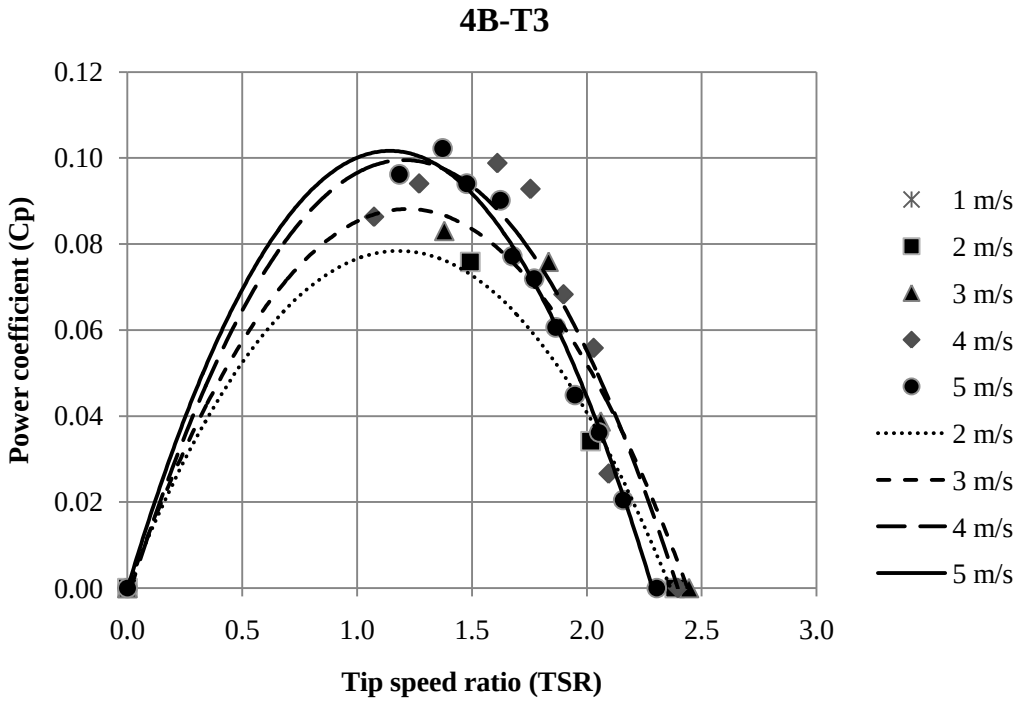

Figure 4.18 Relationship between power coefficient (Cp) and tip speed ratio (TSR) of TSRM 4B-T3 at wind speed 1-5 m/s

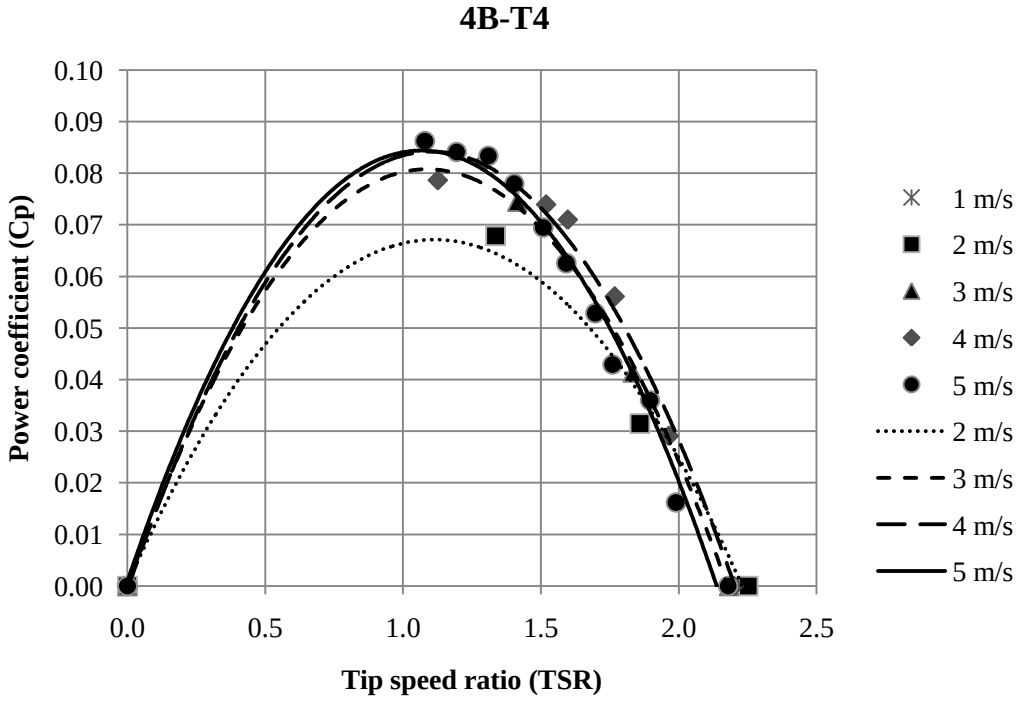

Figure 4.19 Relationship between power coefficient (Cp) and tip speed ratio (TSR) of TSRM 4B-T4 at wind speed 1-5 m/s

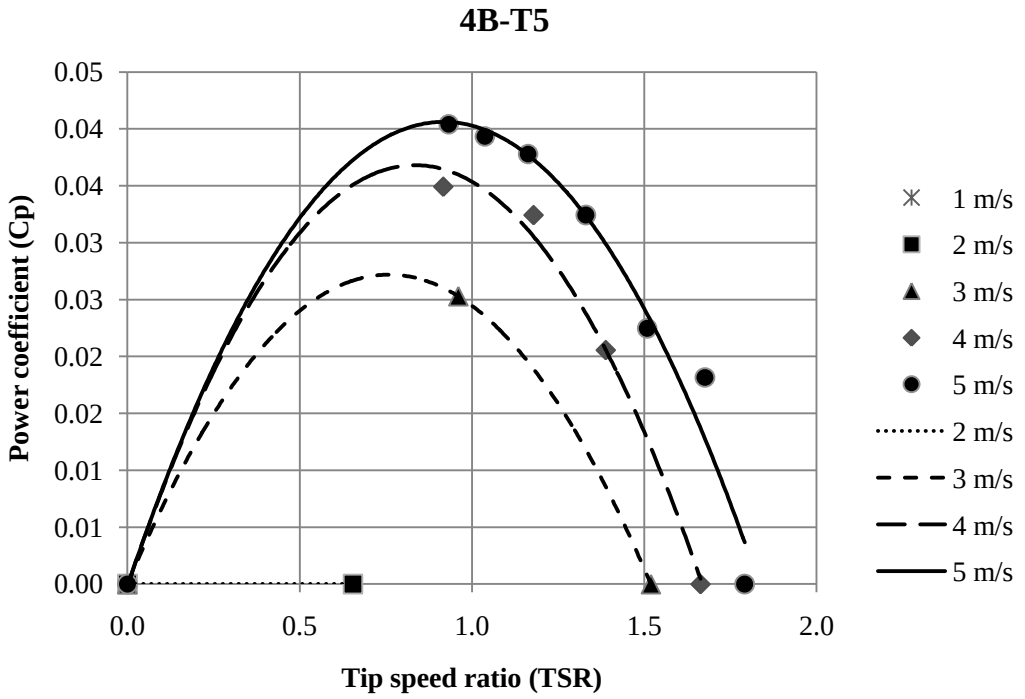

Figure 4.20 Relationship between power coefficient (Cp) and tip speed ratio (TSR) of TSRM 4B-T5 at wind speed 1-5 m/s

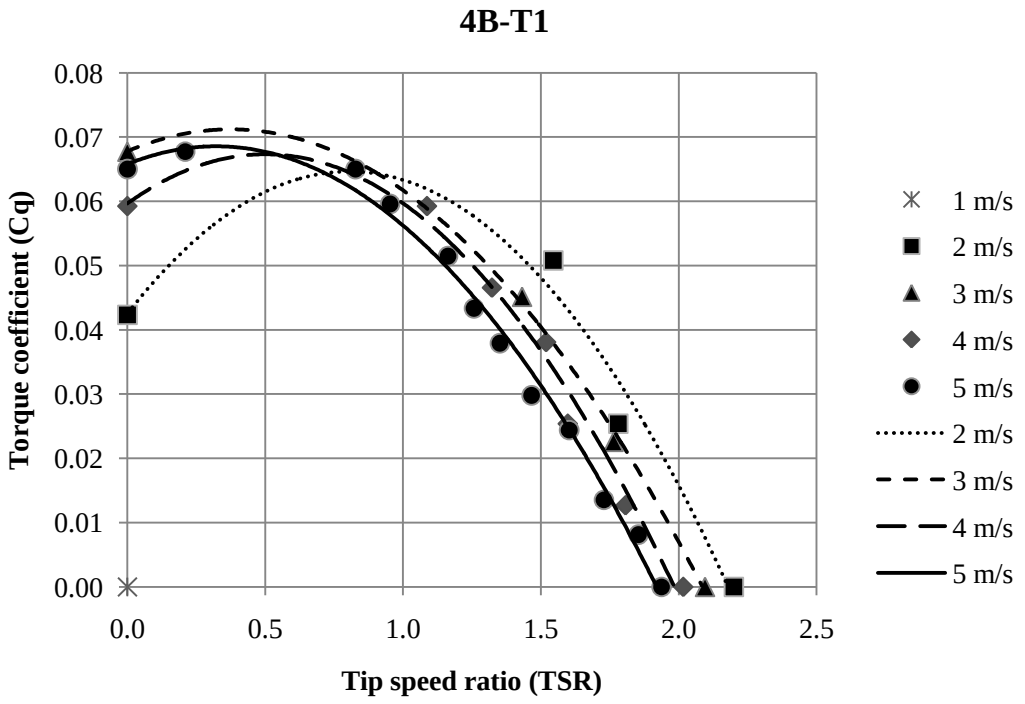

Figure 4.21 Relationship between torque coefficient (Cq) and tip speed ratio (TSR) of TSRM 4B-T1 at wind speed 1-5 m/s

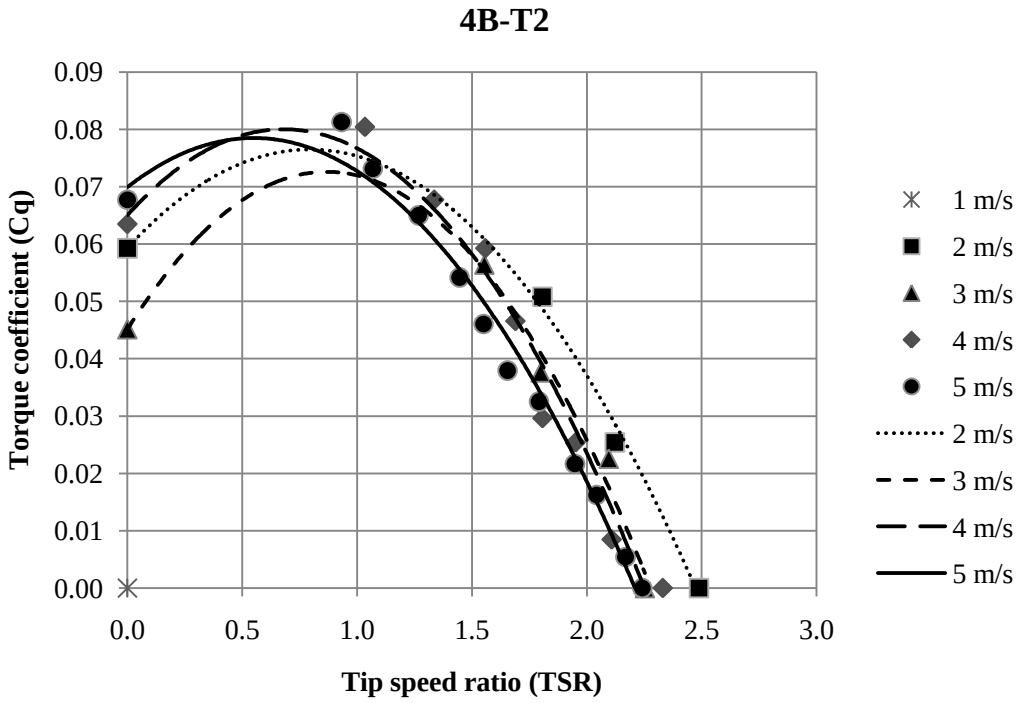

Figure 4.22 Relationship between torque coefficient (Cq) and tip speed ratio (TSR) of TSRM 4B-T2 at wind speed 1-5 m/s

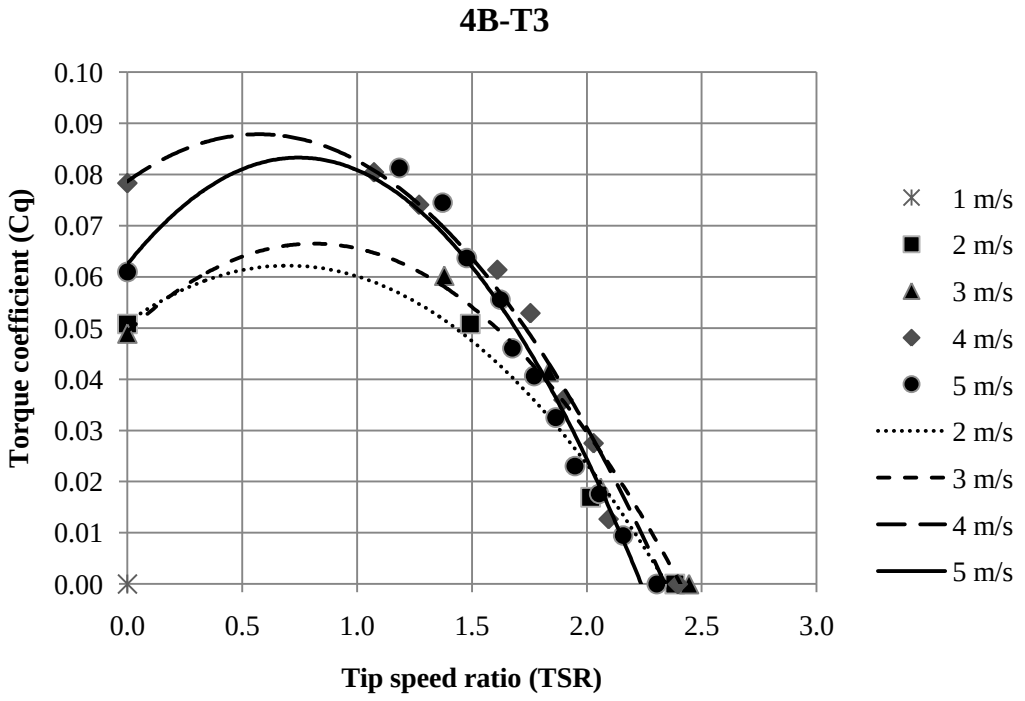

Figure 4.23 Relationship between torque coefficient (Cq) and tip speed ratio (TSR) of TSRM 4B-T3 at wind speed 1-5 m/s

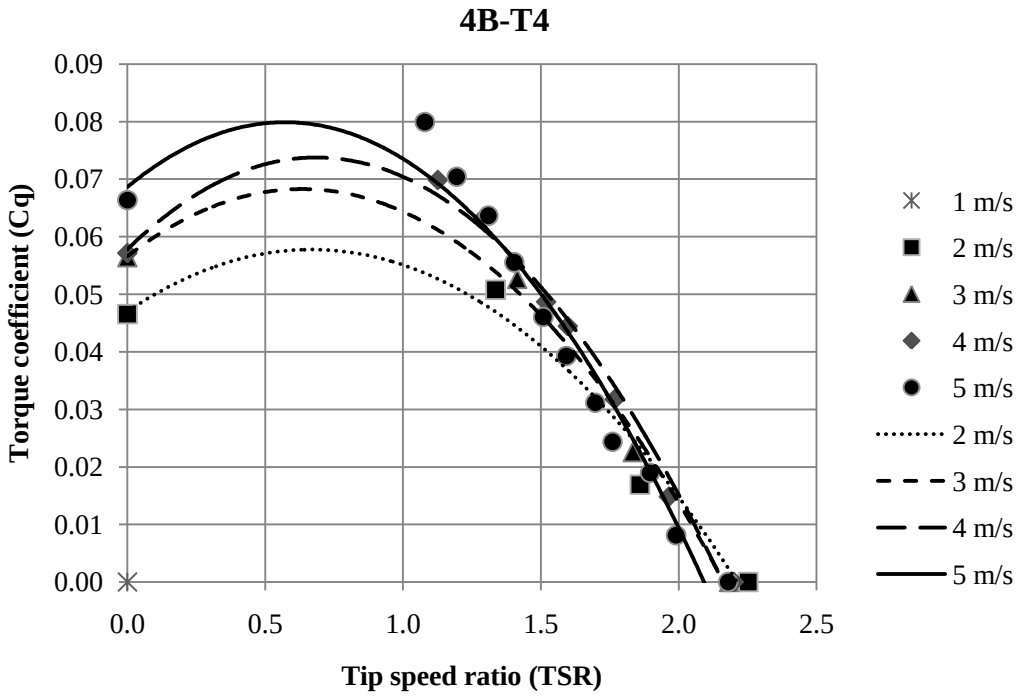

Figure 4.24 Relationship between torque coefficient (Cq) and tip speed ratio (TSR) of TSRM 4B-T4 at wind speed 1-5 m/s

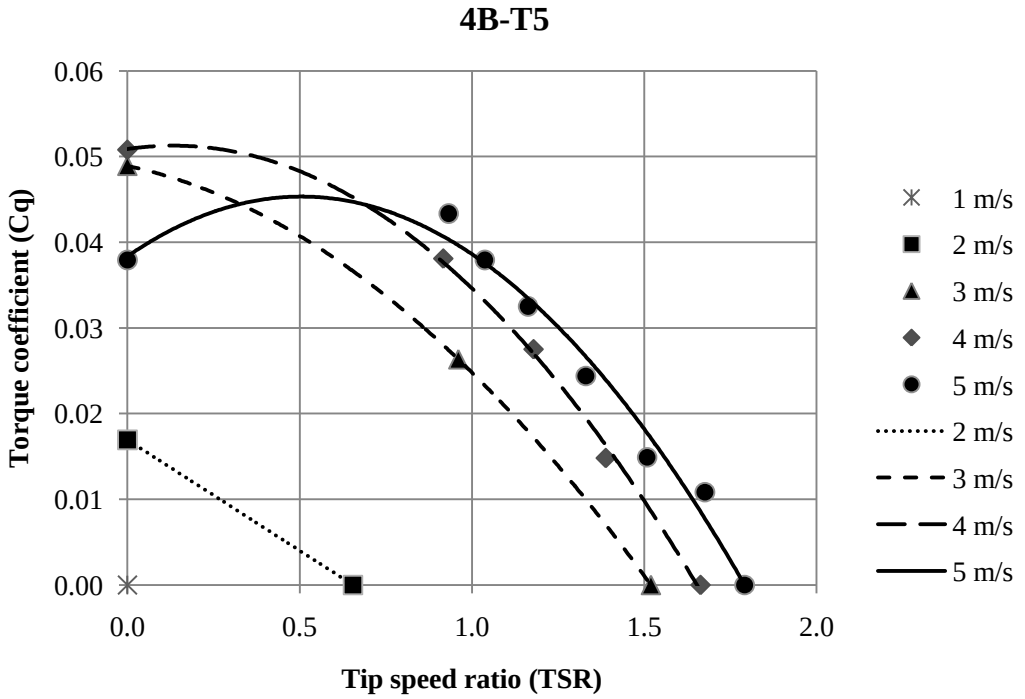

Figure 4.25 Relationship between torque coefficient (Cq) and tip speed ratio (TSR) of TSRM 4B-T5 at wind speed 1-5 m/s

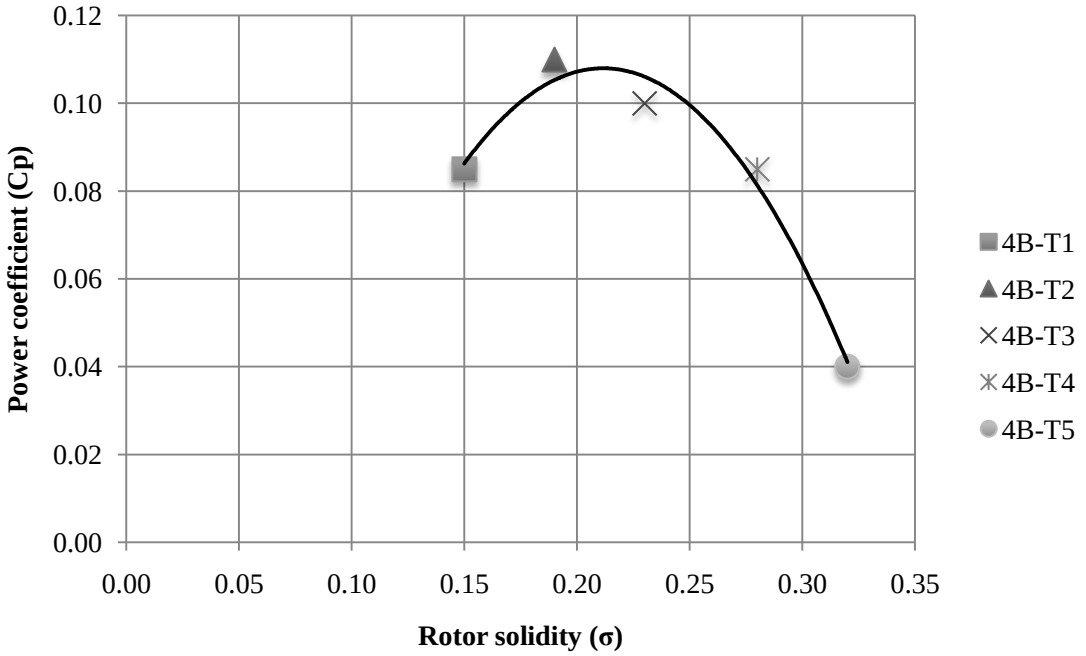

Figure 4.26 Relationship between rotor solidity (σ) and power coefficient (Cp) of TSRM 4B-T1-T2-T3-T4-T5

4.2.2 Thai sail rotor model six blades testing

The power coefficient (Cp) and Tip speed ratio (TSR) for varying between 1 to 5 m/s are shown in Figure 4.27 to Figure 4.35 for the TSRM six blades; 6B-T0, 6B-T1:10°, 6B-T1:15°, 6B-T1:20°, 6B-T2, 6B-T3, 6B-T4, and 6B-T5.

The torque coefficient (Cq) and Tip speed ratio (TSR) for varying between 1 to 5 m/s are shown in Figure 4.36 to Figure 4.44 for the TSRM six blades; 6B-T0, 6B-T1:10°, 6B-T1:15°, 6B-T1:20°, 6B-T2, 6B-T3, 6B-T4, and 6B-T5.

It can be observed that for the six models tested, the optimum power coefficient (Cp) occurs at tip speed ratio (TSR) of about 1.2 as shown in Figure 4.33. The TSRM 6B-T3 rotor solidity of 0.38 gives the highest power coefficient (Cp), as shown in Figure 4.45. The corresponding Cp for the three model is 0.11, 0.12, 0.11, 0.08, 0.09, 0.11, 0.09, and 0.075 respectively.

The optimum torque coefficient (Cq) occurs at tip speed ratio (TSR) of about 0.5 as shown in Figure 4.42. Similarly TSRM 6B-T3 rotor solidity of 0.38 gives the higher optimum torque coefficient (Cq). The corresponding Cq for the three model is 0.11, 0.13, 0.12, 0.12, 0.12, 0.11, 0.11 and 0.11 respectively.

The model tests the optimum power when the degree of sail blade is 15° better than 10° and 20° are shown in Figure 4.28 to Figure 4.31. Based on this testing, the optimum power coefficient (Cp) of TSRM 6B-T1 degree of sail blade is 10°, TSRM 6B-T1 degree of sail blade is 15° and TSRM 6B-T1 degree of sail blade is 20° model are recommended to used degree of sail blade about 15° or moderate degree of sail blade for testing and used for development of the new generation of Thai sail windmill.

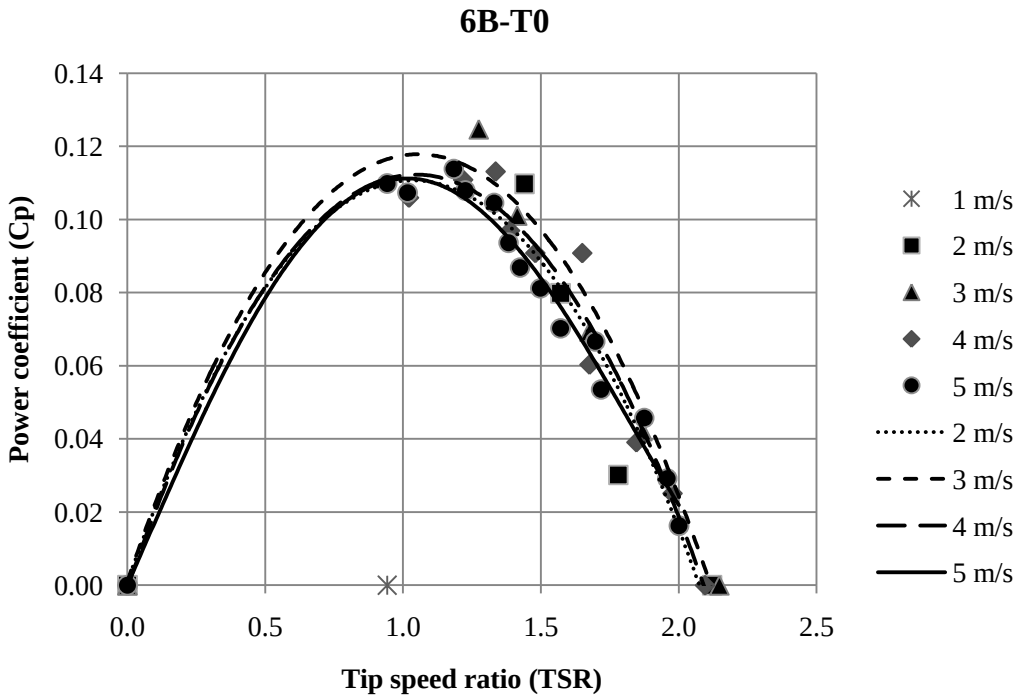

Figure 4.27 Relationship between power coefficient (Cp) and tip speed ratio (TSR) of TSRM 6B-T0 at wind speed 1-5 m/s

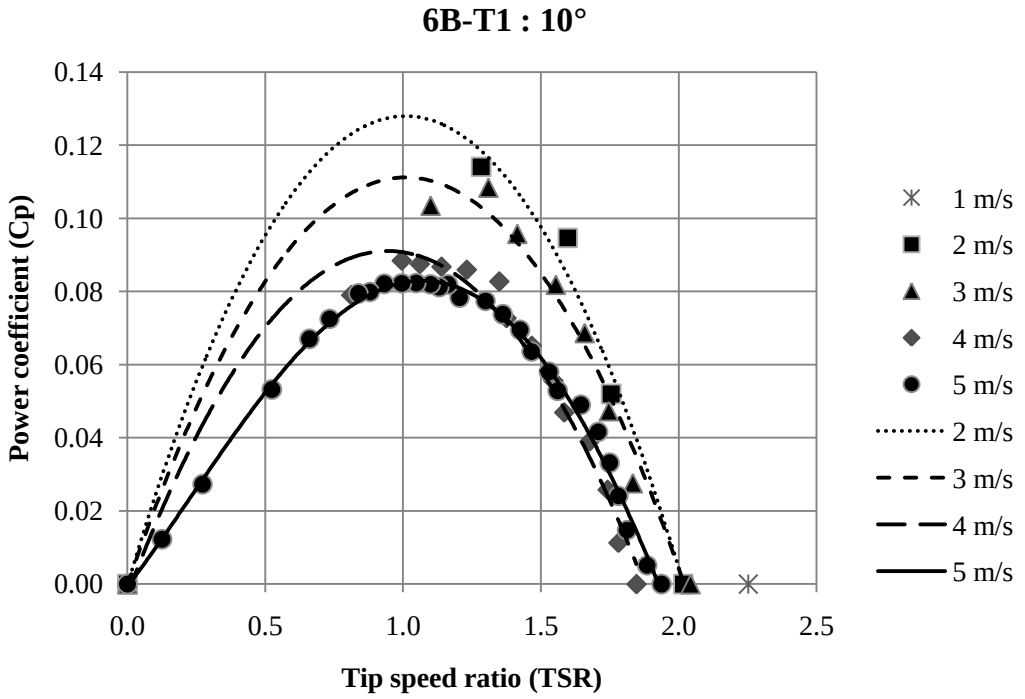

Figure 4.28 Relationship between power coefficient (Cp) and tip speed ratio (TSR) of TSRM 6B-T1 degree of sail blade 10° at wind speed 1-5 m/s

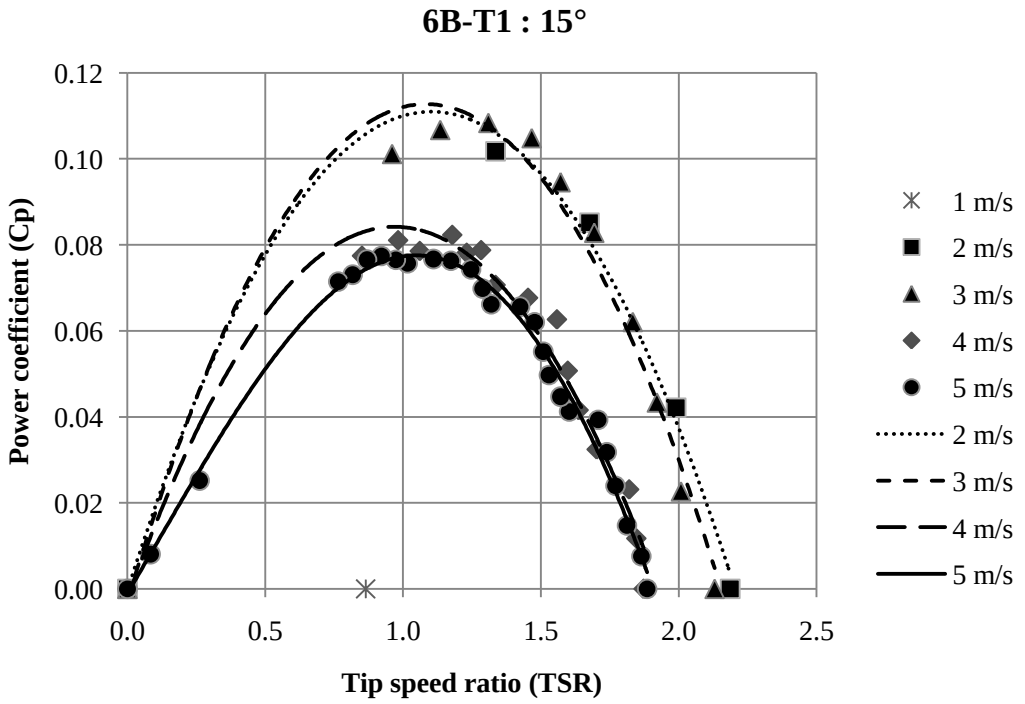

Figure 4.29 Relationship between power coefficient (Cp) and tip speed ratio (TSR) of TSRM 6B-T1 degree of sail blade 15° at wind speed 1-5 m/s

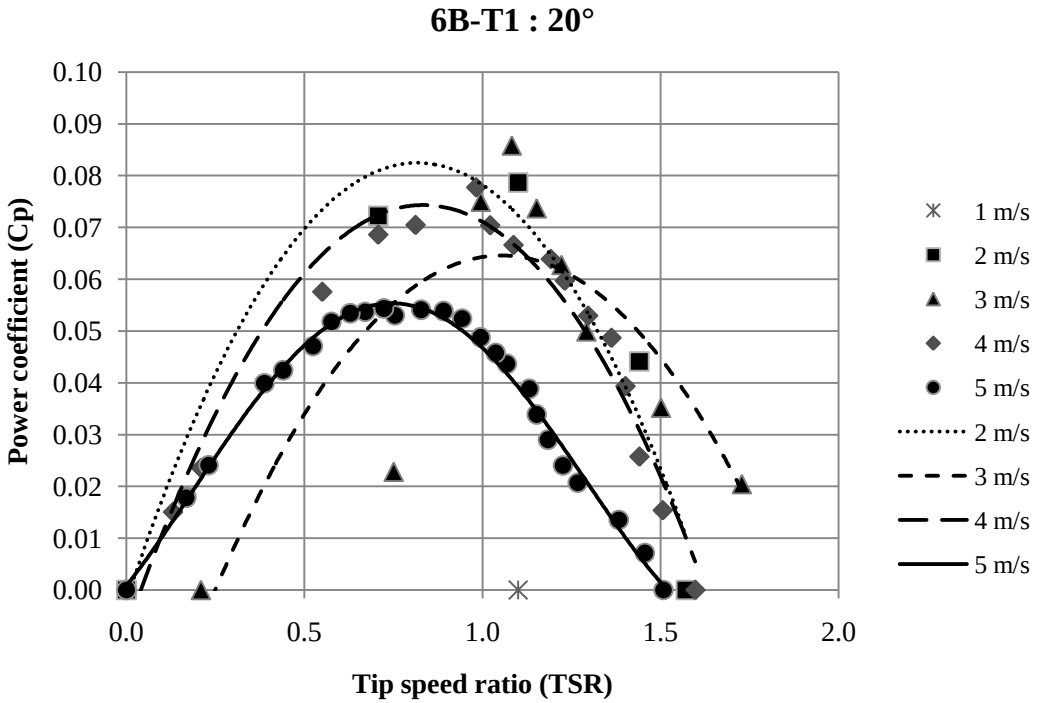

Figure 4.30 Relationship between power coefficient (Cp) and tip speed ratio (TSR) of TSRM 6B-T1 degree of sail blade 20° at wind speed 1-5 m/s

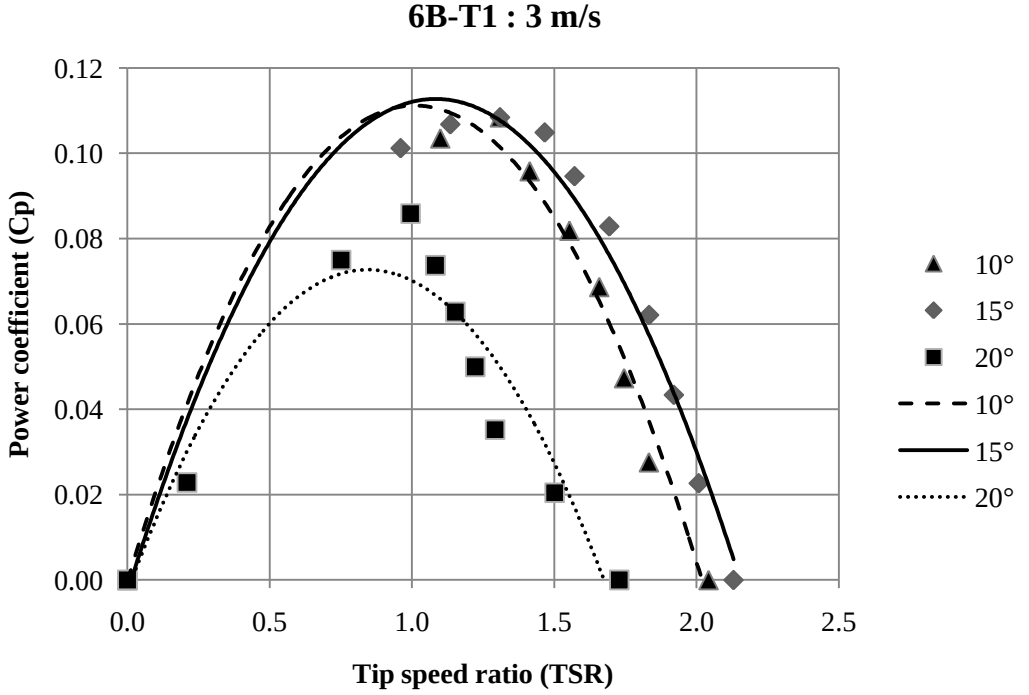

Figure 4.31 Relationship between power coefficient (Cp) and tip speed ratio (TSR) of TSRM 6B-T1 degree of sail blade 10°, 15°, 20° at wind speed 3 m/s

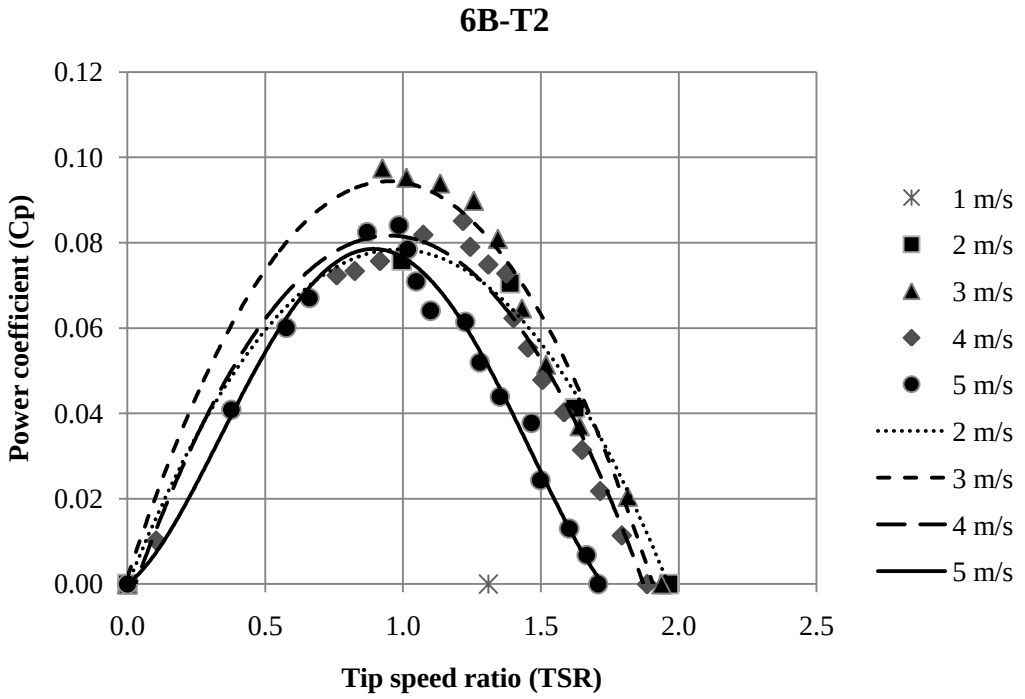

Figure 4.32 Relationship between power coefficient (Cp) and tip speed ratio (TSR) of TSRM 6B-T2 at wind speed 1-5 m/s

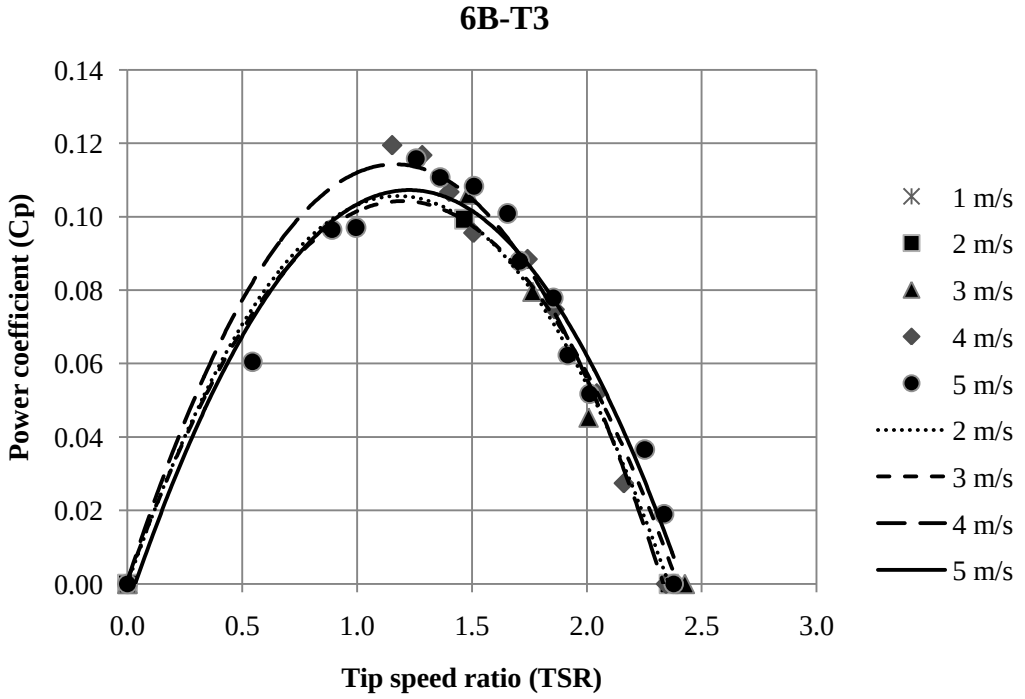

Figure 4.33 Relationship between power coefficient (Cp) and tip speed ratio (TSR) of TSRM 6B-T3 at wind speed 1-5 m/s

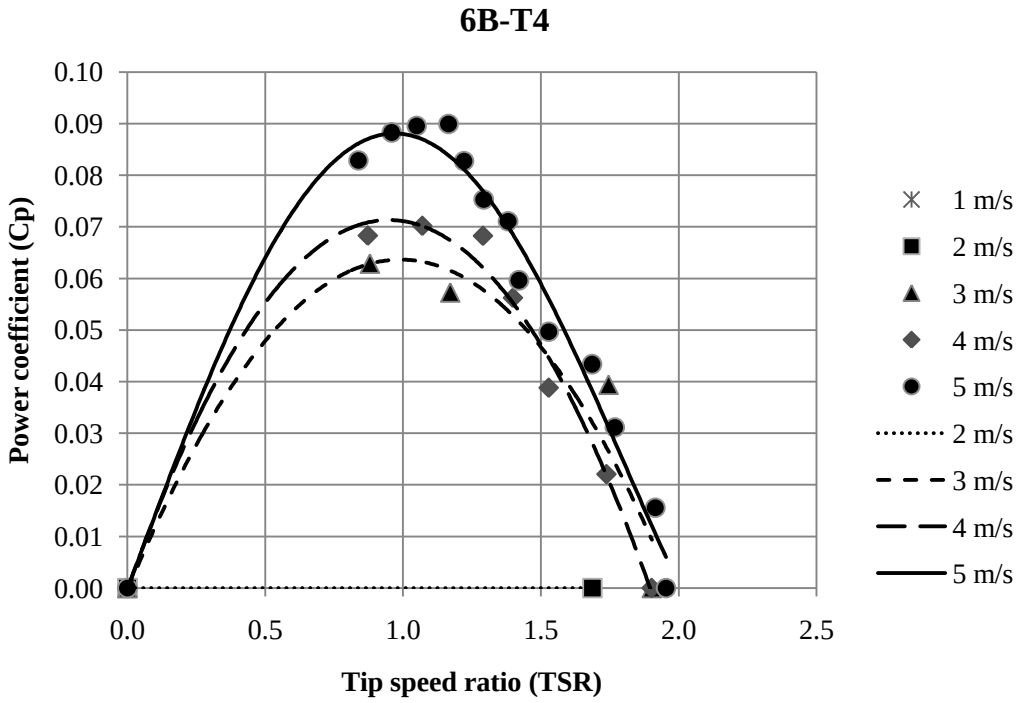

Figure 4.34 Relationship between power coefficient (Cp) and tip speed ratio (TSR) of TSRM 6B-T4 at wind speed 1-5 m/s

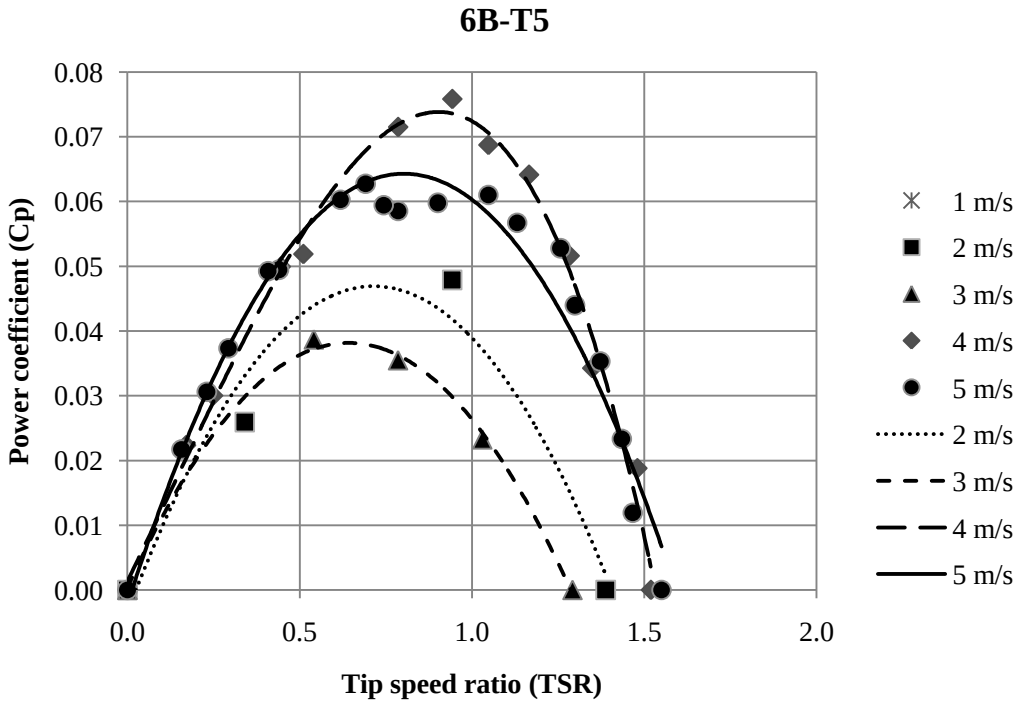

Figure 4.35 Relationship between power coefficient (Cp) and tip speed ratio (TSR) of TSRM 6B-T5 at wind speed 1-5 m/s

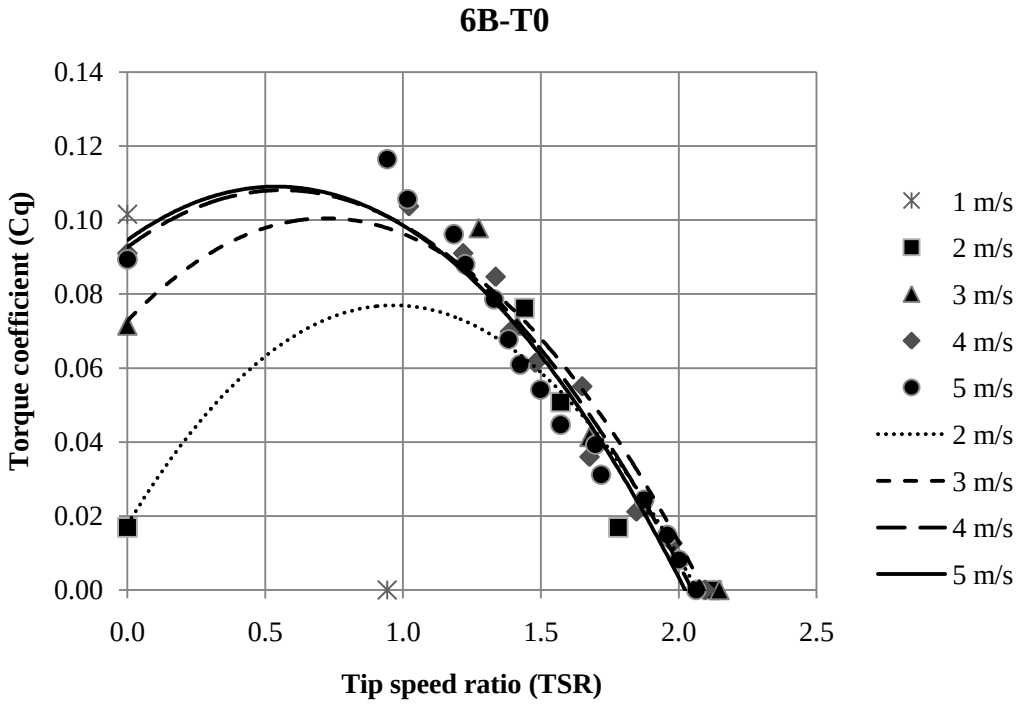

Figure 4.36 Relationship between torque coefficient (Cq) and tip speed ratio (TSR) of TSRM 6B-T0 at wind speed 1-5 m/s

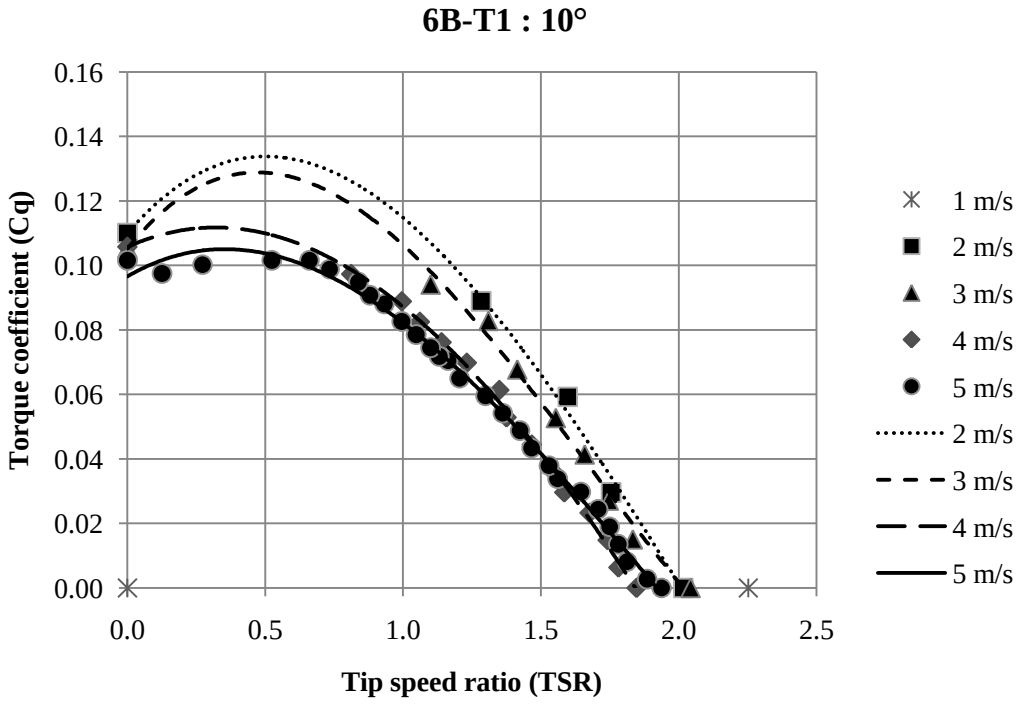

Figure 4.37 Relationship between torque coefficient (Cq) and tip speed ratio (TSR) of TSRM 6B-T1 at wind speed 1-5 m/s of 10°

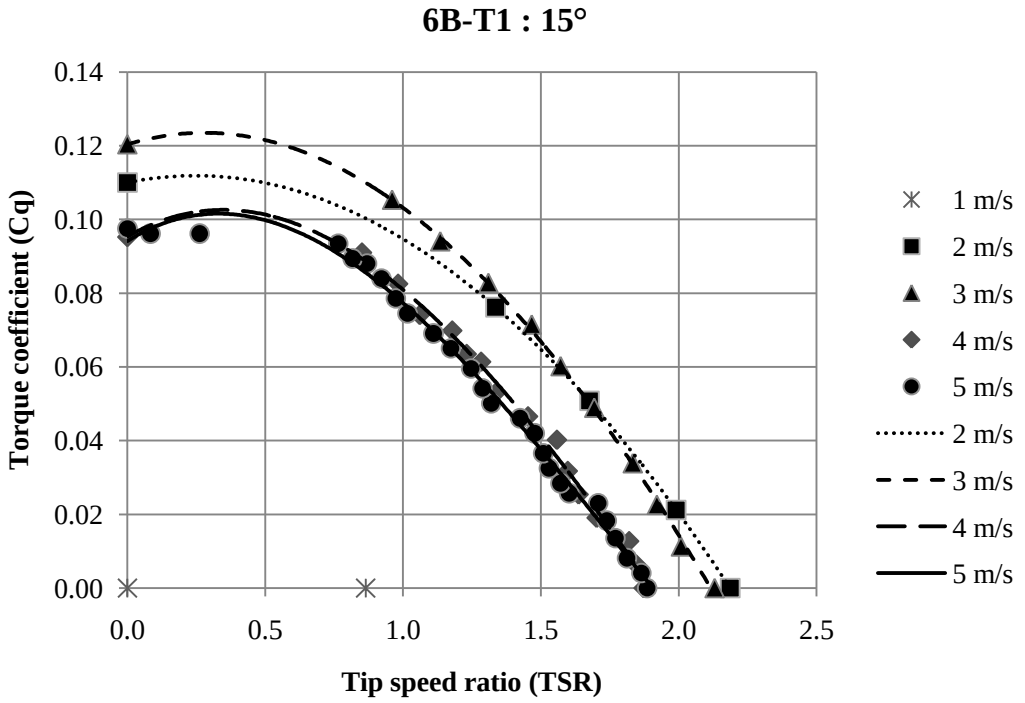

Figure 4.38 Relationship between torque coefficient (Cq) and tip speed ratio (TSR) of TSRM 6B-T1 at wind speed 1-5 m/s of 15°

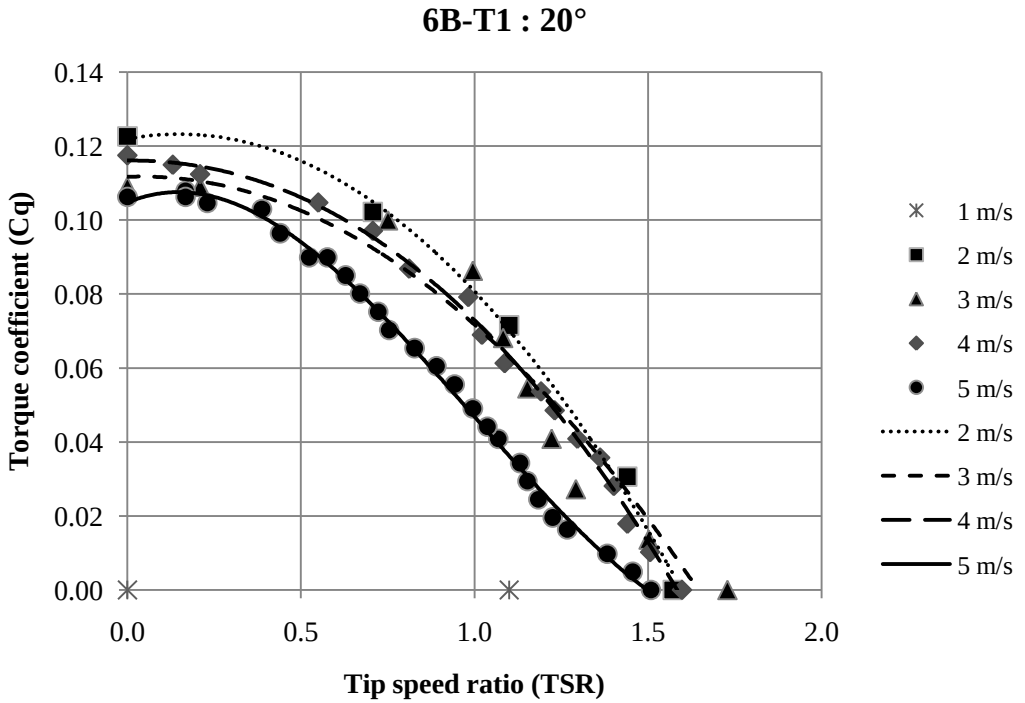

Figure 4.39 Relationship between torque coefficient (Cq) and tip speed ratio (TSR) of TSRM 6B-T1 at wind speed 1-5 m/s of 20°

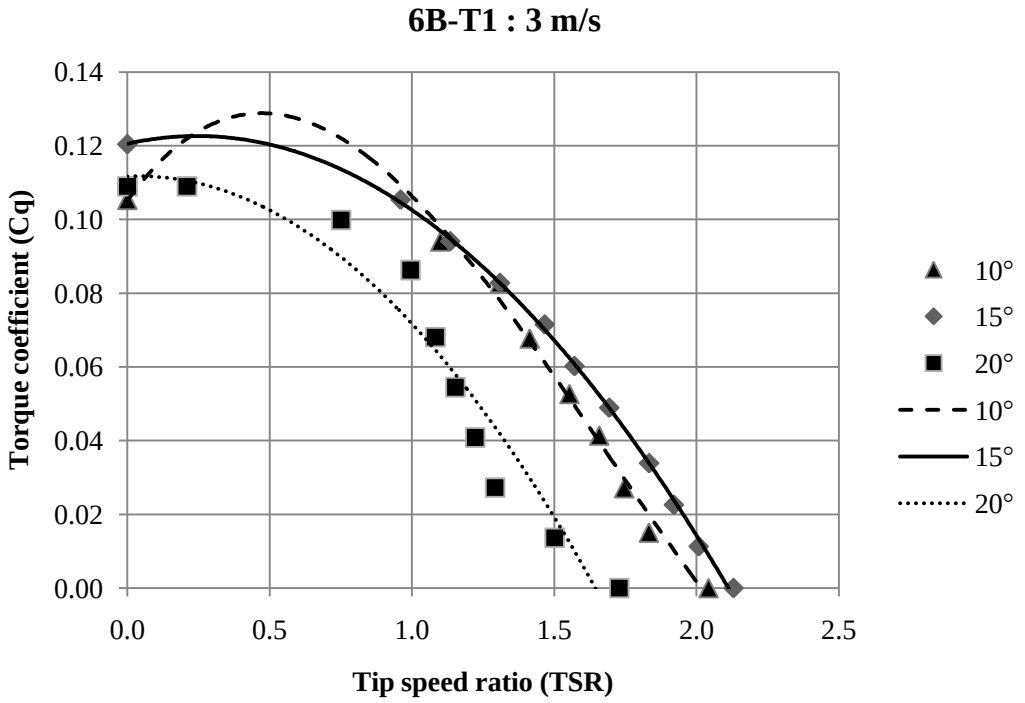

Figure 4.40 Relationship between torque coefficient (Cq) and tip speed ratio (TSR) of TSRM 6B-T1 degree of sail blade 10°, 15°, 20° at wind speed 3 m/s

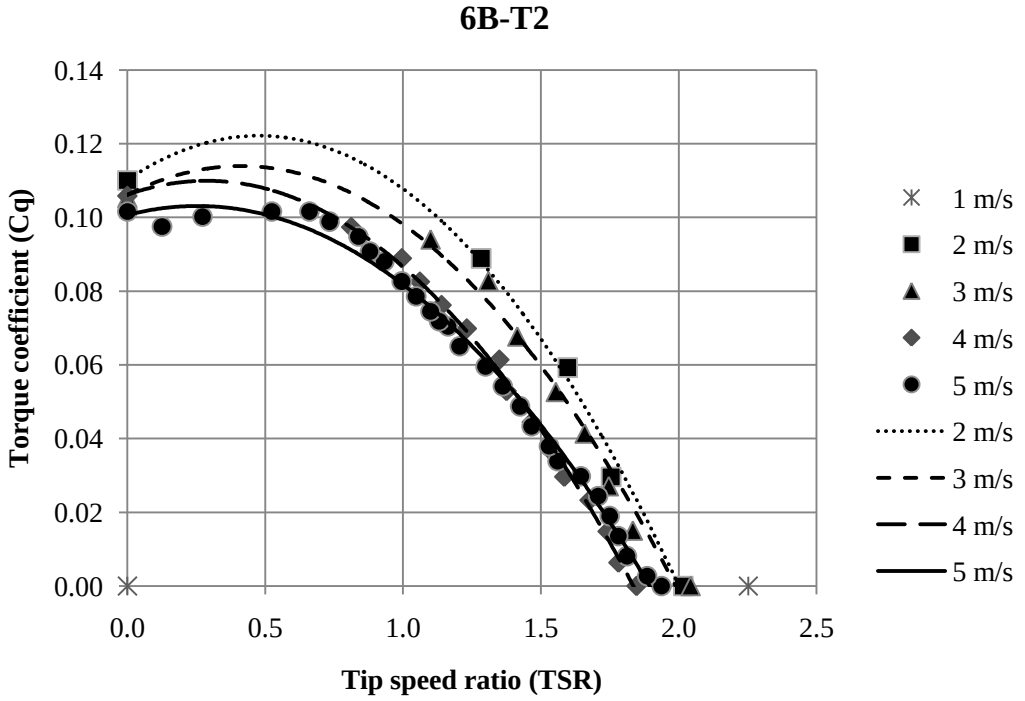

Figure 4.41 Relationship between torque coefficient (Cq) and tip speed ratio (TSR) of TSRM 6B-T2 at wind speed 1-5 m/s

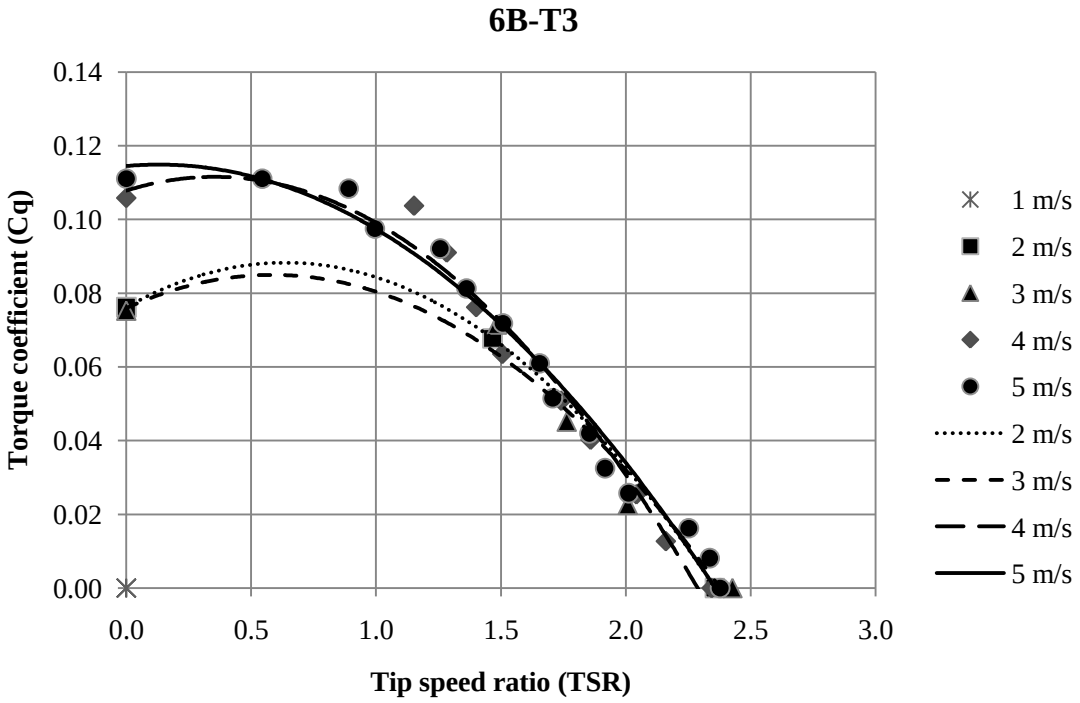

Figure 4.42 Relationship between torque coefficient (Cq) and tip speed ratio (TSR) of TSRM 6B-T3 at wind speed 1-5 m/s

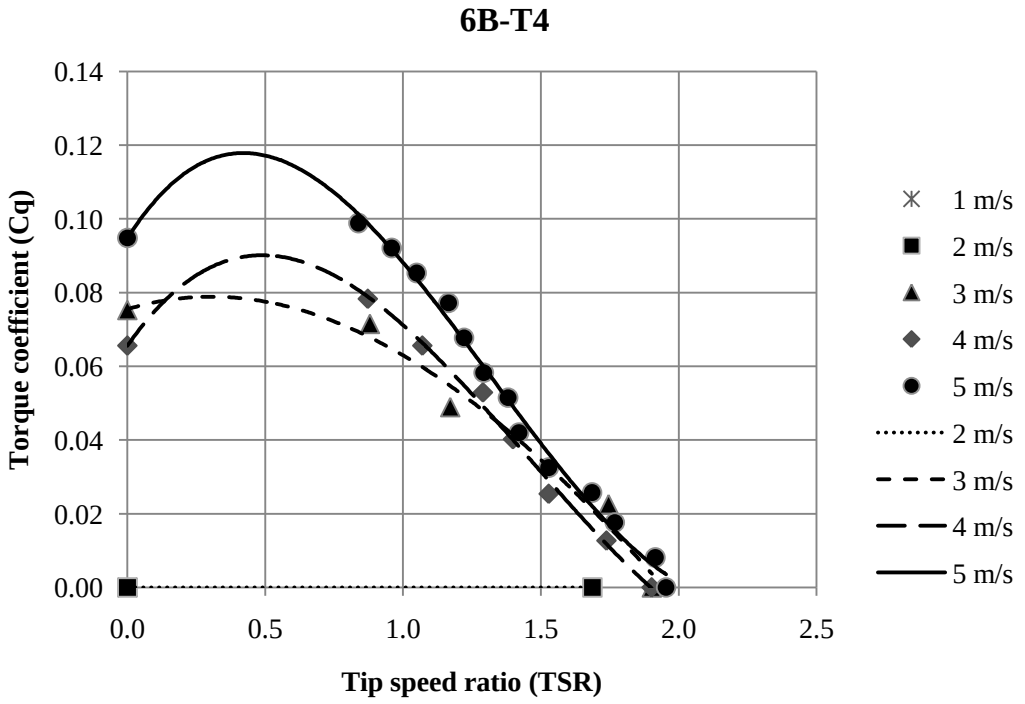

Figure 4.43 Relationship between torque coefficient (Cq) and tip speed ratio (TSR) of TSRM 6B-T4 at wind speed 1-5 m/s

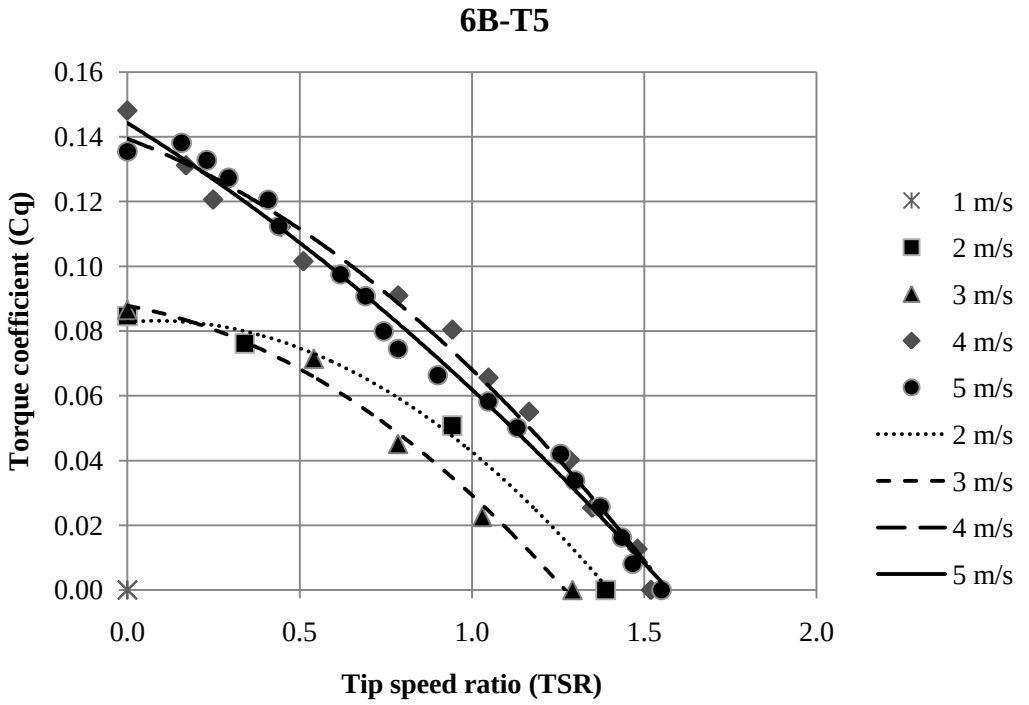

Figure 4.44 Relationship between torque coefficient (Cq) and tip speed ratio (TSR) of TSRM 6B-T5 at wind speed 1-5 m/s

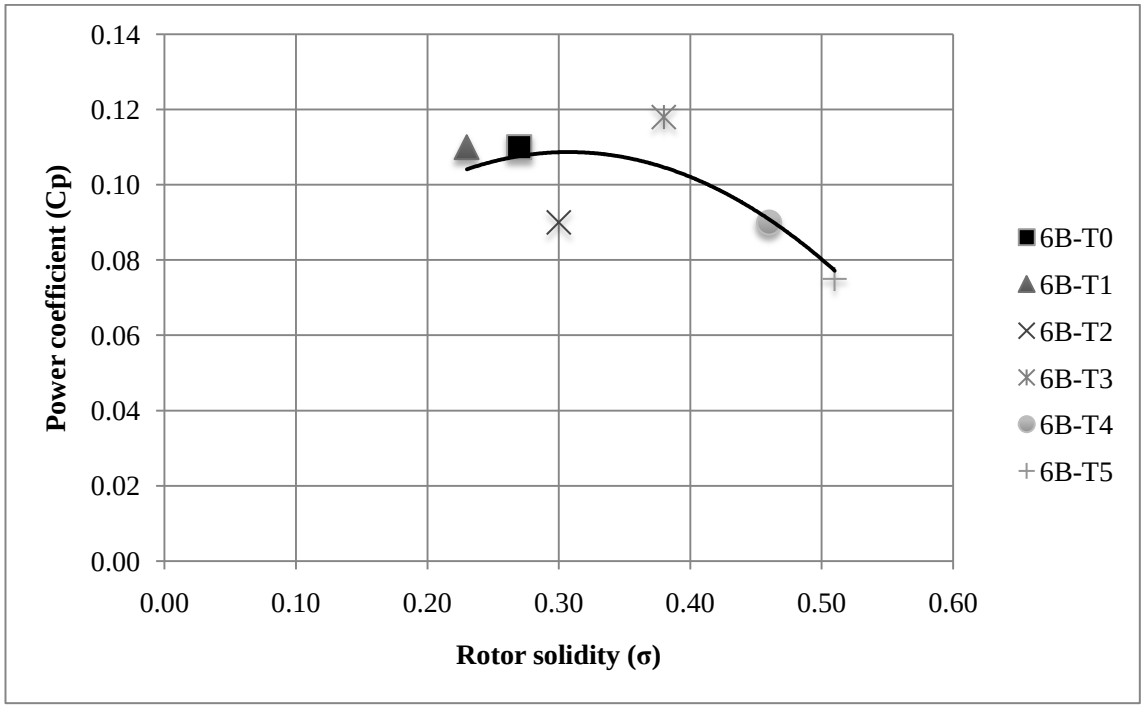

Figure 4.45 Relationship between rotor solidity (σ) and power coefficient (Cp) of TSRM 6B-T0-T1-T2-T3-T4-T5

4.2.3 Thai sail rotor model eight blades testing

The power coefficient (Cp) and Tip speed ratio (TSR) for varying between 1 to 5 m/s are shown in Figure 4.46 to Figure 4.48 for the TSRM eight blades; 8B-T1, 8B-T2 and 8B-T3.

The torque coefficient (Cq) and Tip speed ratio (TSR) for varying between 1 to 5 m/s are shown in Figure 4.49 to Figure 4.51 for the TSRM eight blades; 8B-T1, 8B-T2 and 8B-T3.

It can be observed that for the three models tested, the optimum power coefficient (Cp) occurs at tip speed ratio (TSR) of about 1.0 as shown in Figure 4.48. The TSRM 8B-T3 rotor solidity of 0.51 gives the highest power coefficient (Cp), as shown in Figure 4.52. The corresponding Cp for the three model is 0.10, 0.11and 0.12 respectively.

The optimum torque coefficient (Cq) occurs at tip speed ratio (TSR) of about 0.5 as shown in Figure 4.51. Similarly TSRM 8B-T3 rotor solidity of 0.51 gives the higher optimum torque coefficient (Cq). The corresponding Cq for the three model is 0.135, 0.13 and 0.16 respectively.

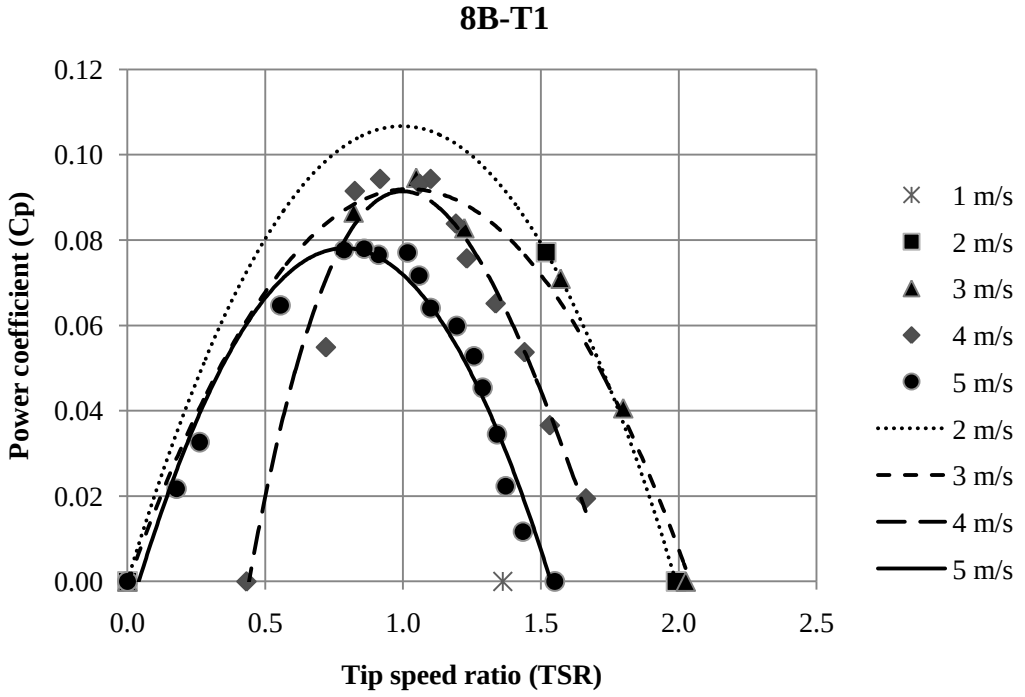

Figure 4.46 Relationship between power coefficient (Cp) and tip speed ratio (TSR) of TSRM 8B-T1 at wind speed 1-5 m/s

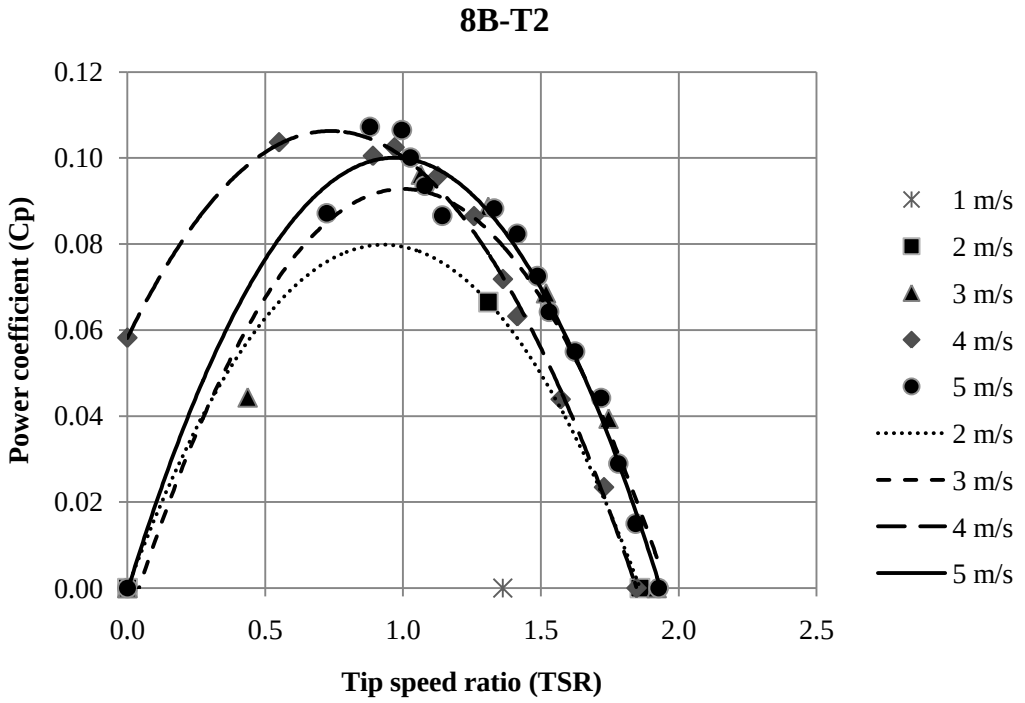

Figure 4.47 Relationship between power coefficient (Cp) and tip speed ratio (TSR) of TSRM 8B-T2 at wind speed 1-5 m/s

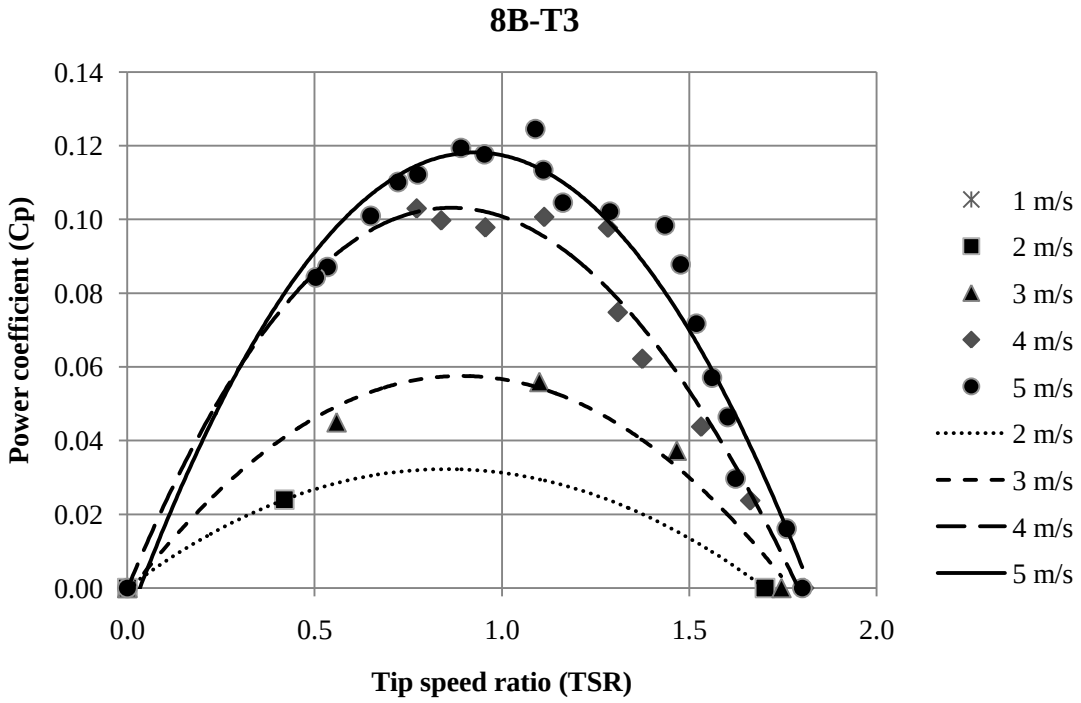

Figure 4.48 Relationship between power coefficient (Cp) and tip speed ratio (TSR) of TSRM 8B-T3 at wind speed 1-5 m/s

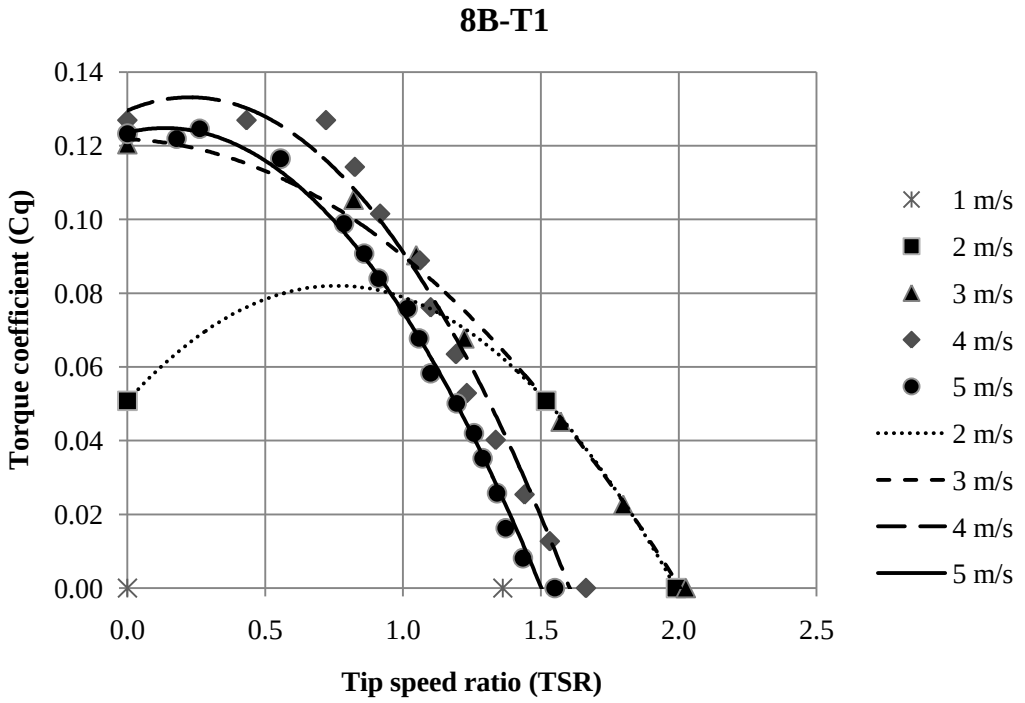

Figure 4.49 Relationship between torque coefficient (Cq) and tip speed ratio (TSR) of TSRM 8B-T1 at wind speed 1-5 m/s

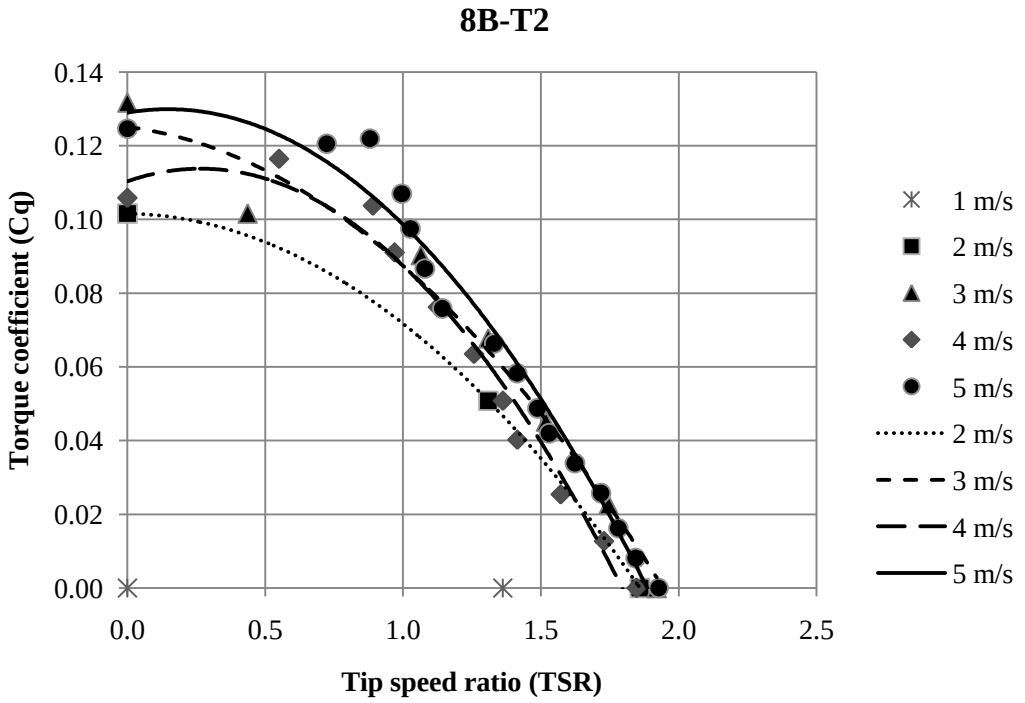

Figure 4.50 Relationship between torque coefficient (Cq) and tip speed ratio (TSR) of TSRM 8B-T2 at wind speed 1-5 m/s

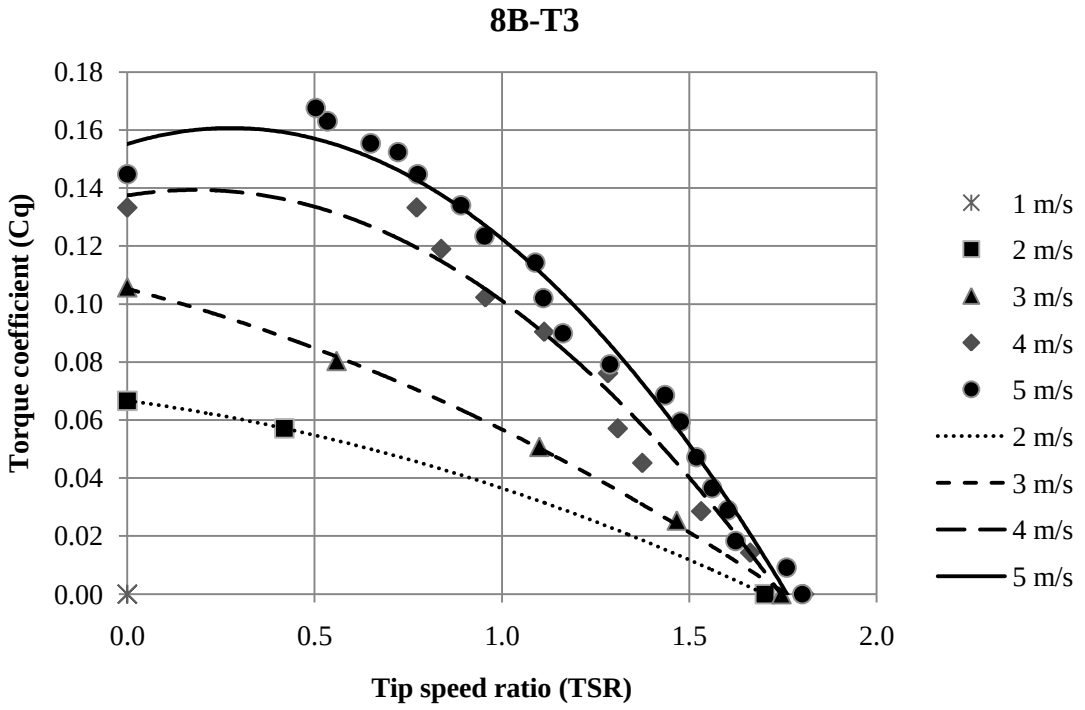

Figure 4.51 Relationship between torque coefficient (Cq) and tip speed ratio (TSR) of TSRM 8B-T3 at wind speed 1-5 m/s

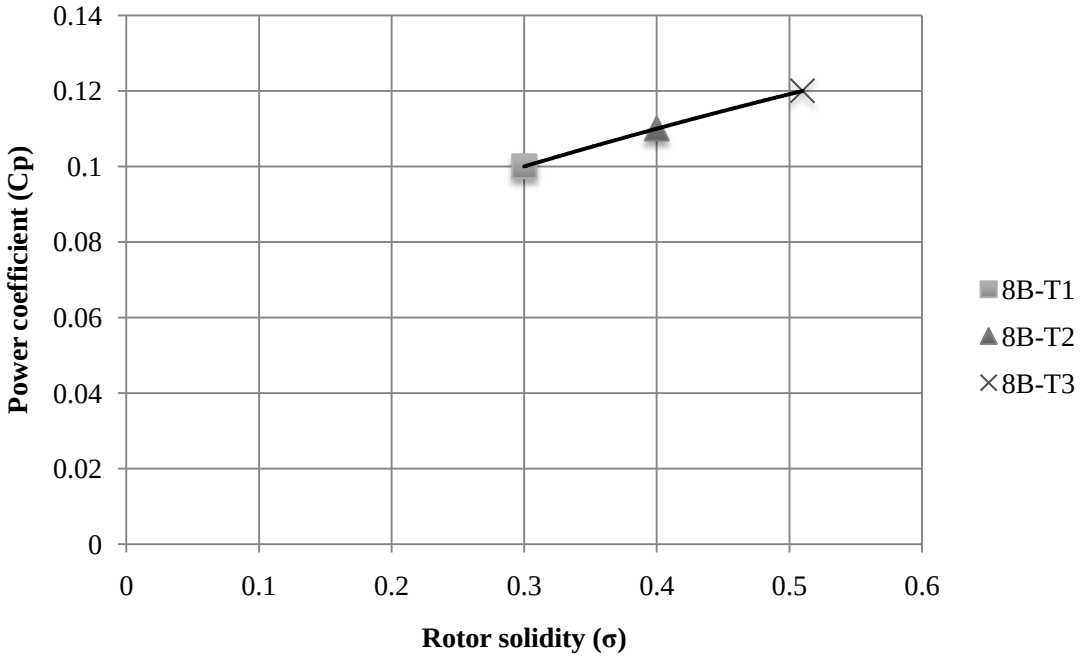

Figure 4.52 Relationship between rotor solidity (σ) and power coefficient (Cp) of TSRM 8B-T1-T2-T3

4.2.4 Thai sail rotor model twelve blades testing

The power coefficient (Cp) and Tip speed ratio (TSR) for varying between 1 to 5 m/s are shown in Figure 4.53 to Figure 4.55 for the TSRM twelve blades; 12B-T0, 12B-T1 and 12B-T2.

The torque coefficient (Cq) and Tip speed ratio (TSR) for varying between 1 to 5 m/s are shown in Figure 4.56 to Figure 4.58 for the TSRM twelve blades; 12B-T0, 12B-T1 and 12B-T2.

It can be observed that for the three models tested, the optimum power coefficient (Cp) occurs at tip speed ratio (TSR) of about 0.9 as shown in Figure 4.53. The TSRM 12B-T0 rotor solidity of 0.51 gives the highest power coefficient (Cp), as shown in Figure 5.59. The corresponding Cp for the three model is 0.16, 0.12 and 0.04 respectively.

The optimum torque coefficient (Cq) occurs at tip speed ratio (TSR) of about 0.25 as shown in Figure 4.56. Similarly TSRM 12B-T0 rotor solidity of 0.51 gives the higher optimum torque coefficient (Cq). The corresponding Cq for the three model is 0.30, 0.23 and 0.08 respectively.

Based on above conclusion for laboratory scale of Thai sail rotor model four blades, six blades, eight blades and twelve blades testing, the optimum power coefficient (Cp), the optimum torque coefficient (Cq) and the optimum solidity (σ) of TSRM 12B-T0 model are recommended for the development of the new generation of Thai sail windmill.

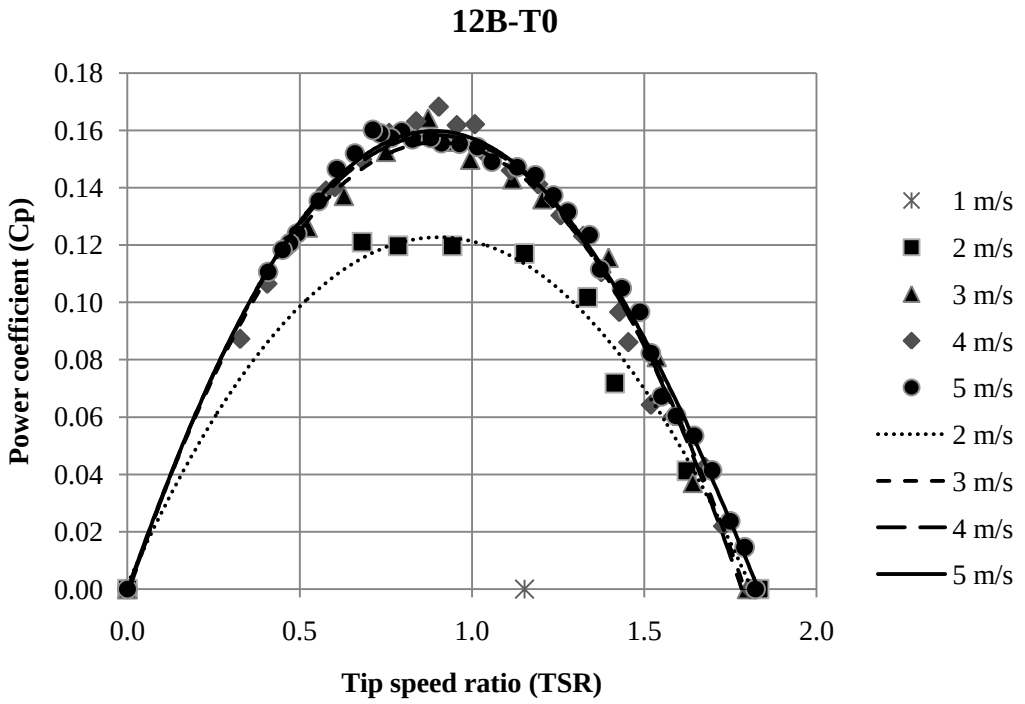

Figure 4.53 Relationship between power coefficient (Cp) and tip speed ratio (TSR) of TSRM 12B-T0 at wind speed 1-5 m/s

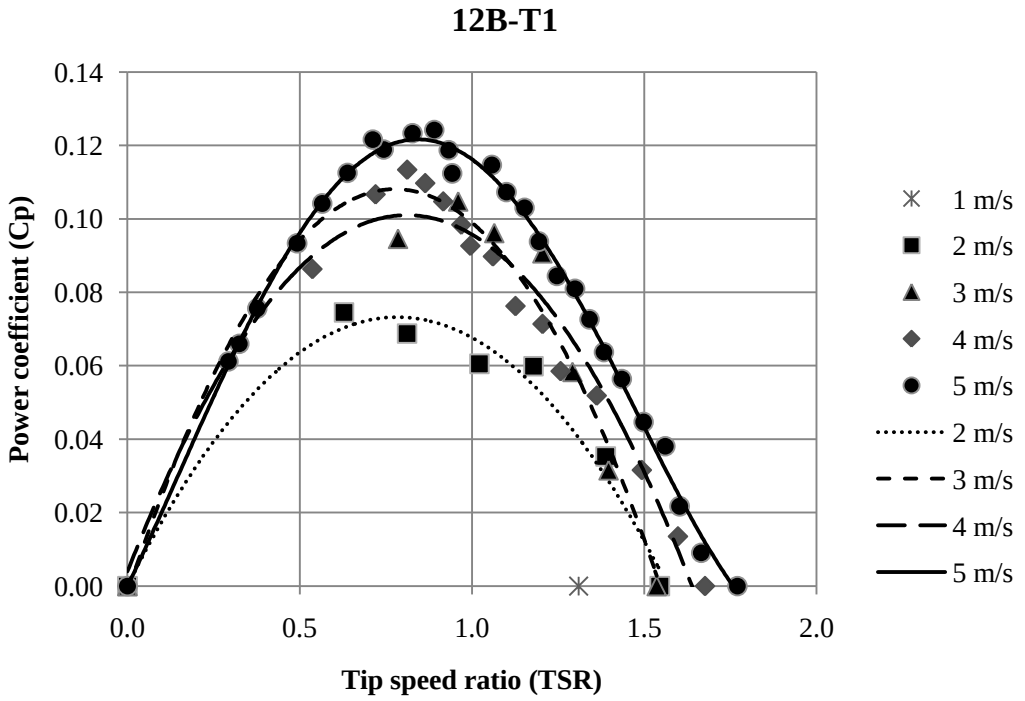

Figure 4.54 Relationship between power coefficient (Cp) and tip speed ratio (TSR) of TSRM 12B-T1 at wind speed 1-5 m/s

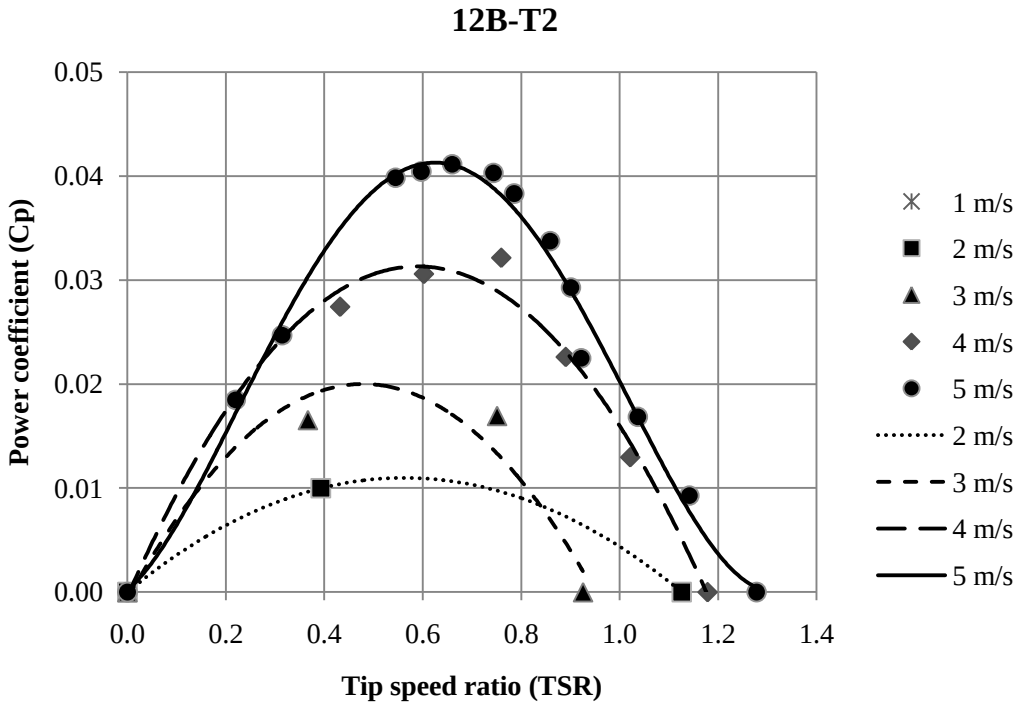

Figure 4.55 Relationship between power coefficient (Cp) and tip speed ratio (TSR) of TSRM 12B-T2 at wind speed 1-5 m/s

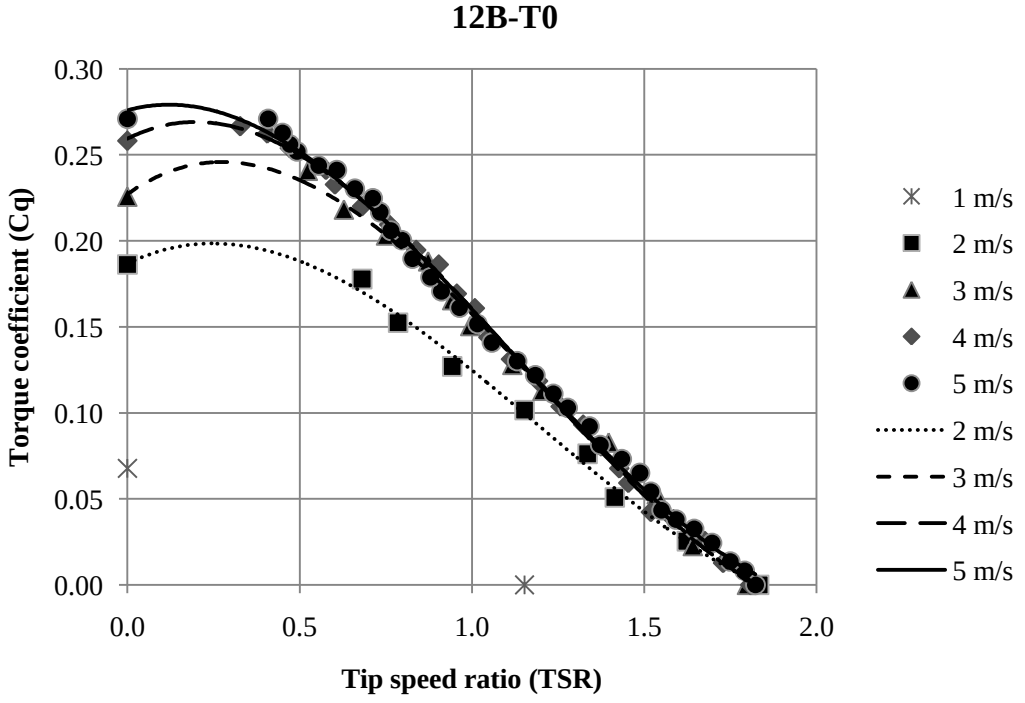

Figure 4.56 Relationship between torque coefficient (Cq) and tip speed ratio (TSR) of TSRM 12B-T0 at wind speed 1-5 m/s

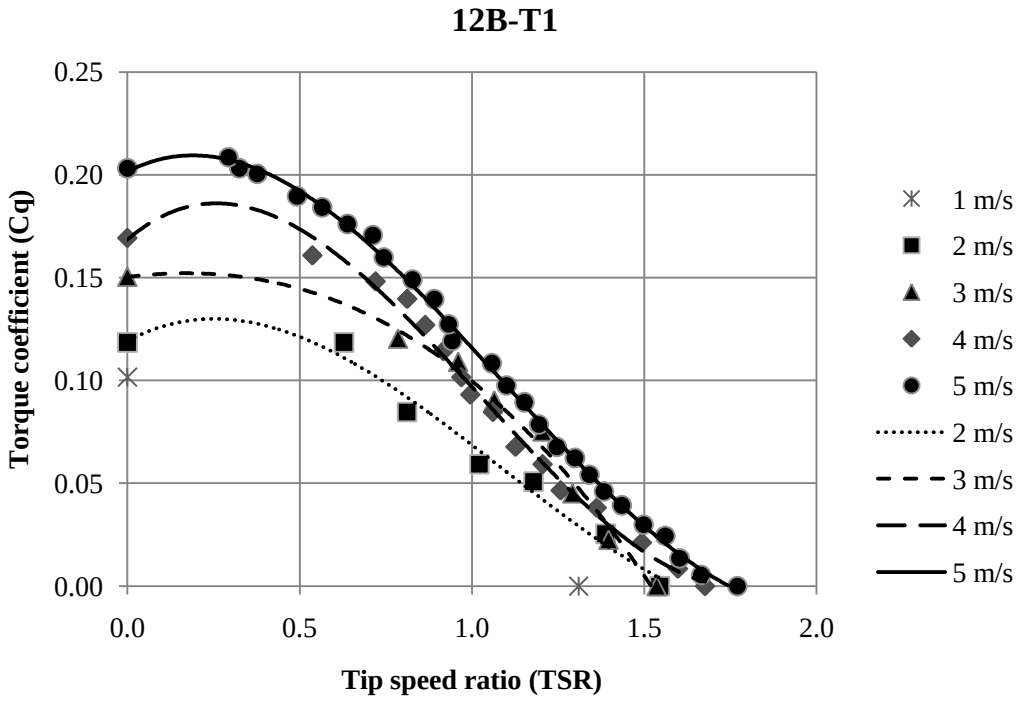

Figure 4.57 Relationship between torque coefficient (Cq) and tip speed ratio (TSR) of TSRM 12B-T1 at wind speed 1-5 m/s

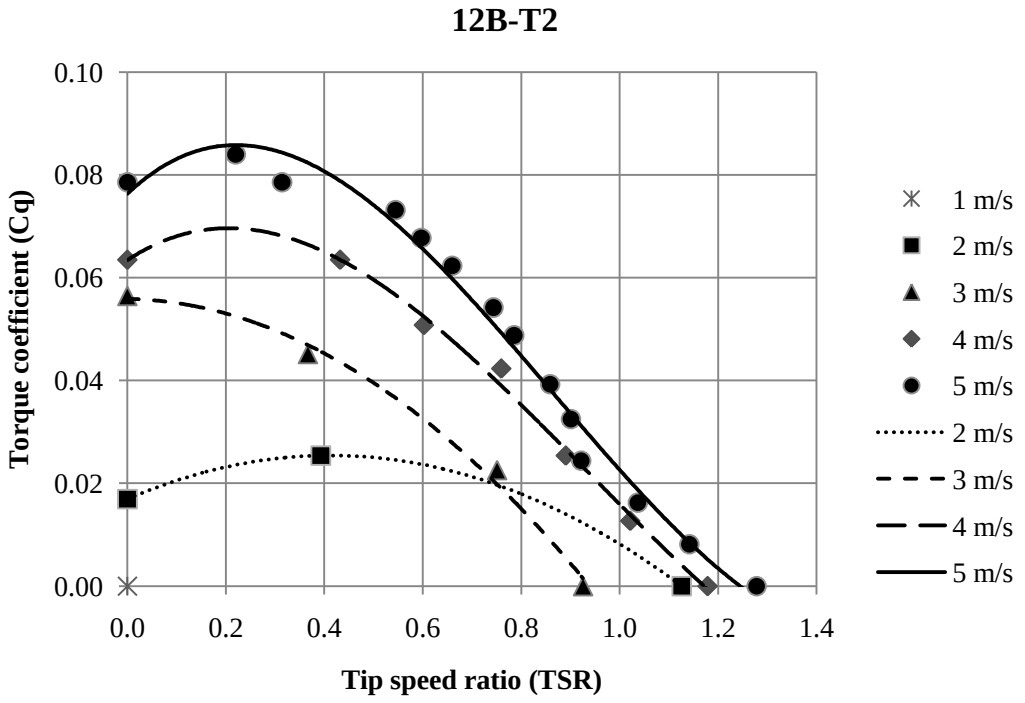

Figure 4.58 Relationship between torque coefficient (Cq) and tip speed ratio (TSR) of TSRM 12B-T2 at wind speed 1-5 m/s

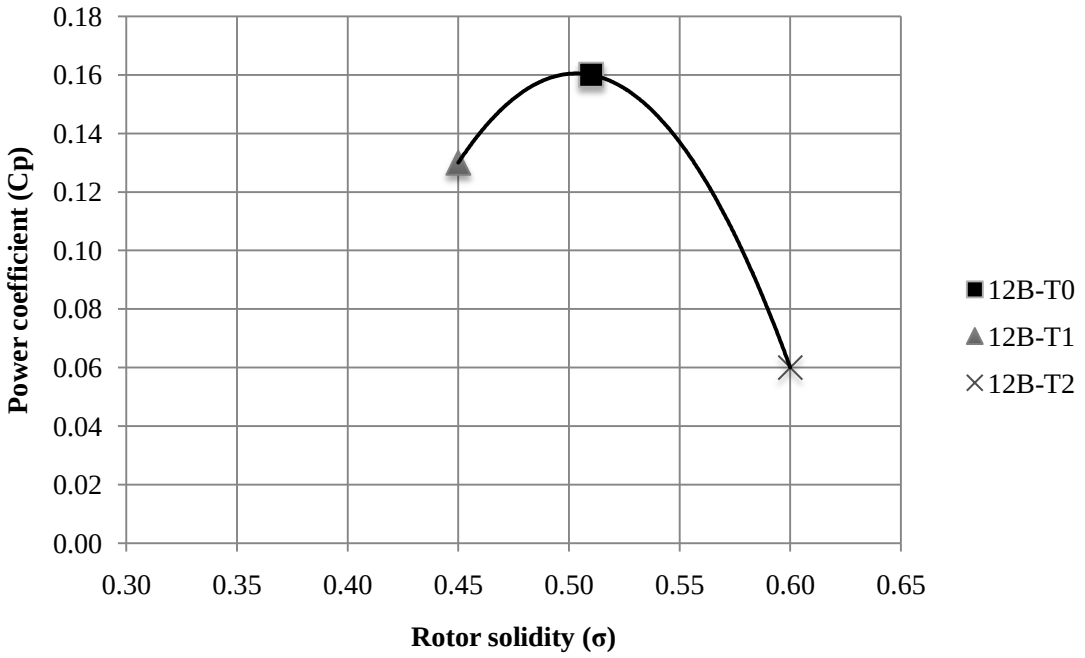

Figure 4.59 Relationship between rotor solidity (σ) and power coefficient (Cp) of TSRM 12B-T0-T1-T2

4.3 Test performance of Archimedean's pipe-screw model

Water pumping tests were conducted to assess the performance of characteristics of Archimedean's pipe-screw model, were carried out single Archimedean's pipe-screw (APS) blade to optimize the different parameters.

4.3.1 Effect of the pitch

For the pitch of Archimedean's pipe-screw testing are the pitch Archimedean's pipe-screw (P) is 0.6D, 0.8D, 0.6D, 1.0D, 1.2D, 1.4D, 1.6D, 1.8D and 2.0D, average discharge of Archimedean's pipe-screw (APS) ϕ5/8", ϕ1/2" and ϕ3/8" at α = 20°, 25° and 30°, the optimize of pitch Archimedean's pipe-screw (P) is 1.4D are shown in Figure 4.60.

4.3.2 Effect of the rotation speed of the pump shaft (n)

For the rotation speed of the pump shaft (n) of Archimedean's pipe-screw testing are the pitch Archimedean's pipe-screw (n) are 6, 15, 33, 55, 73 and 80 rpm at the pitch of Archimedean's pipe-screw testing 0.6D, 0.8D, 0.6D, 1.0D, 1.2D, 1.4D, 1.6D, 1.8D and 2.0D, average discharge of Archimedean's pipe-screw (APS) ϕ5/8", ϕ1/2" and ϕ3/8" at

α = 20°, 25° and 30°, the maximum discharge of Archimedean's pipe-screw is 80 rpm as shown in Figure 4.60.

4.3.3 Effect of the angle slope and lift head

For the angle slope and lift head of the Archimedean's pipe-screw (APS) ϕ5/8", ϕ1/2" and ϕ3/8" with the horizontal (α) is 20°, 25°, 30°, the maximum discharge of Archimedean's pipe-screw is 20° and the minimum discharge of Archimedean's pipe-screw is 30° are shown in Figures 4.60 to Figures 4.68, the optimize of pitch Archimedean's pipe-screw (P) is 1.4D.

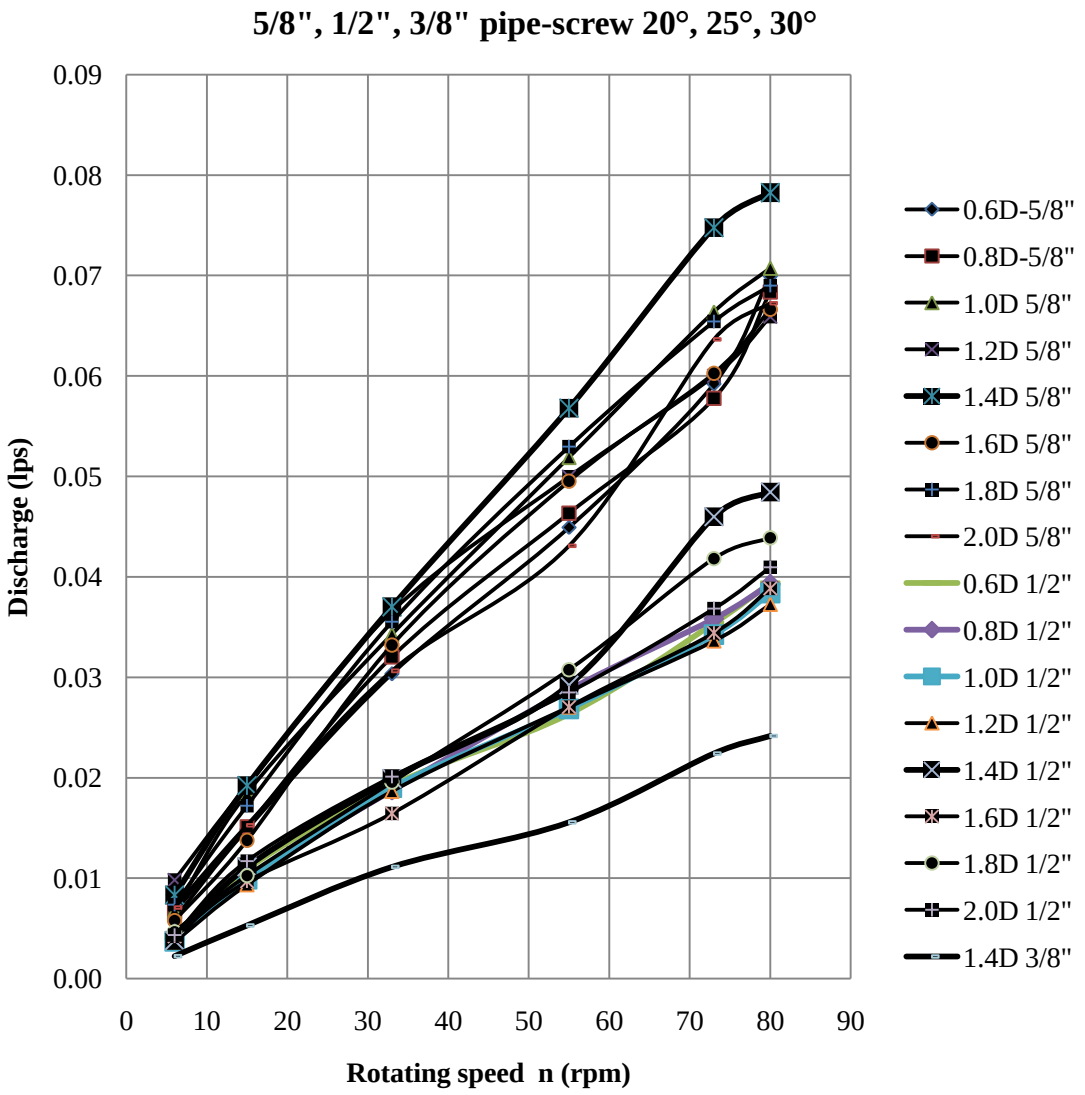

Figure 4.60 Average discharge of Archimedean's pipe-screw (APS) ϕ5/8", ϕ1/2" and ϕ3/8" at α = 20°, 25° and 30°

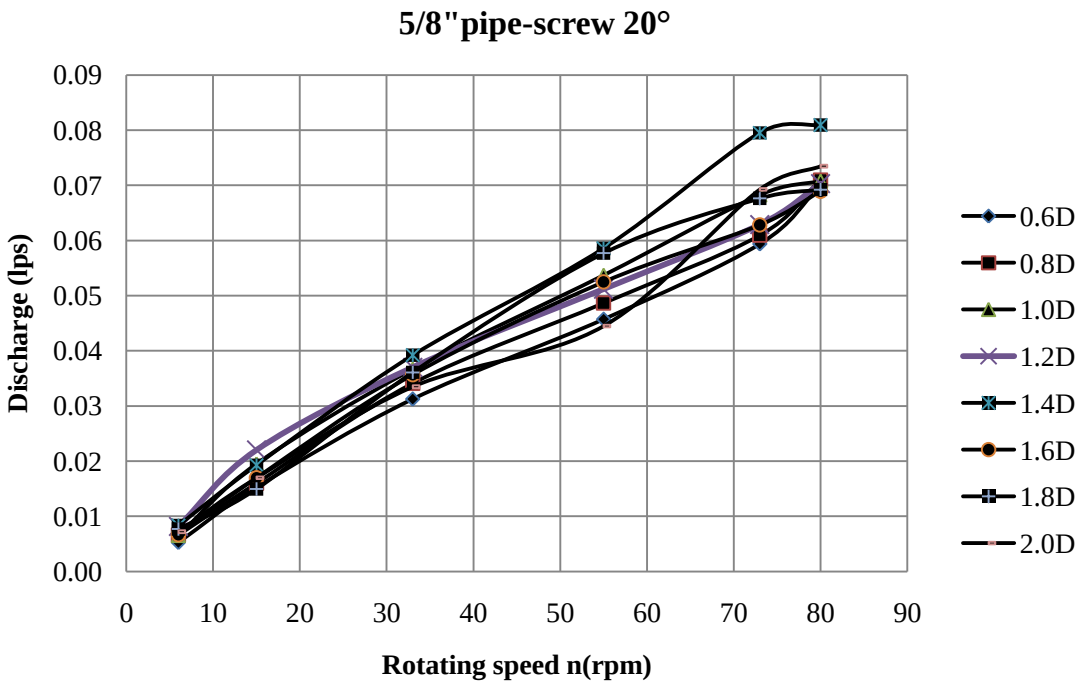

Figure 4.61 Discharge of Archimedean's pipe-screw (APS) ϕ5/8" at α = 20°

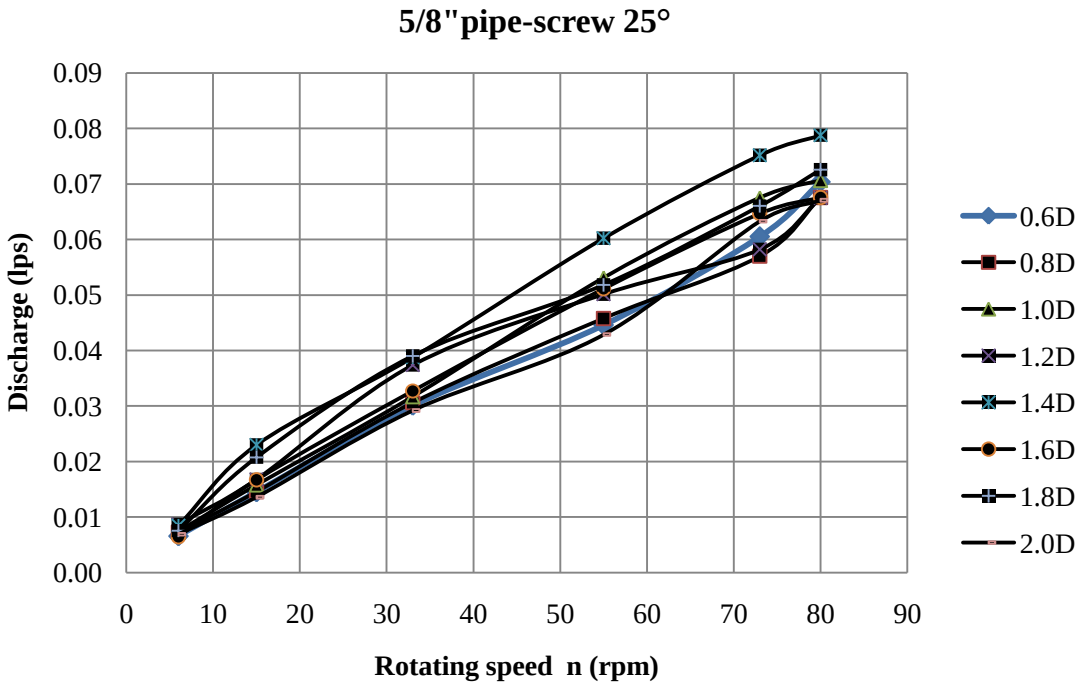

Figure 4.62 Discharge of Archimedean's pipe-screw (APS) ϕ5/8" at α = 25°

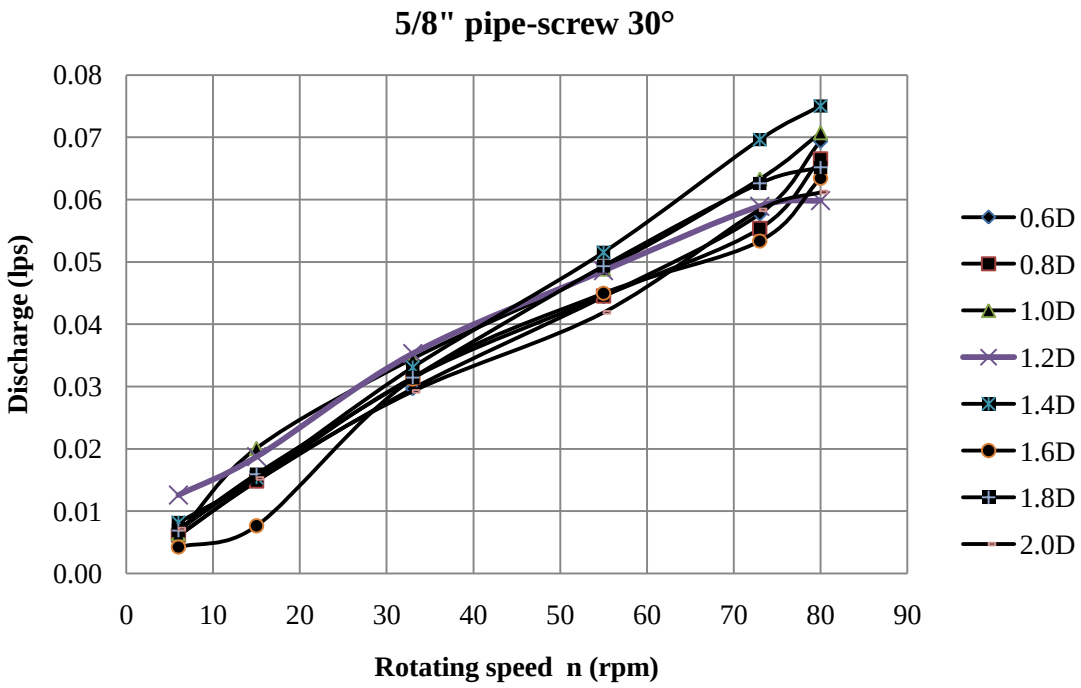

Figure 4.63 Discharge of Archimedean's pipe-screw (APS) ϕ5/8" at α = 30°

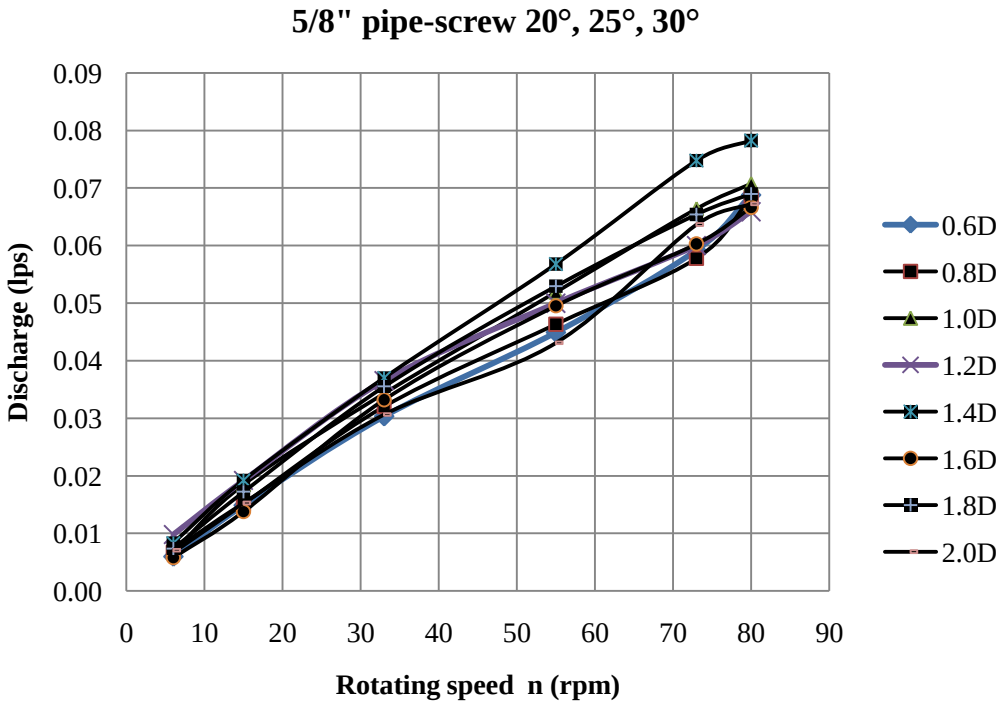

Figure 4.64 Average discharge of Archimedean's pipe-screw (APS) ϕ5/8" at α = 20°, 25° and 30°

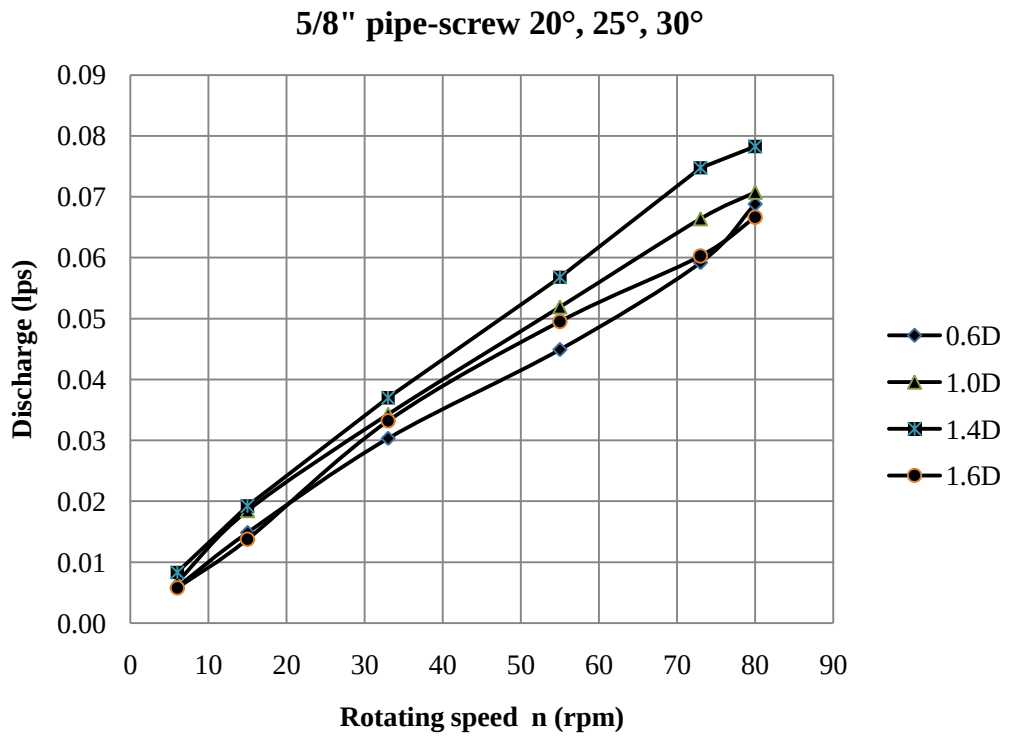

Figure 4.65 Optimize discharge of Archimedean's pipe-screw (APS) ϕ5/8" at α = 20°, 25° and 30°

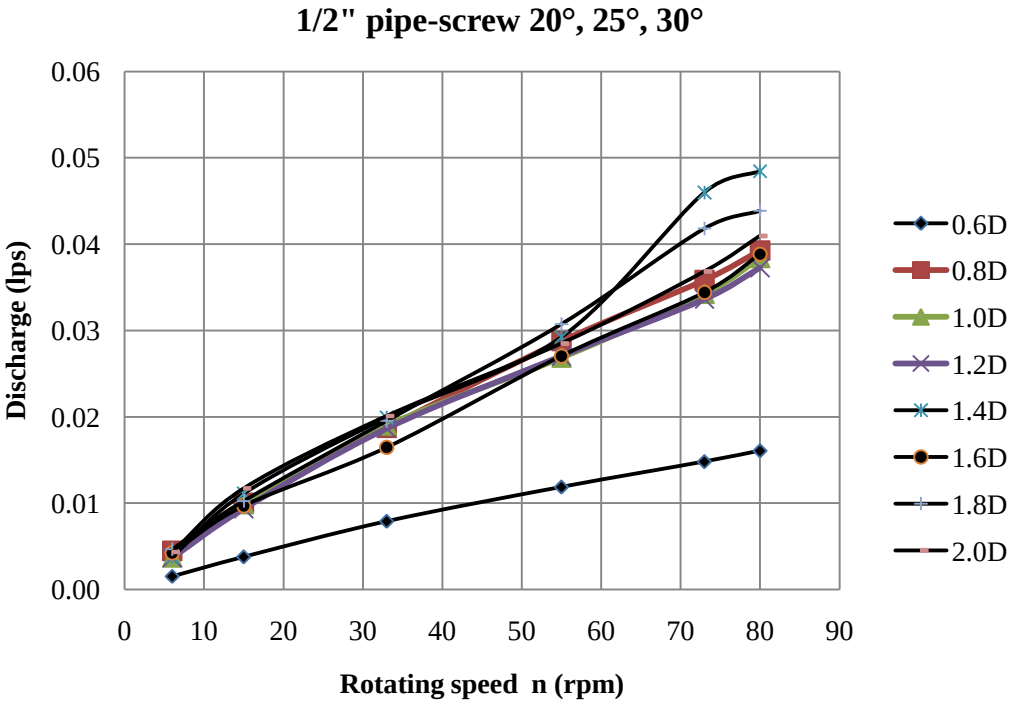

Figure 4.66 Average discharge of Archimedean's pipe-screw (APS) ϕ1/2" at α = 20°, 25° and 30°

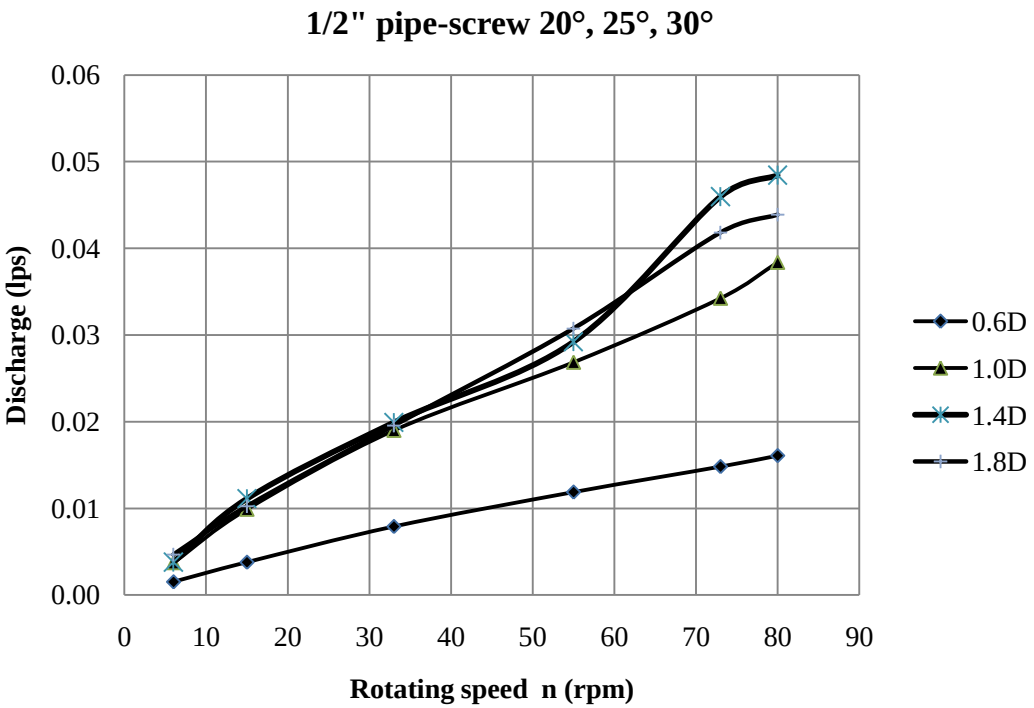

Figure 4.67 Optimize discharge of Archimedean's pipe-screw (APS) ϕ1/2" at α = 20°, 25° and 30°

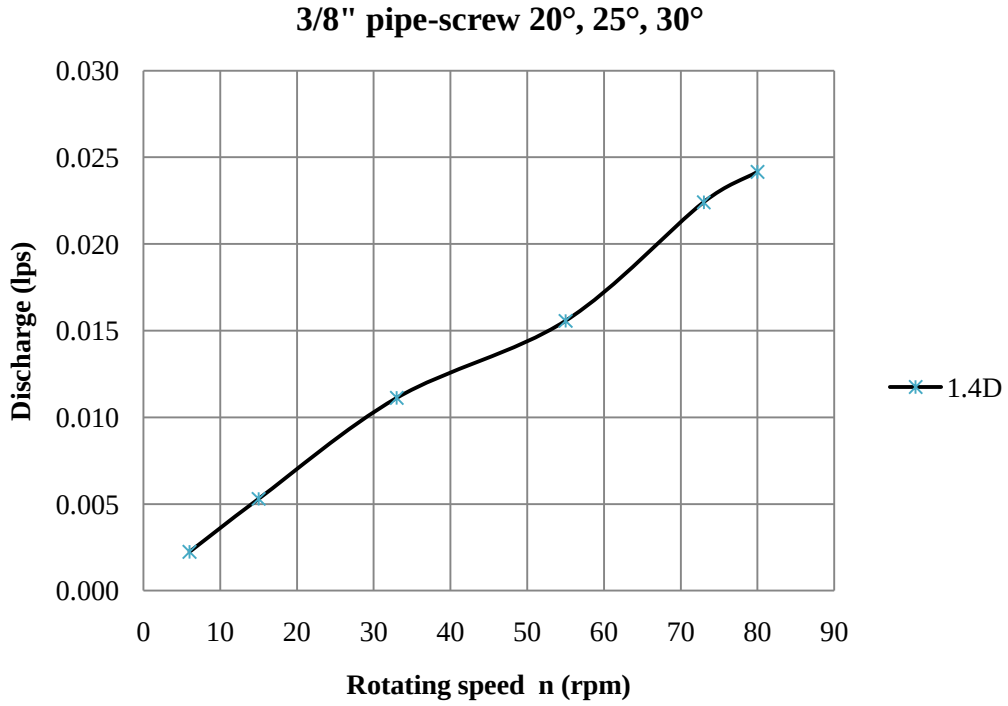

Figure 4.68 Optimize discharge of Archimedean's pipe-screw (APS) ϕ3/8" at α = 20°, 25° and 30°

4.3.4 Effect of the intake submergence

For the intake submergence of Archimedean's pipe-screw are testing at the downstream of Archimedean's pipe-screw 50% and 25%, the optimize discharge intake submergence of Archimedean's pipe-screw is 50% as shown in Figure 4.69.

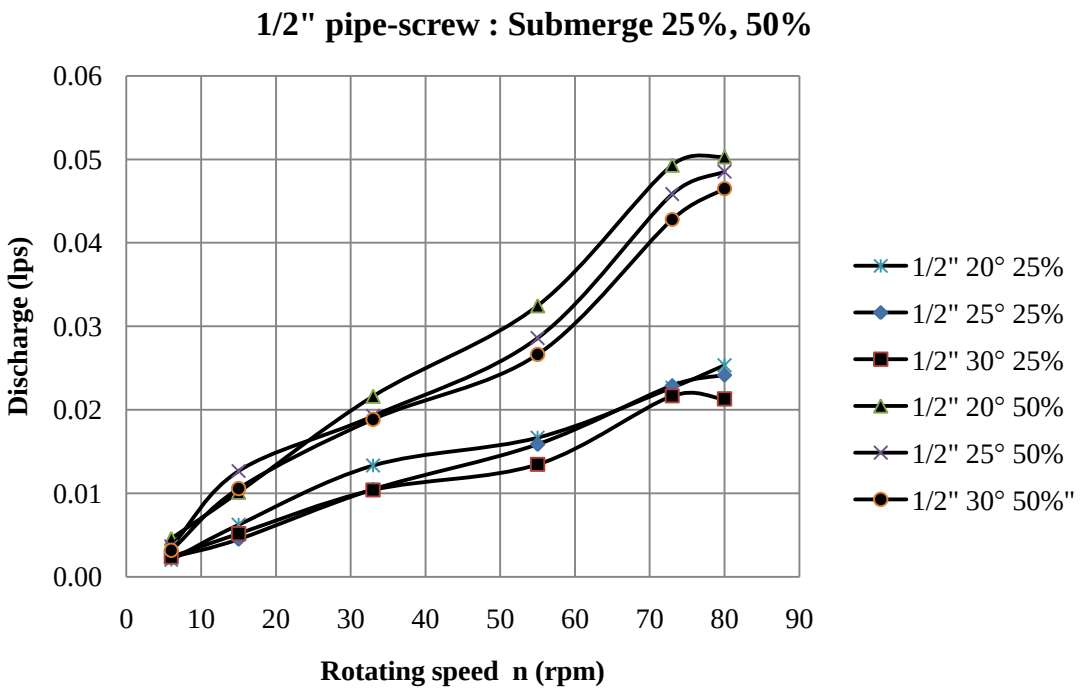

Figure 4.69 Discharge curve of Archimedean's pipe-screw (APS) ϕ1/2" at the pitch 1.4D and intake submergence 50% and 25%

4.3.5 The optimize discharge of Archimedean's pipe-screw (APS)

For water pumping tests were conducted to assess the performance of characteristics of Archimedean's pipe-screw model. The optimize output and discharge curve of the experiments recommenced for development the prototype of Archimedean's pipe-screw pump for the Thai sail windmill are the Archimedean's pipe-screw pump which the pitch 1.4D are shown in Figures 4.70 to Figures 4.73.

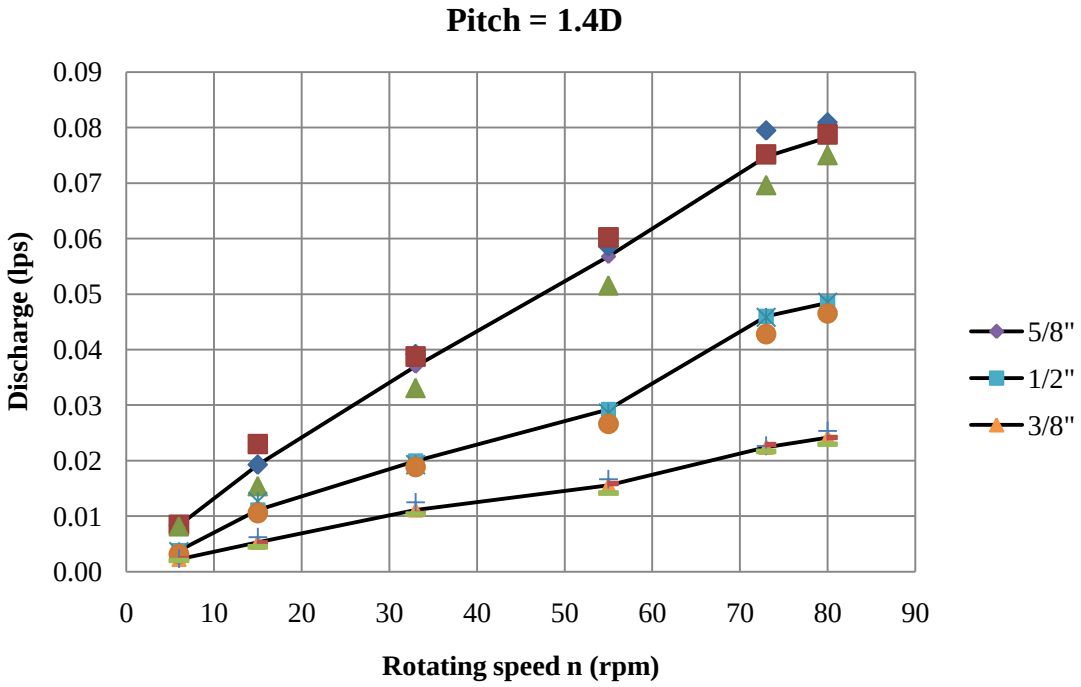

Figure 4.70 Optimize discharge of Archimedean's pipe-screw (APS) ϕ5/8",ϕ1/2" and ϕ3/8" at the pitch 1.4D

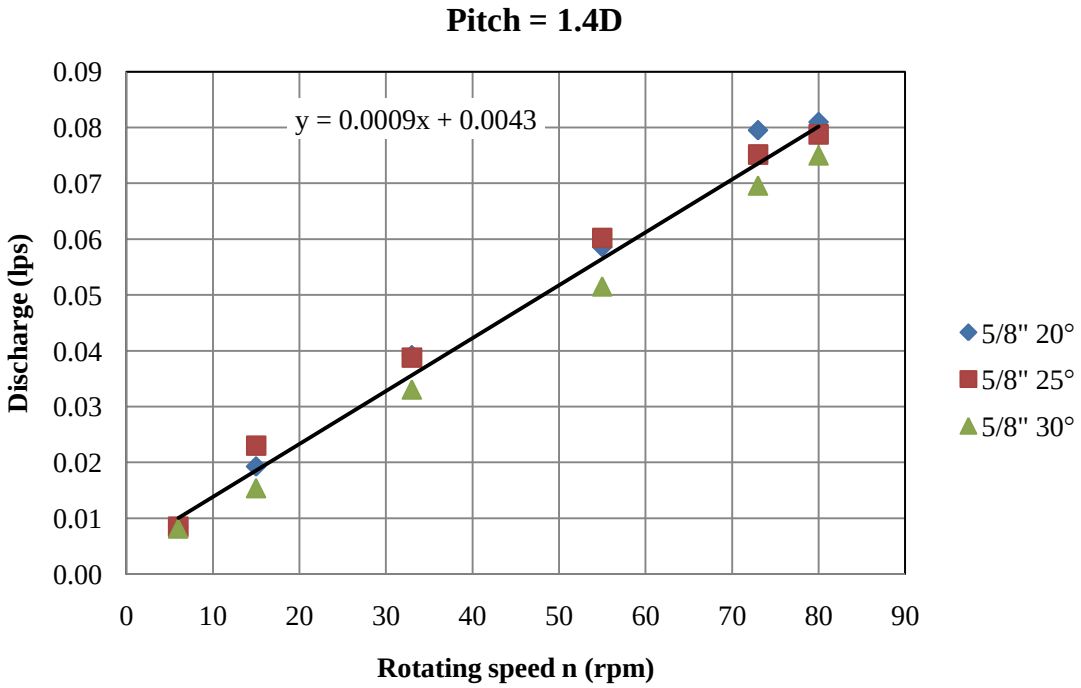

Figure 4.71 Optimize discharge curve of Archimedean's pipe-screw (APS) ϕ5/8" at the pitch 1.4D

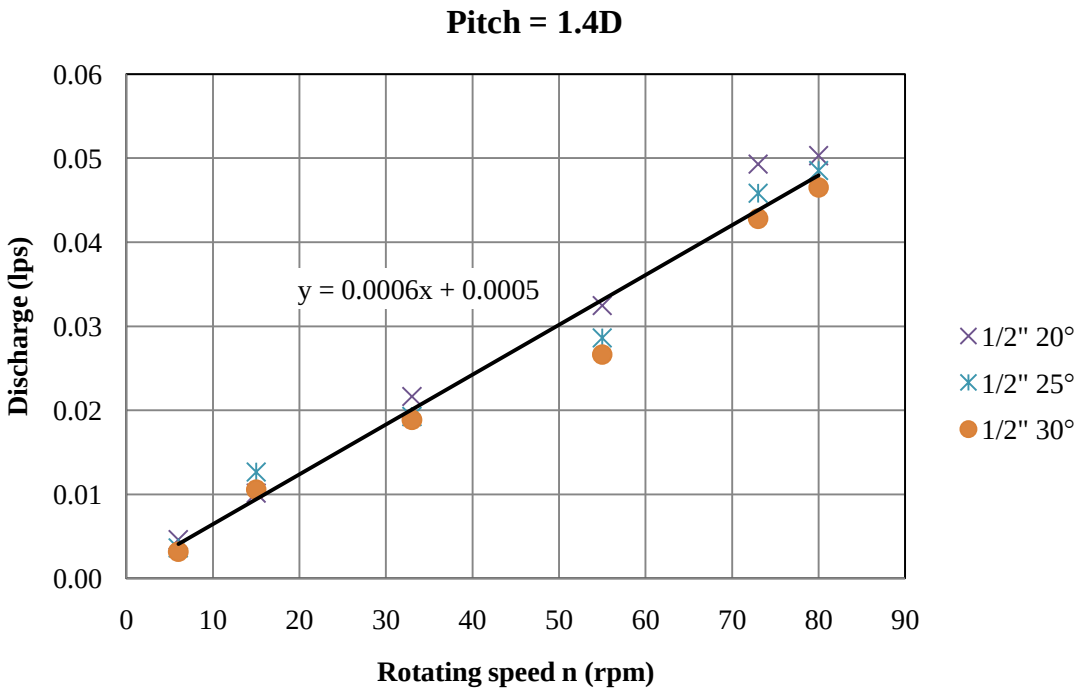

Figure 4.72 Optimize discharge curve of Archimedean's pipe-screw (APS) ϕ1/2" at the pitch 1.4D

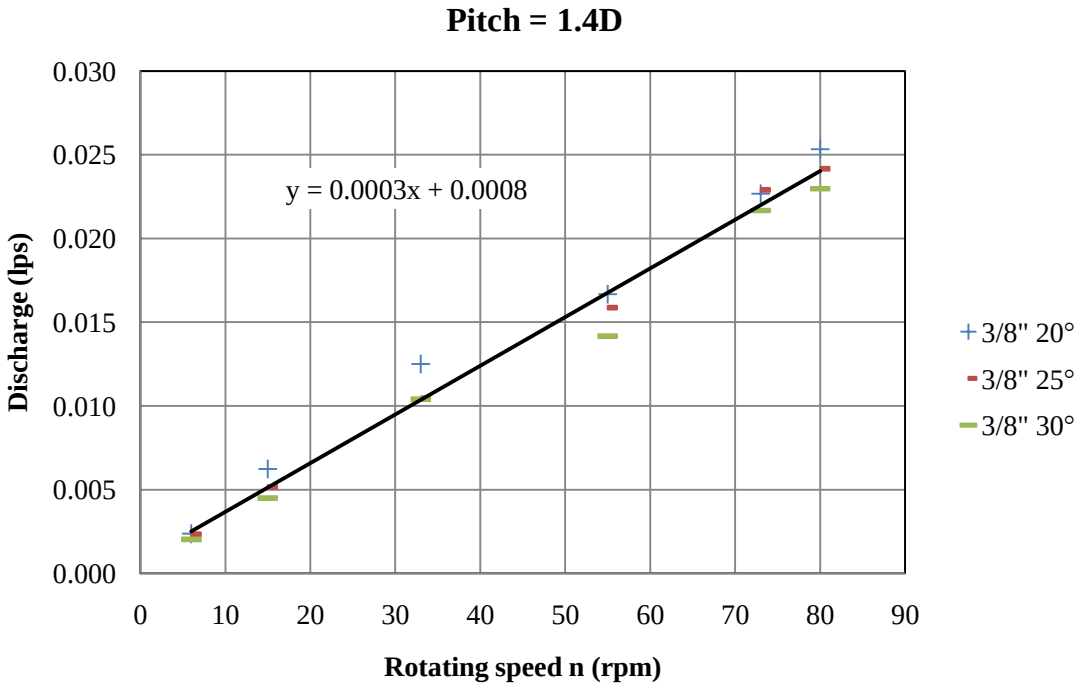

Figure 4.73 Optimize discharge curve of Archimedean's pipe-screw (APS) ϕ3/8" at the pitch 1.4D

4.4 Large scale the new prototype of Thai sail windmill

Relationship between wind speed and rotating speed of Thai sail windmill 12B-T0 rotor model in free load as shown in Figure 4.74, for wind speed from 1.5- 6.5 m/s, rotating speed of a Thai sail windmill rotor assembly from 10-45 rpm and rotating speed of drive shaft from 20-90 rpm**.** During tests wind direction varies continuously and the new Thai sail windmill operated correctly.

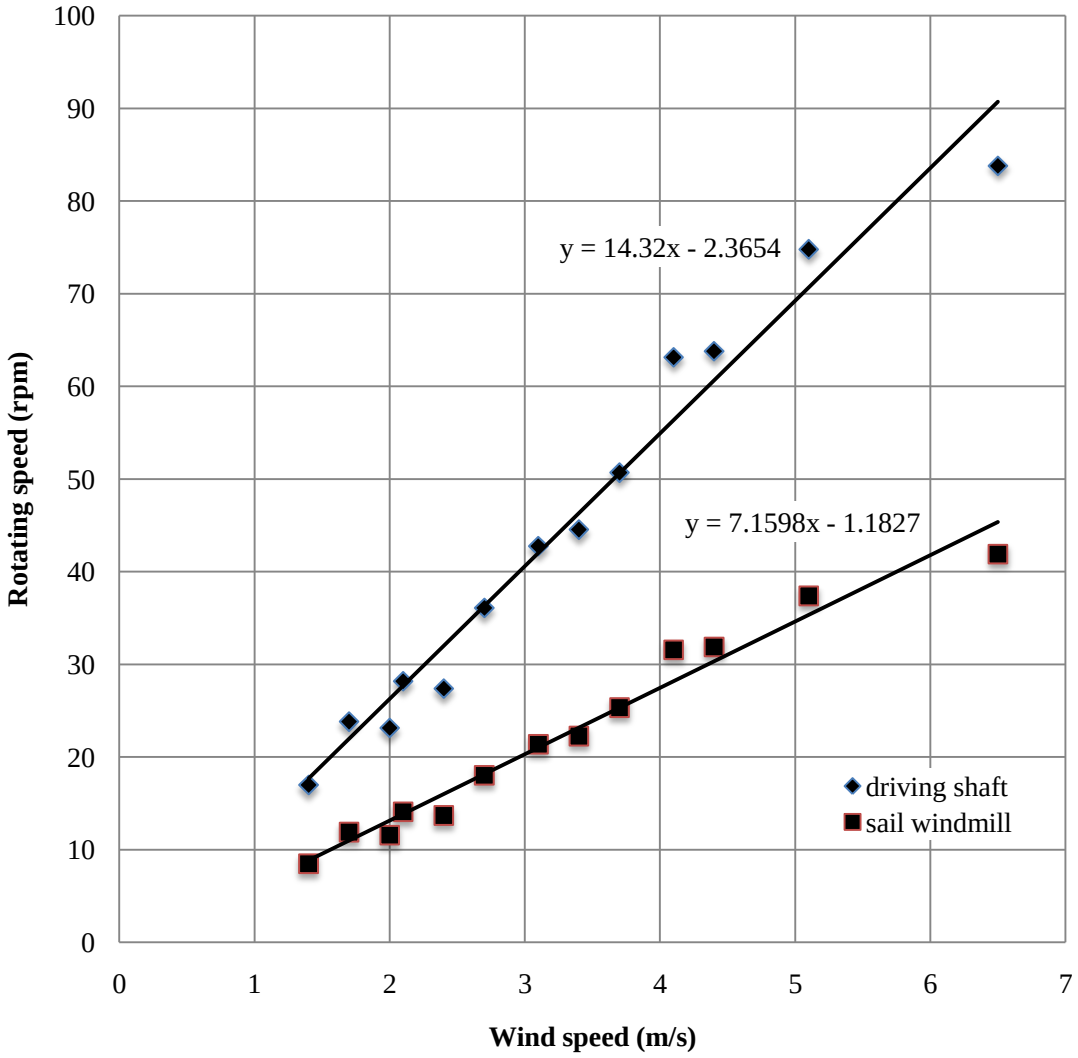

Figure 4.74 Relationship between wind speed and rotating speed of the new Thai sail windmill in free load

4.5 Large scale of Water ladder pump coupled by the prototype of Thai sail windmill Testing

Relationship between rotating speed and discharge of water ladder pump coupled to adjustable rotating speed motor as shown in Figure 4.75, rotating speed of drive shaft of water ladder pump from 13-50 rpm and discharge of water ladder pump from 8-85 m^3/hr.

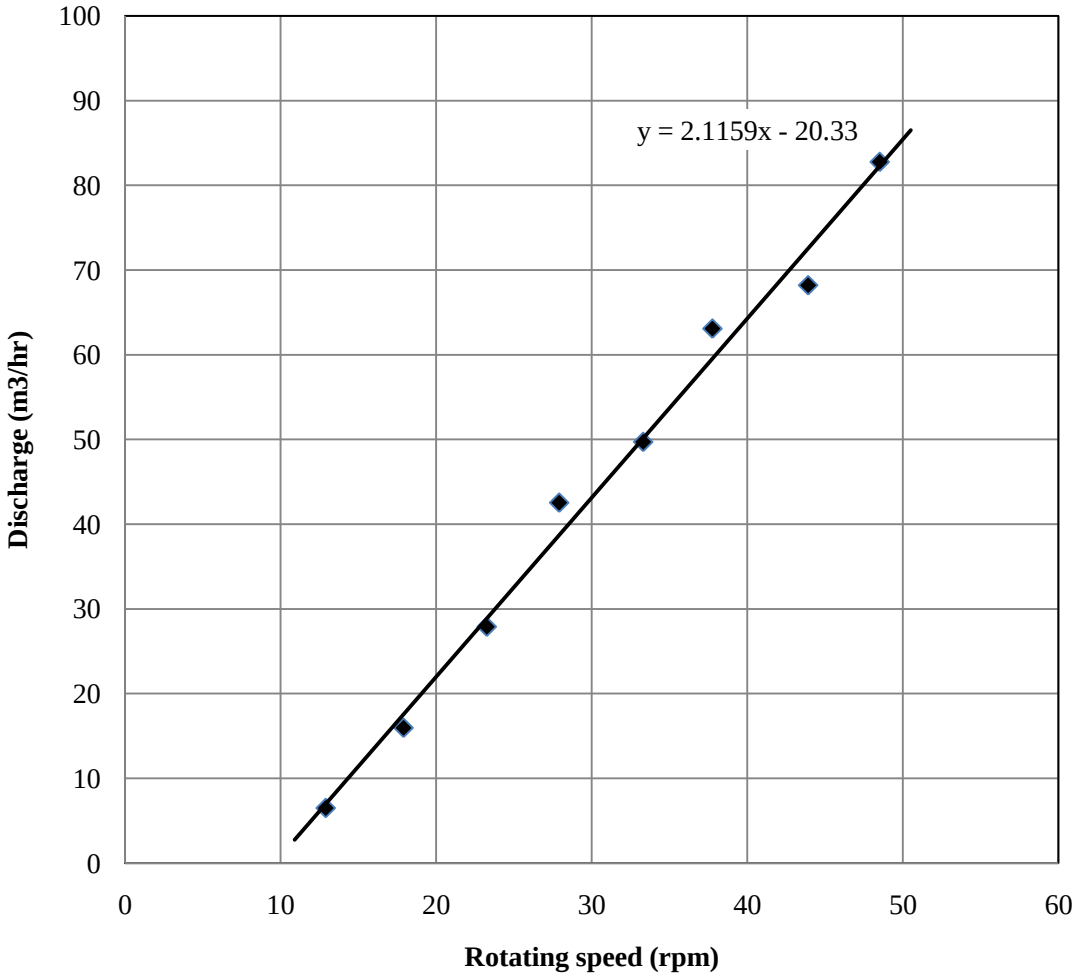

Figure 4.75 Relationship between rotating speed and discharge of water ladder pump coupled to adjustable rotating speed motor

Relationship between wind speed and rotating speed of Thai sail windmill coupled to water ladder pump as shown in Figure 4.76, wind speed from 1.0- 4.5 m/s, rotating speed of drive shaft of water ladder pump from 9-33 rpm.

Performance curve of the prototype of Thai sail windmill 12B-T0 of wind speed and discharge of water ladder pump are shown in Figure 4.78 and compared to the original six blades Thai sail windmill of about wind speed from 1.5- 4.5 m/s. It can be observed that the discharge of water ladder pump was increased depending on wind speed. The discharge amount varied between 8-50 m^3/hr. When compared to the traditional windmill, the pumped amount is much larger that confirmed the good performance of the new windmill. In addition, the new model can operate at low speed starting from 1.5 m/s, that's extremely important. Above results confirmed that the prototype of Thai sail windmill 12B-T0 model is better than the original six blades Thai sail windmill.

Relationship between wind speed and the overall efficiency of Thai sail windmill coupled to water ladder pump are shown in Figure 4.77 and Table 4.1. It was found that the overall efficiency of this windmill for water pumping was highest (33.68%) at wind speed of 1.4 m/s and the value would decrease as the wind speed increased.

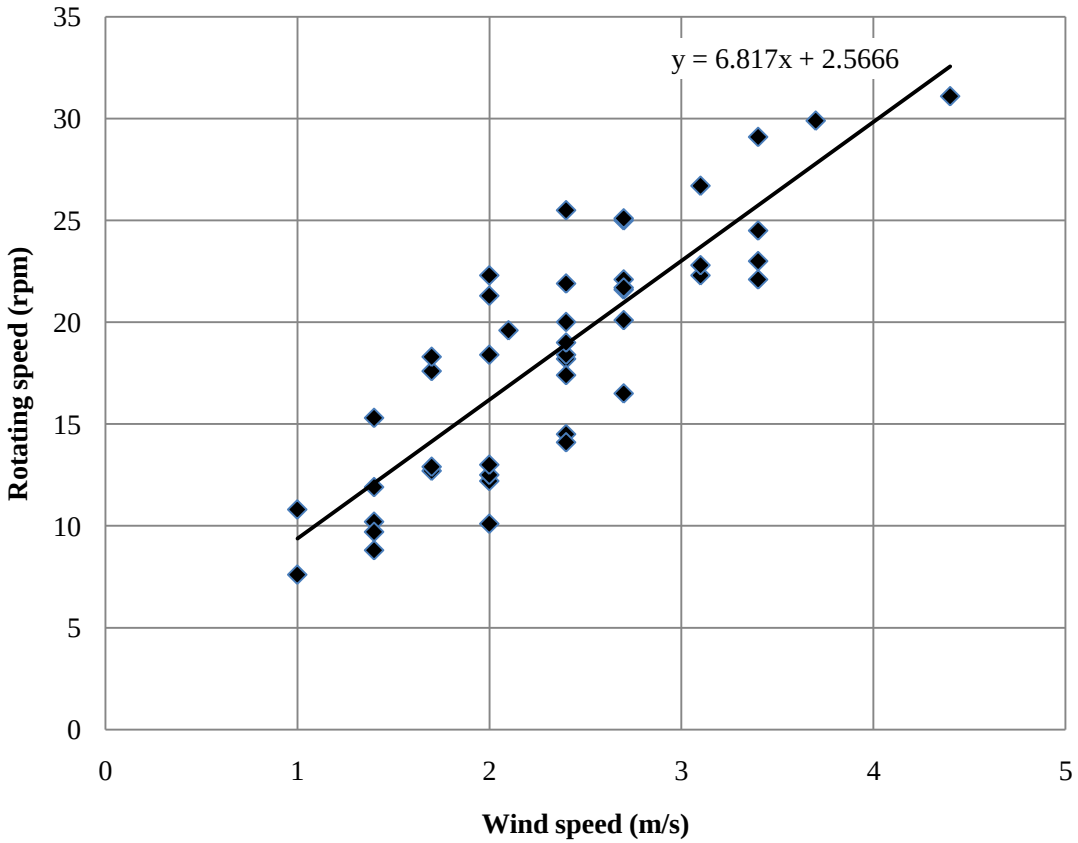

Figure 4.76 Relationship between wind speed and rotating speed of the new Thai sail windmill coupled to water ladder pump

Table 4.1 Test results of wind speed and discharge of water ladder pump coupled by the new Thai sail windmill

Wind speed (m/s)	Average rotating speed (rpm)	Discharge Q (m^3/hr)	Discharge Q (lps)	Water power (W)	Wind power (W)	The overall efficiency (%)
1.40	11.18	6.66	1.85	27.19	80.72	33.68
1.70	15.38	10.81	3.00	44.15	144.53	30.55
2.00	15.69	14.97	4.16	61.11	235.34	25.97
2.10	19.60	16.35	4.54	66.76	272.43	24.51
2.40	18.78	20.50	5.70	83.72	406.66	20.59
2.70	21.73	24.66	6.85	100.68	579.02	17.39
3.10	23.93	30.19	8.39	123.29	876.37	14.07
3.40	24.68	34.35	9.54	140.25	1156.21	12.13
3.70	29.90	38.50	10.69	157.21	1490.07	10.55
4.40	31.10	48.19	13.39	196.79	2505.87	7.85

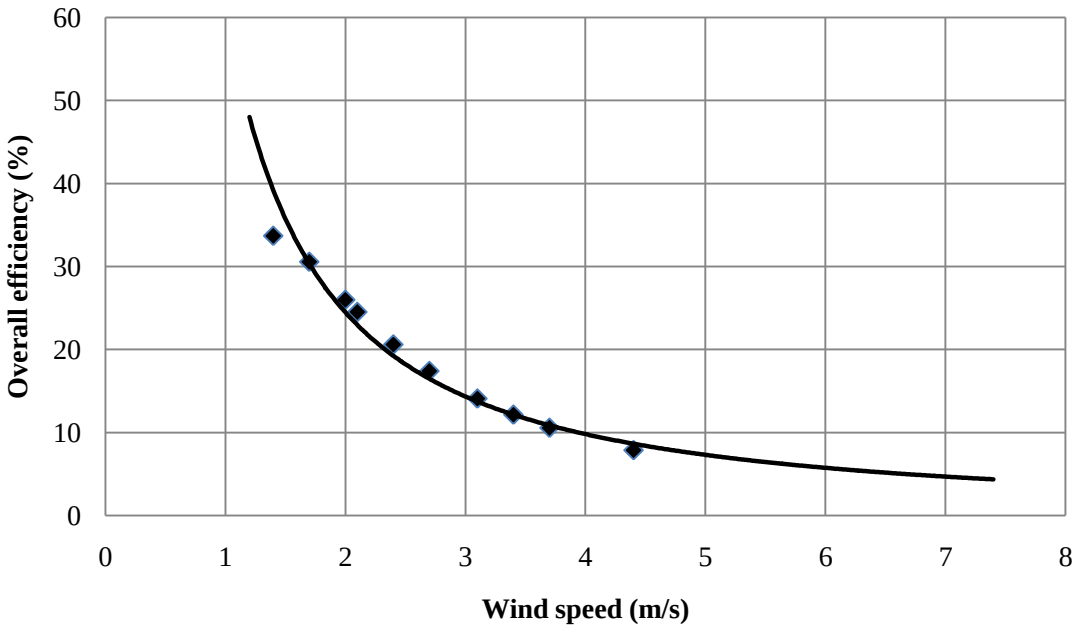

Figure 4.77 Relationship between wind speed and overall efficiency of water ladder pump coupled by the new Thai sail windmill

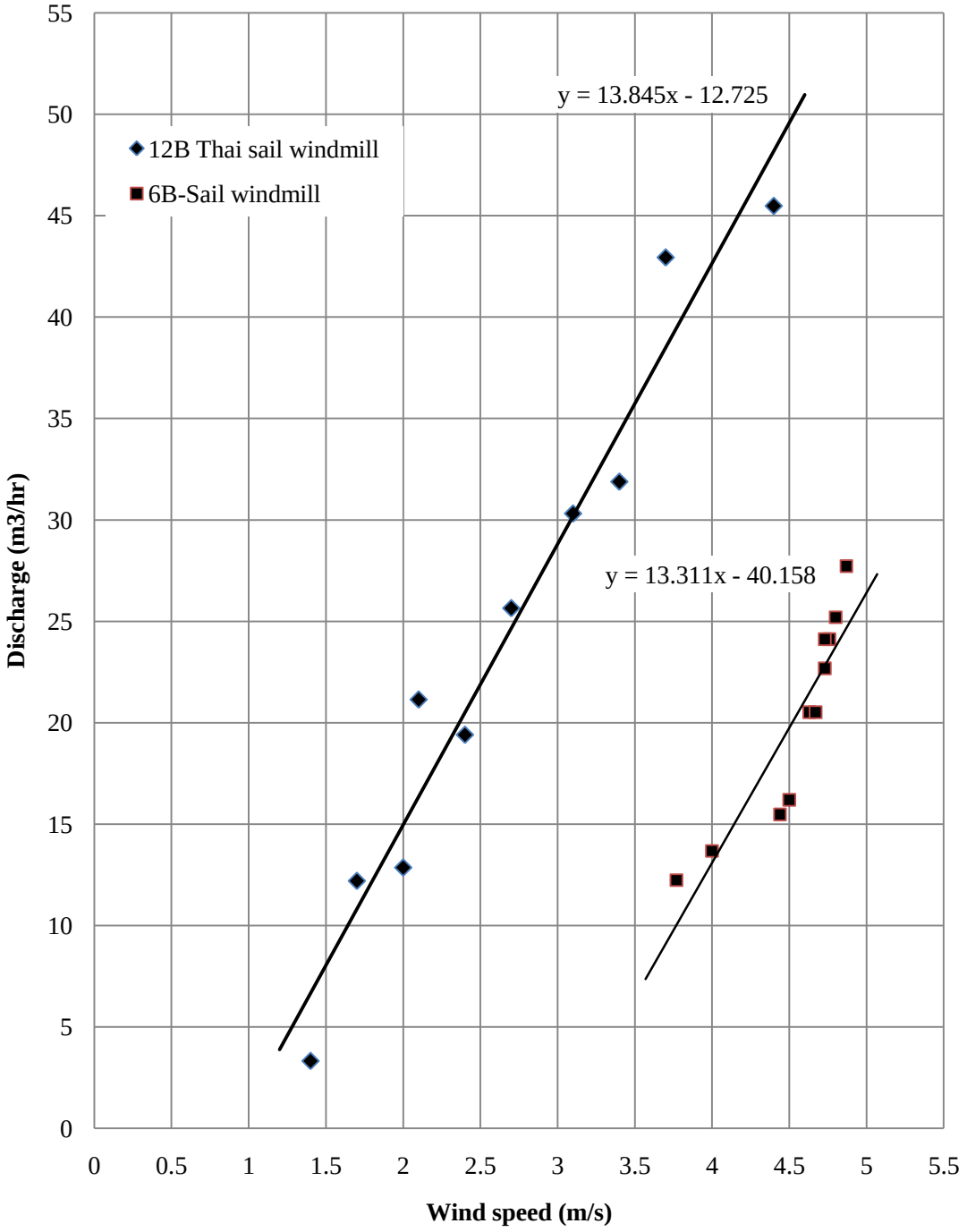

Figure 4.78 Performance curve of wind speed and discharge of water ladder pump of the new Thai sail windmill compared to the traditional one

4.6 Large scale of Archimedean's pipe-screw coupled by the prototype of Thai sail windmill testing

Relationship between rotating speed and discharge of Archimedean's pipe-screw pump coupled to adjustable rotating speed motor as shown in Figure 4.79 to Figure 4.90.

Rotating speed of drive shaft of one Archimedean's pipe-screw (3-APS) pump from 10.37-54.70 rpm and discharge of Archimedean's pipe-screw pump from 0.21-1.04 lps, discharge equation is y = 0.017x + 0.0618 as shown in Figure 4.79.

Rotating speed of drive shaft of two Archimedean's pipe-screw (2-APS) pump from 10.27-53.90 rpm and discharge of Archimedean's pipe-screw pump from 0.37-2.10 lps, discharge equation is y = 0.0374x - 0.0097as shown in Figure 4.80.

Rotating speed of drive shaft of three Archimedean's pipe-screw (3-APS) pump from 10.07-53.72 rpm and discharge of Archimedean's pipe-screw pump from 0.51-2.87 lps, discharge equation is y = 0.0516x - 0.0197as shown in Figure 4.81.

Rotating speed of drive shaft of four Archimedean's pipe-screw (4-APS) pump from 9.87-53.53 rpm and discharge of Archimedean's pipe-screw pump from 0.82-4.52 lps, discharge equation is y = 0.0833x - 0.0544 as shown in Figure 4.82.

Rotating speed of drive shaft of five Archimedean's pipe-screw (5-APS) pump from 9.70-53.43 rpm and discharge of Archimedean's pipe-screw pump from 0.94-5.26 lps, discharge equation is y = 0.0981x - 0.0108 as shown in Figure 4.83.

Rotating speed of drive shaft of six Archimedean's pipe-screw (6-APS) pump from 9.53-53.33 rpm and discharge of Archimedean's pipe-screw pump from 1.11-6.29 lps, discharge equation is y = 0.1195x + 0.075 as shown in Figure 4.84.

Rotating speed of drive shaft of seven Archimedean's pipe-screw (7-APS) pump from 9.35-53.10 rpm and discharge of Archimedean's pipe-screw pump from 1.27-7.51 lps, discharge equation is y = 0.1469x - 0.0273 as shown in Figure 4.85.

Rotating speed of drive shaft of eight Archimedean's pipe-screw (8-APS) pump from 9.17-52.87 rpm and discharge of Archimedean's pipe-screw pump from 1.49-9.33 lps, discharge equation is y = 0.1895x - 0.238 as shown in Figure 4.86.

Rotating speed of drive shaft of nine Archimedean's pipe-screw (9-APS) pump from 8.30-52.03 rpm and discharge of Archimedean's pipe-screw pump from 1.60-11.85 lps, discharge equation is y = 0.2319x - 0.4131 as shown in Figure 4.87.

Rotating speed of drive shaft of ten Archimedean's pipe-screw (10-APS) pump from 8.20-54.70 rpm and discharge of Archimedean's pipe-screw pump from 1.74-13.46 lps, discharge equation is y = 0.2578x - 0.3881 as shown in Figure 4.88.

Rotating speed of drive shaft of eleven Archimedean's pipe-screw (11-APS) pump from 7.80-50.87 rpm and discharge of Archimedean's pipe-screw pump from 1.67-13.95 lps, discharge equation is y = 0.2841x - 0.3863 as shown in Figure 4.89.

Rotating speed of drive shaft of twelve Archimedean's pipe-screw (12-APS) pump from 11.47-48.37 rpm and discharge of Archimedean's pipe-screw pump from 3.82-14.53 lps, discharge equation is y = 0.2897x + 0.2272 as shown in Figure 4.90.

Relationship between wind speed and rotating speed of Thai sail windmill coupled to twelve Archimedean's pipe-screw (12-APS) pump is equation y = 6.8731x + 1.5082 as shown in Figure 4.91, wind speed from 1.0 - 5.1 m/s, rotating speed of drive shaft of twelve Archimedean's pipe-screw (12-APS) pump from 8.56-37.7 rpm as shown in Table 4.2.

Performance curve of the prototype of Thai sail windmill 12B-T0 of wind speed and discharge of Archimedean's pipe-screw pump are shown in Figure 4.94 and Figure 4.93. It can be observed that the discharge of twelve Archimedean's pipe-screw (12-APS) pump was increased depending on wind speed. The discharge amount varied between 9.56 – 38.23 m^3/hr at wind speed from 1.0 - 5.0 m/s.

Relationship between wind speed and the overall efficiency of Thai sail windmill coupled to twelve Archimedean's pipe-screw (12-APS) pump are shown in Figure 4.93 and Table 4.2. It was found that the overall efficiency of this windmill for water pumping was highest (76.96%) at wind speed of 1.4 m/s and the value would decrease as the wind speed increased.

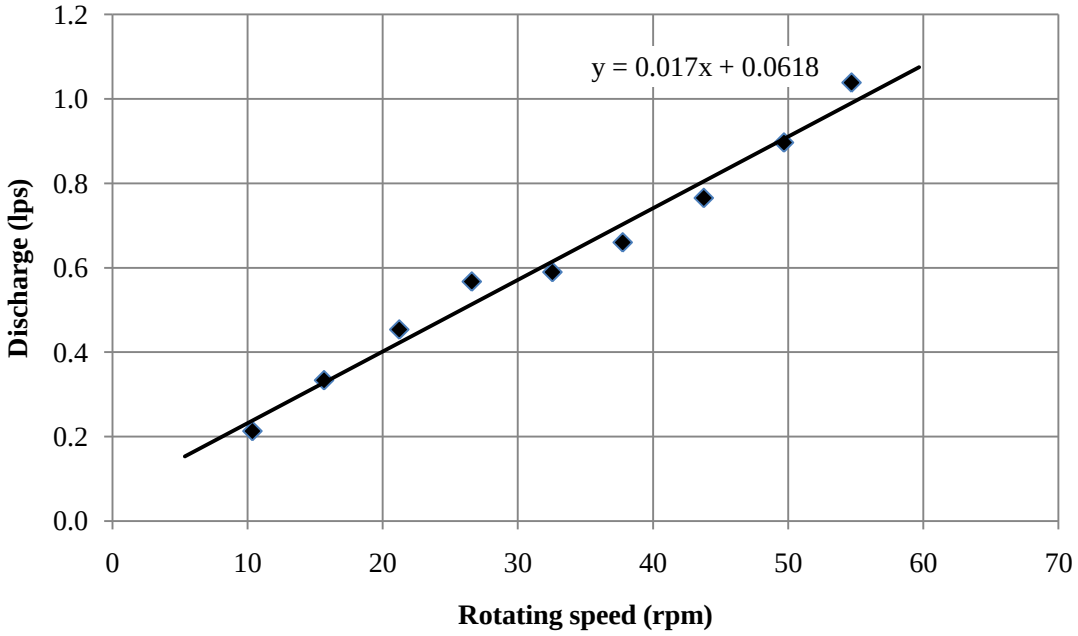

Figure 4.79 Relationship between rotating speed and discharge of one Archimedean's pipe-screw (1-APS) pump coupled to adjustable rotating speed motor

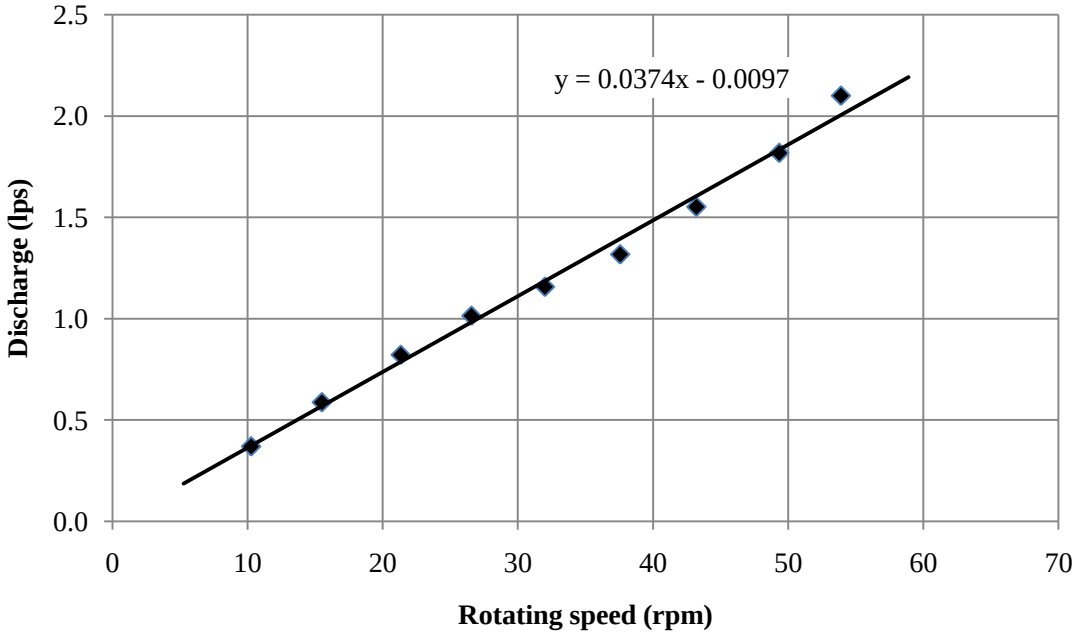

Figure 4.80 Relationship between rotating speed and discharge of two Archimedean's pipe-screw (2-APS) pump coupled to adjustable rotating speed motor

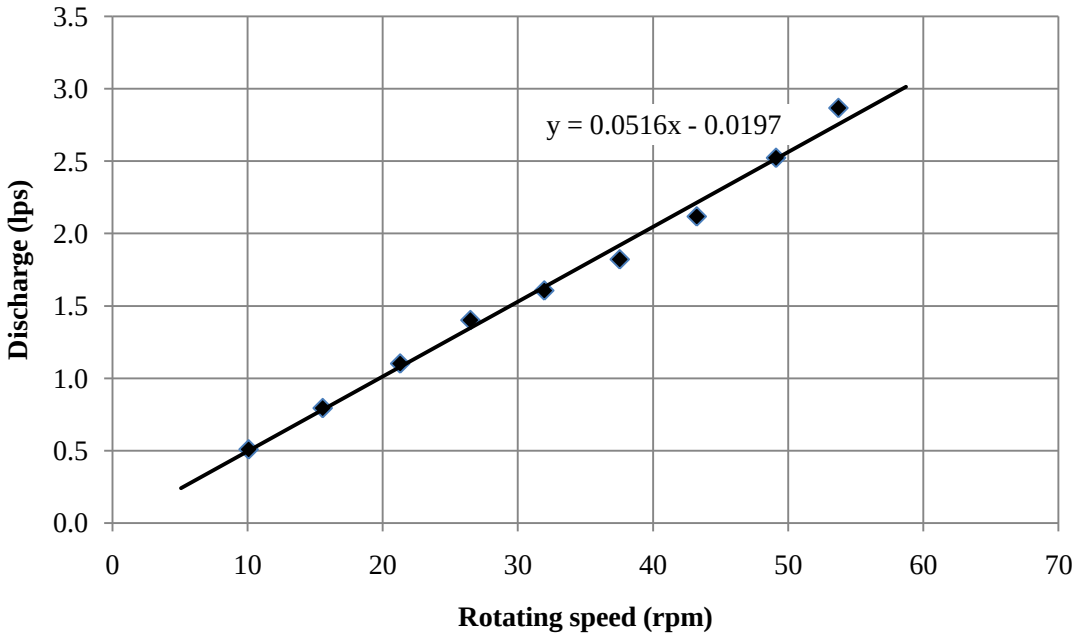

Figure 4.81 Relationship between rotating speed and discharge of three Archimedean's pipe-screw (3-APS) pump coupled to adjustable rotating speed motor

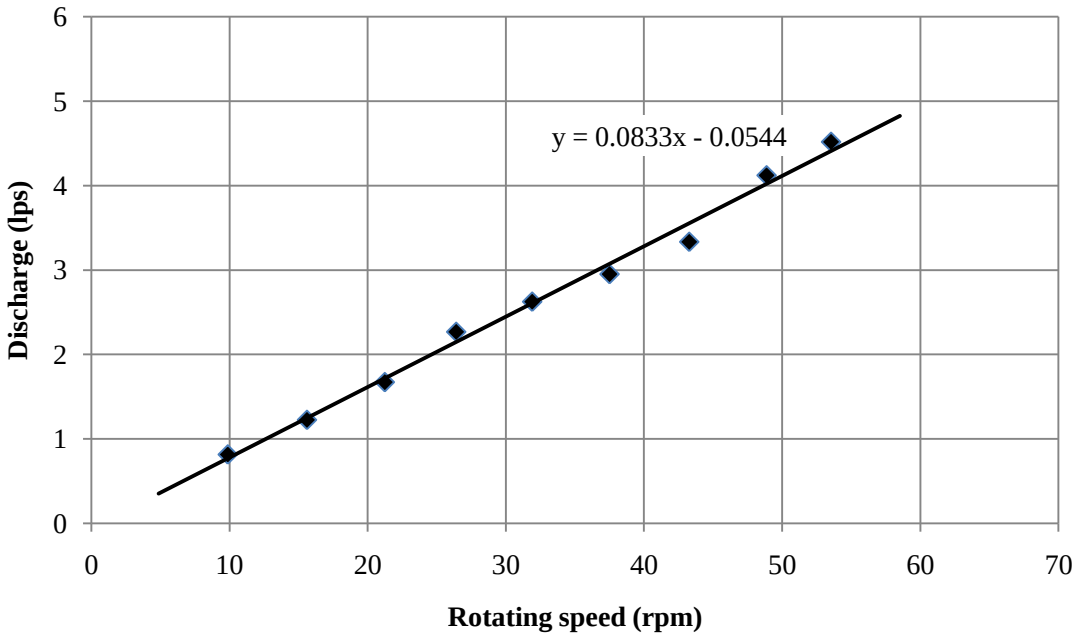

Figure 4.82 Relationship between rotating speed and discharge of four Archimedean's pipe-screw (4-APS) pump coupled to adjustable rotating speed motor

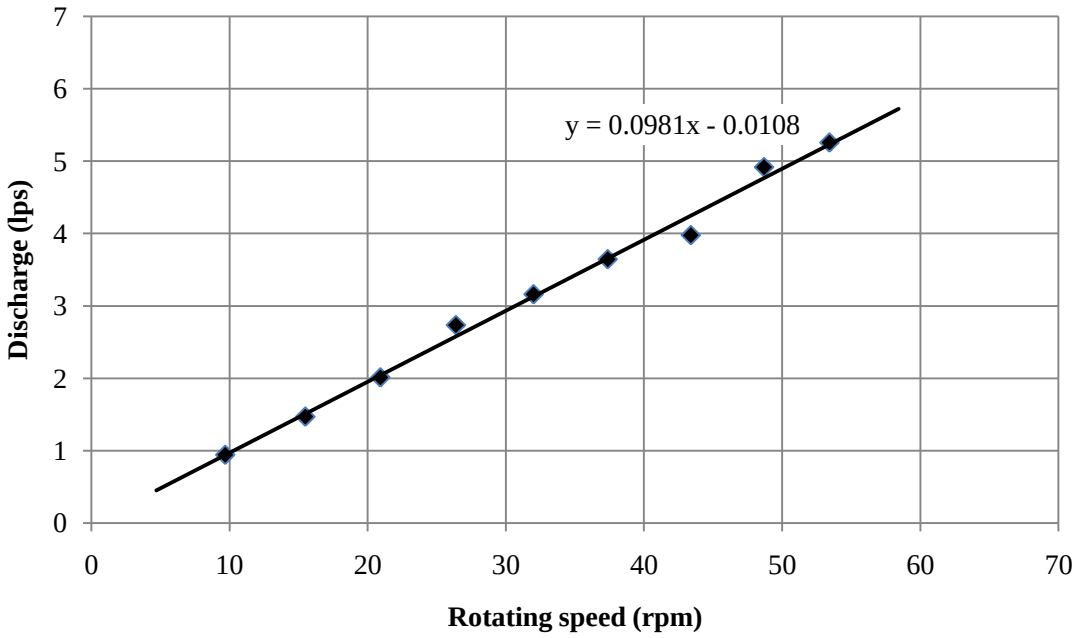

Figure 4.83 Relationship between rotating speed and discharge of five Archimedean's pipe-screw (5-APS) pump coupled to adjustable rotating speed motor

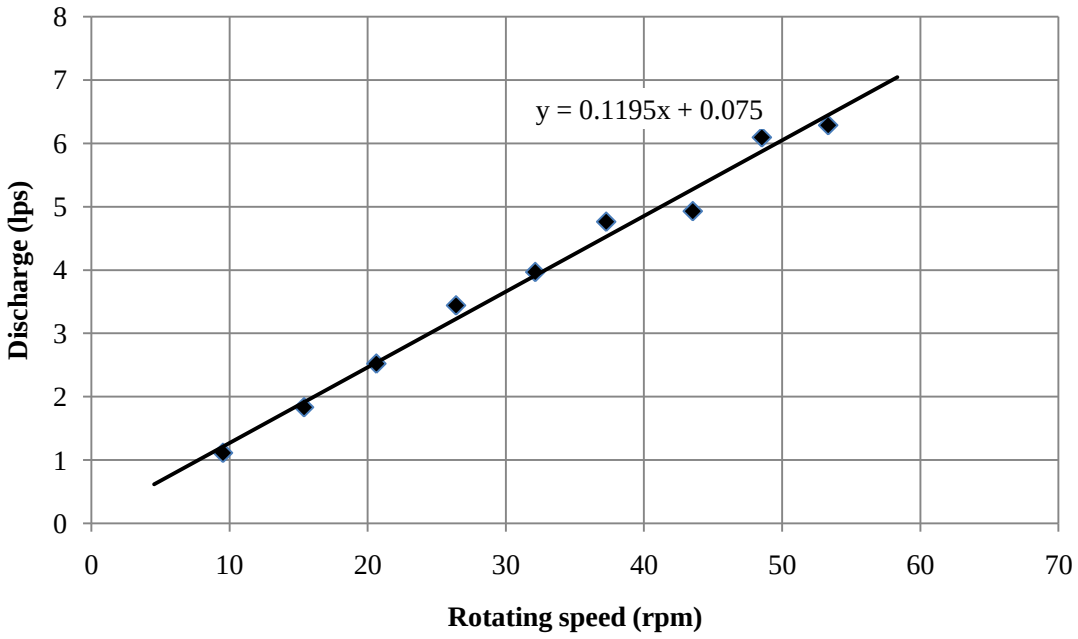

Figure 4.84 Relationship between rotating speed and discharge of six Archimedean's pipe-screw (6-APS) pump coupled to adjustable rotating speed motor

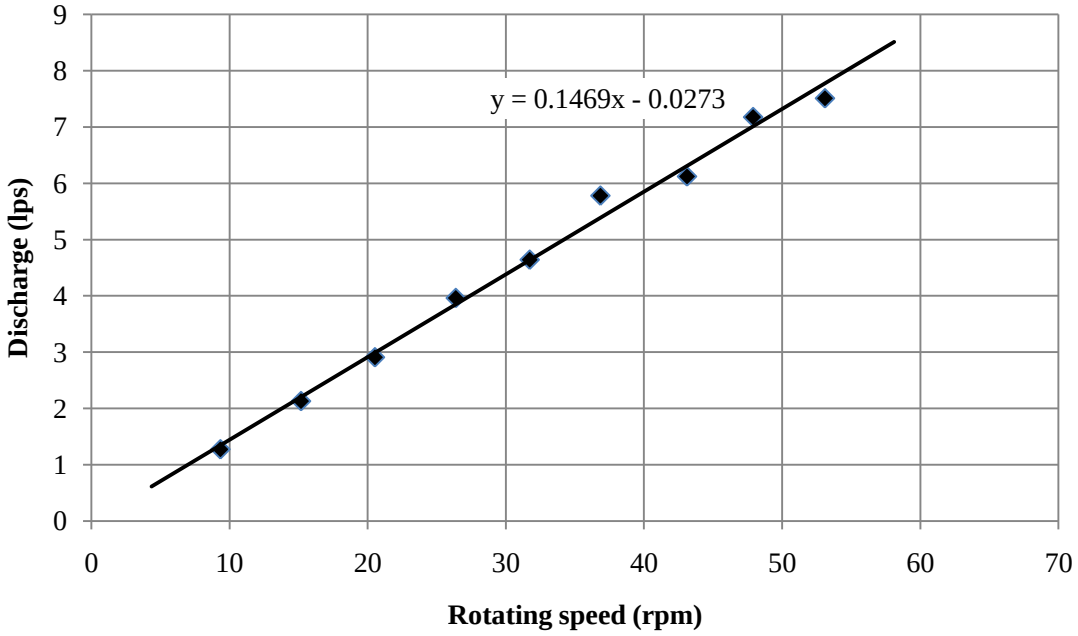

Figure 4.85 Relationship between rotating speed and discharge of seven Archimedean's pipe-screw (7-APS) pump coupled to adjustable rotating speed motor

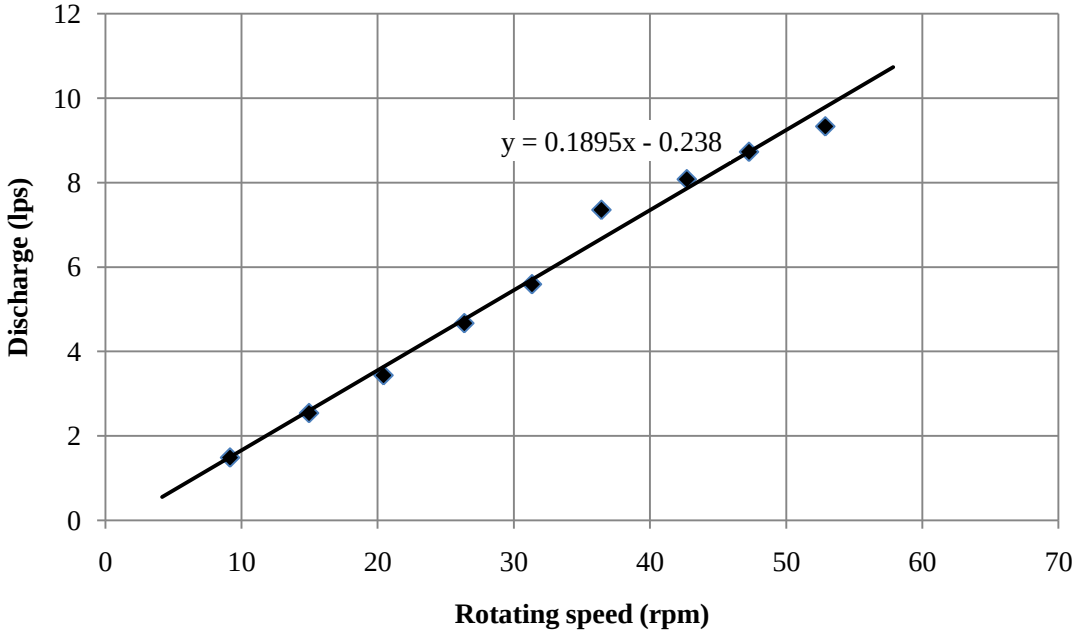

Figure 4.86 Relationship between rotating speed and discharge of eight Archimedean's pipe-screw (8-APS) pump coupled to adjustable rotating speed motor

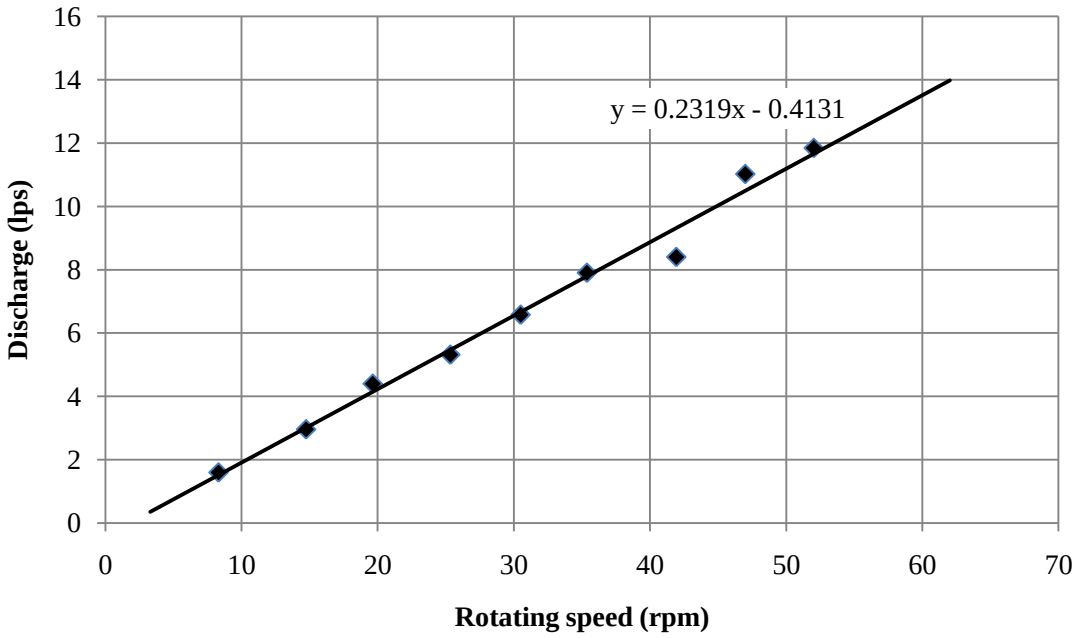

Figure 4.87 Relationship between rotating speed and discharge of nine Archimedean's pipe-screw (9-APS) pump coupled to adjustable rotating speed motor

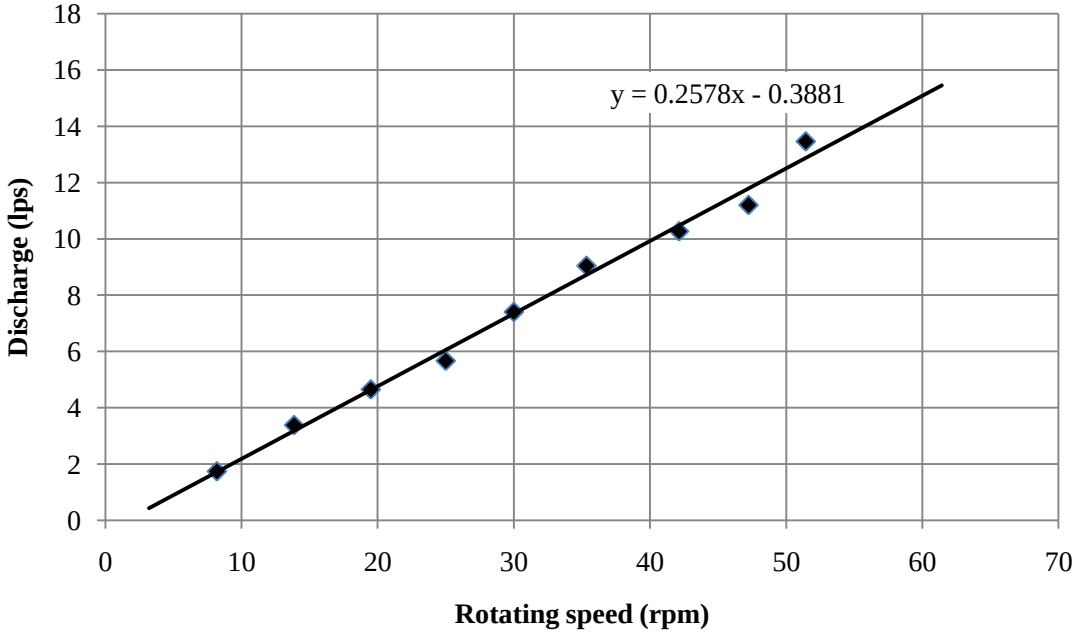

Figure 4.88 Relationship between rotating speed and discharge of ten Archimedean's pipe-screw (10-APS) pump coupled to adjustable rotating speed motor

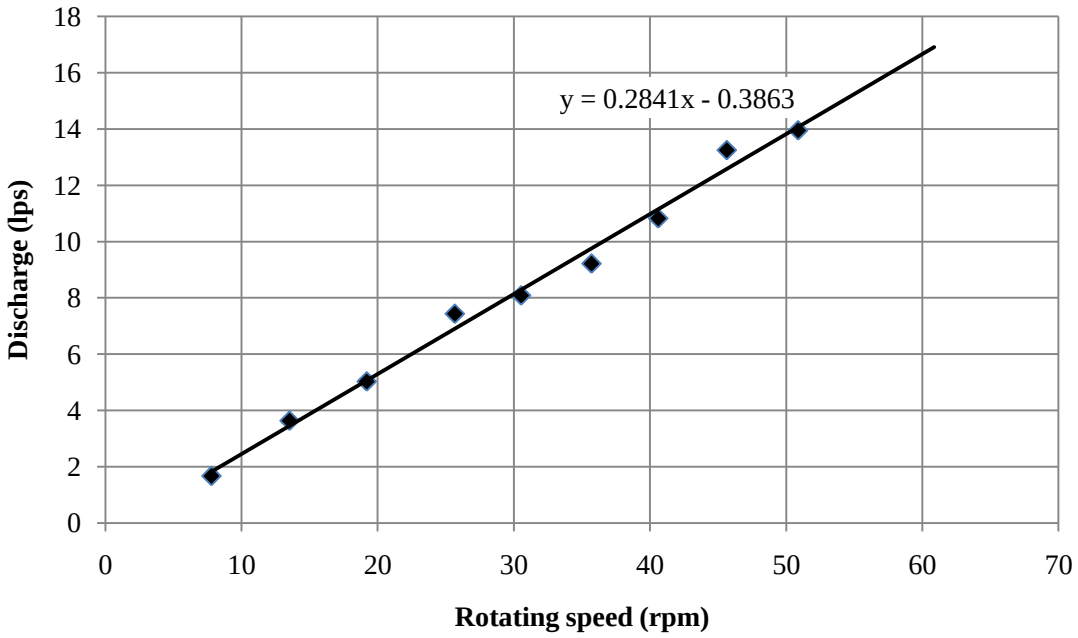

Figure 4.89 Relationship between rotating speed and discharge of eleven Archimedean's pipe-screw (11-APS) pump coupled to adjustable rotating speed motor

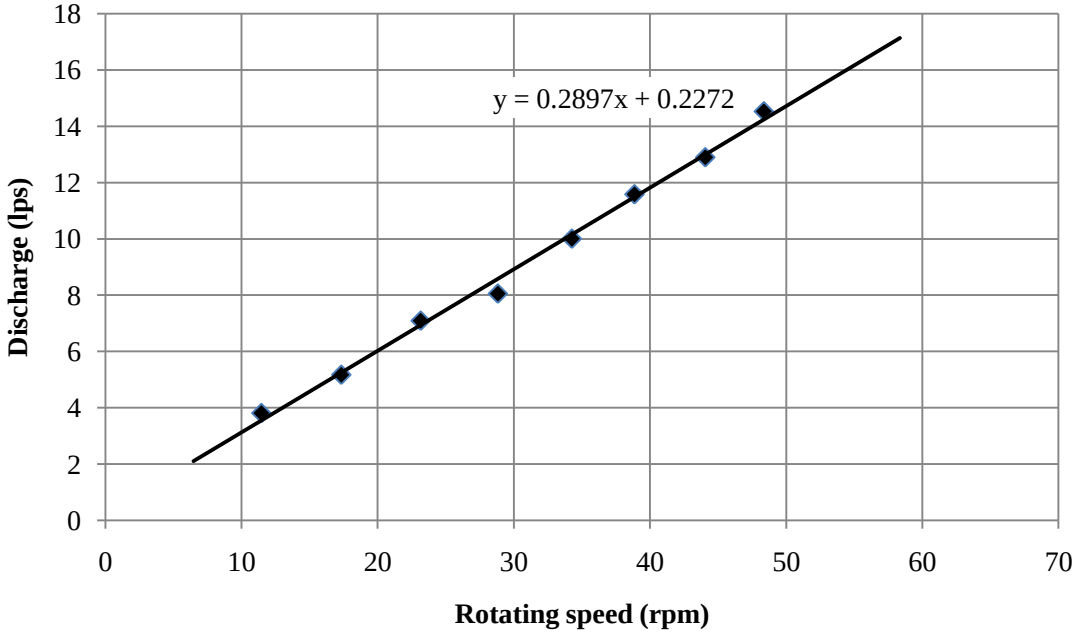

Figure 4.90 Relationship between rotating speed and discharge of twelve Archimedean's pipe-screw (12-APS) pump coupled to adjustable rotating speed motor

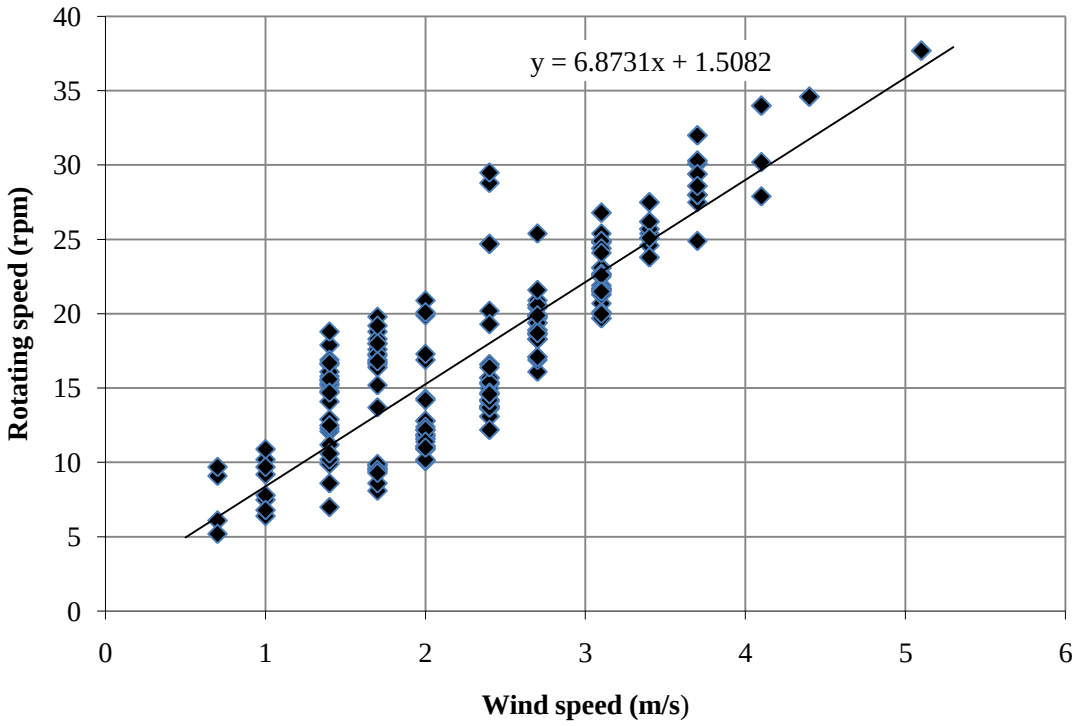

Figure 4.91 Relationship between wind speed and rotating speed of the new Thai sail windmill coupled to twelve Archimedean's pipe-screw (12-APS) pump

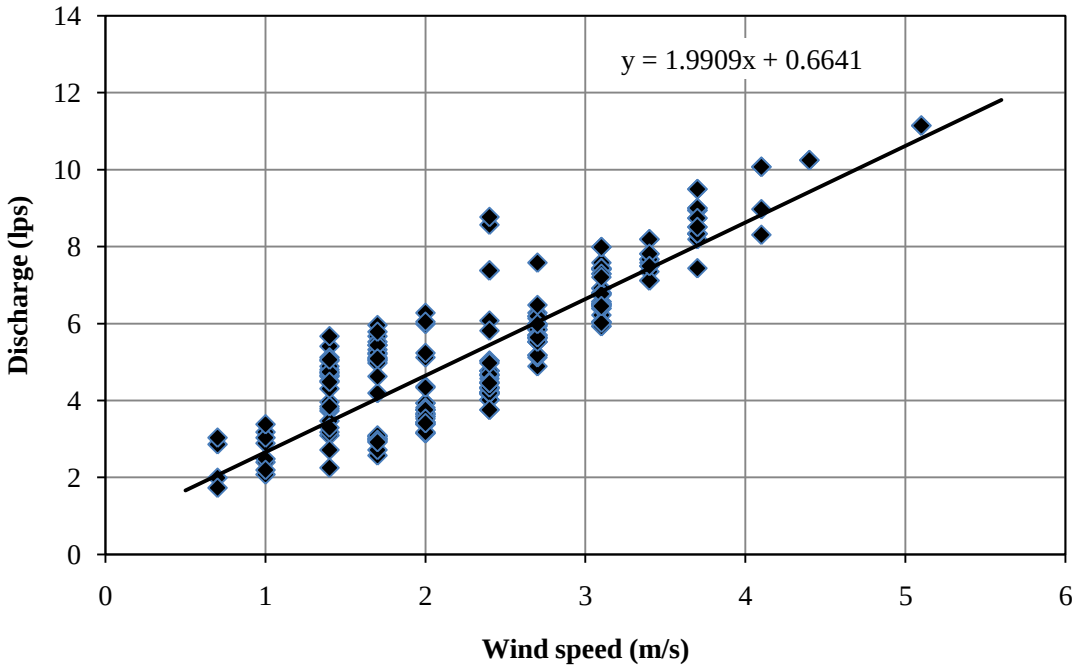

Figure 4.92 Performance curve of wind speed and discharge (lps) of twelve Archimedean's pipe-screw (12-APS) pump coupled by the new Thai sail windmill

Table 4.2 Test results of wind speed and discharge (m^3/hr) of twelve Archimedean's pipe screw (12-APS) pump coupled by the new Thai sail windmill

Wind speed (m/s)	Average rotating speed (rpm)	Discharge Q (m^3/hr)	Discharge Q (lps)	Water power (W)	Wind power (W)	The overall efficiency (%)
1.40	13.80	15.21	4.23	62.12	80.72	76.96
1.70	14.23	15.66	4.35	63.95	144.53	44.25
2.00	13.10	14.48	4.02	59.12	235.34	25.12
2.40	16.10	17.60	4.89	71.88	406.66	17.68
2.70	19.36	21.00	5.83	85.77	579.02	14.81
3.10	22.53	24.31	6.75	99.28	876.37	11.33
3.40	25.55	27.46	7.63	112.14	1156.21	9.70
3.70	29.08	31.14	8.65	127.14	1490.07	8.53
4.10	31.53	33.69	9.36	137.58	2027.46	6.79
4.40	34.60	36.90	10.25	150.67	2505.87	6.01

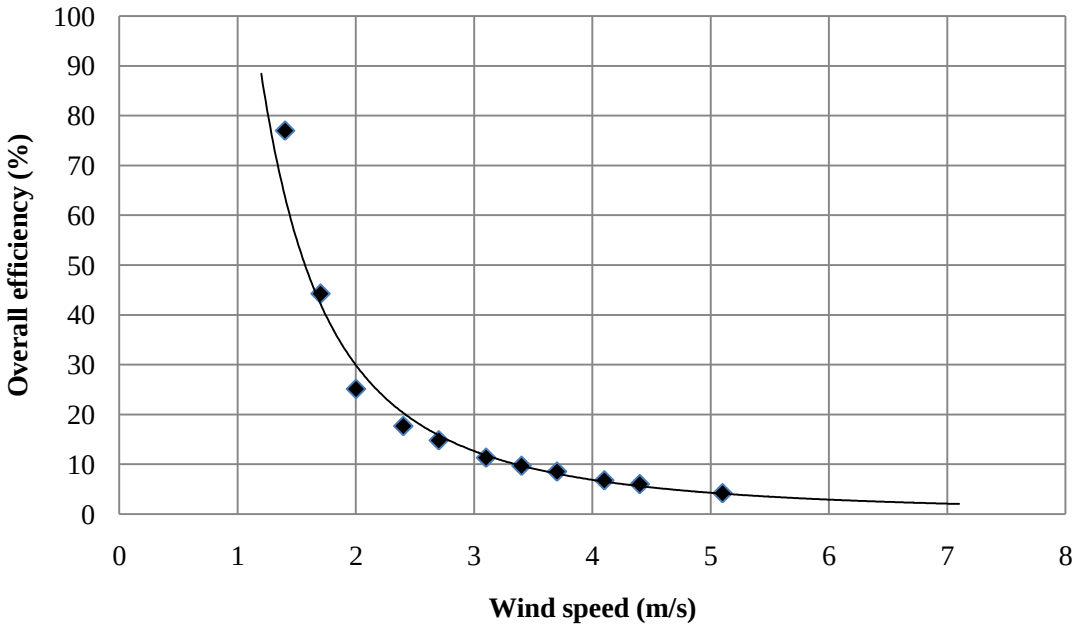

Figure 4.93 Relationship between wind speed and overall efficiency of twelve Archimedean's pipe-screw (12-APS) pump coupled by the new Thai sail windmill

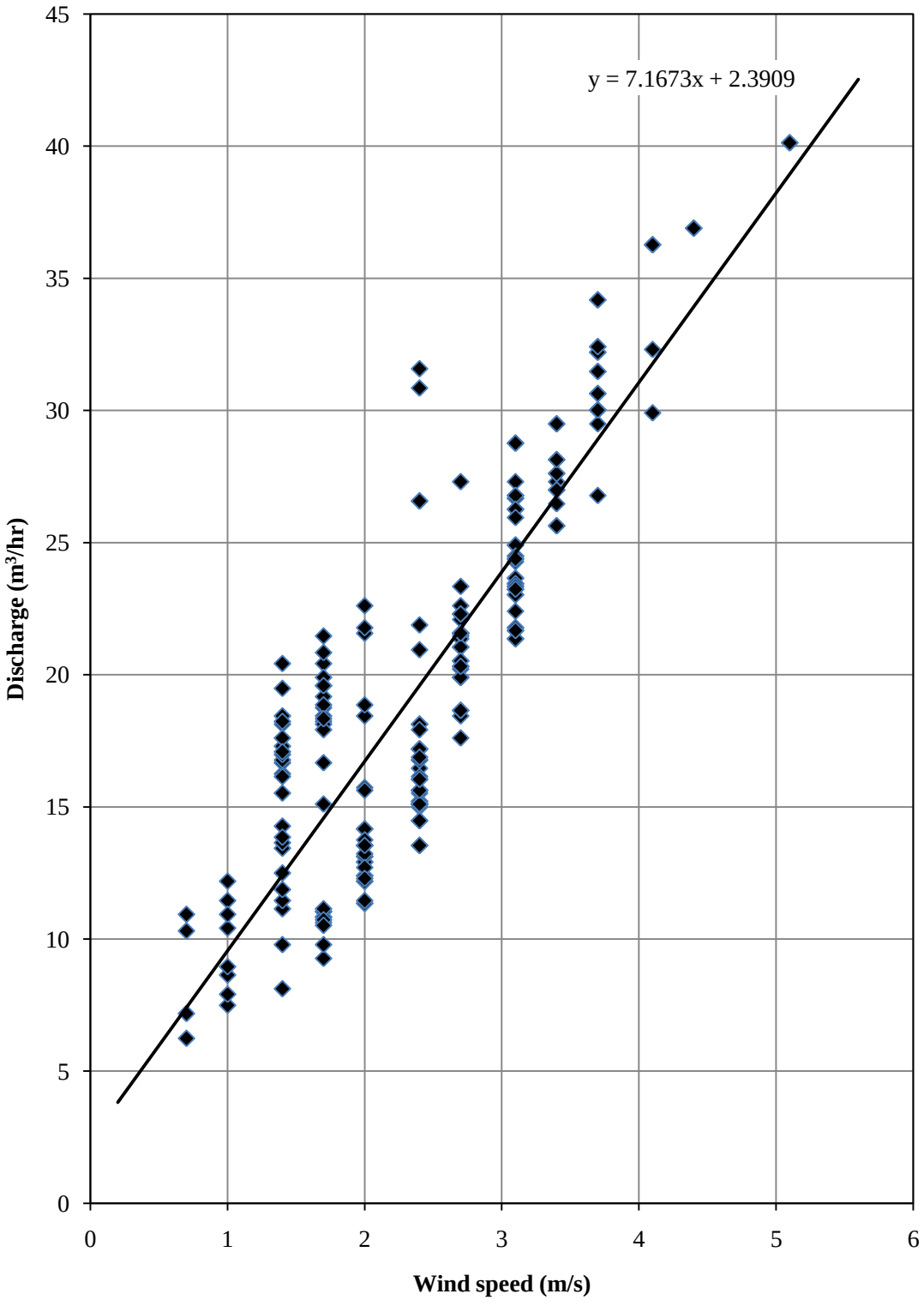

Figure 4.94 Performance curve of wind speed and discharge (m^3/hr) of twelve Archimedean's pipe-screw (12-APS) pump coupled by the new Thai sail windmill

4.7 Cost of windmill for water pumping

An estimate of parts used for construction of the prototype of the new generation of Thai sail windmill is given in Table 4.3, the total cost of windmill is 150,000 Baht for water pumping with water ladder pump and 145,000 Baht for water pumping Archimedean's pipe-screw pump.

Table 4.3 A list of components used in the prototype and cost of the new generation of Thai sail windmill

Components	Total cost of the new generation of Thai sail windmill (Baht*)	
	water ladder pump	Archimedean's pipe-screw pump
Rotor assembly : hub plate, tubular steel spars, support pipe, nylon rope	12,000	12,000
Sail : cloth, nylon rope	3,000	3,000
Power transmission : rear axle, drive shaft, universal joint, lower gear box	9,000	9,000
Tail assembly : steel pipe, galvanized sheet metal, cable	10,000	10,000
Turntable : steel structure, bearings	6,000	6,000
Tower structure : steel pipe, plat form, foundation	90,000	90,000
Pump : water ladder pump	20,000	15,000
Total	150,000	145,000

*1 USD ≅ 30 Baht, rate of 22/10/2013

The cost is quite reasonable and could be acceptable by farmers. Implementing the use of our new windmill would help improve farmer productivity.